MICROCOPY RESOLUTION TEST CHART

NATIONAL BUREAU OF STANDARDS-1963-A

R83-916100-1

AFOSR-TR- 83 - 0724
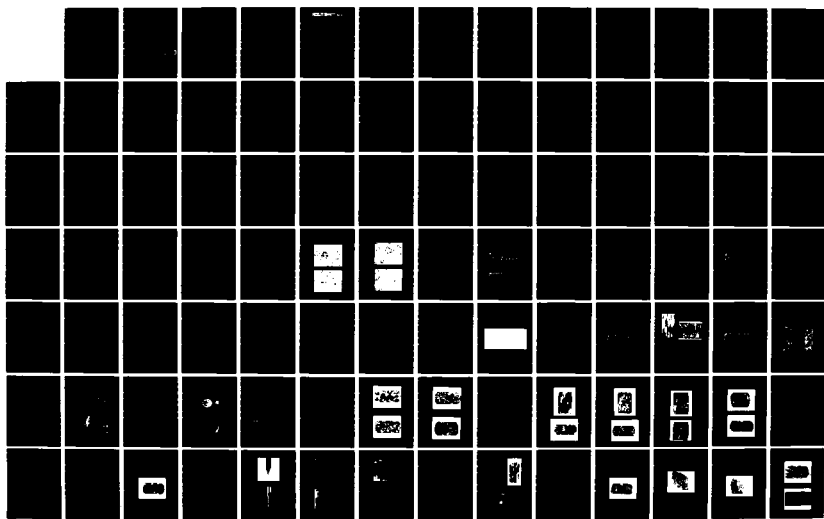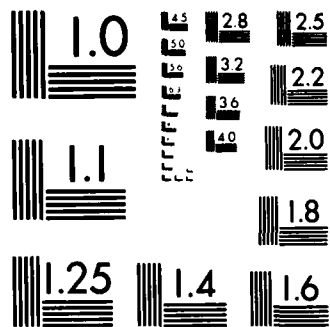
ADA131606

DEFORMATION STUDIES IN WORKABLE SUPERALLOYS

Prepared by
A.F. Giamei

FINAL REPORT

Contract F49620-82-C-0028

for

Air Force Office of Scientific Research
Building 410
Bolling Air Force Base
Washington, DC 20332

DTIC
SELECTED
AUG 2 2 1983
A

May 31, 1983

DTIC FILE COPY

"The views and conclusions contained in this document are those of the author and should not be interpreted as necessarily representing the official policies or endorsements, either expressed or implied, of the Air Force Office of Scientific Research or the U.S. Government."

**UNITED
TECHNOLOGIES
RESEARCH
CENTER**

East Hartford, Connecticut 06108

UNCLASSIFIED

SECURITY CLASSIFICATION OF THIS PAGE (When Data Entered)

REPORT DOCUMENTATION PAGE		READ INSTRUCTIONS BEFORE COMPLETING FORM
1. REPORT NUMBER AFOSR-TR- 83-0724	2. GOVT ACCESSION NO. AD- A131606	3. RECIPIENT'S CATALOG NUMBER
4. TITLE (and Subtitle) DEFORMATION STUDIES IN WORKABLE SUPERALLOYS		5. TYPE OF REPORT & PERIOD COVERED Final Report 1 Oct 1979 - 31 May 1983
		6. PERFORMING ORG. REPORT NUMBER
7. AUTHOR(s) A. F. Giamei		8. CONTRACT OR GRANT NUMBER(s) F49620-82-C-0028
9. PERFORMING ORGANIZATION NAME AND ADDRESS United Technologies Research Center East Hartford, CT 06108		10. PROGRAM ELEMENT. PROJECT, TASK AREA & WORK UNIT NUMBERS 61102F 2306-A1
11. CONTROLLING OFFICE NAME AND ADDRESS Air Force Office of Scientific Research Bolling Air Force Base, Washington, DC 20332		12. REPORT DATE May 31, 1983
		13. NUMBER OF PAGES
14. MONITORING AGENCY NAME & ADDRESS(if different from Controlling Office)		15. SECURITY CLASS. (of this report) Unclassified
		15a. DECLASSIFICATION/DOWNGRADING SCHEDULE

16. DISTRIBUTION STATEMENT (of this Report)

Approved for public release;
distribution unlimited.

17. DISTRIBUTION STATEMENT (of the abstract entered In Block 20, If different from Report)

18. SUPPLEMENTARY NOTES

Approved for Public Release - Distribution Unlimited

19. KEY WORDS (Continue on reverse side if necessary and identify by block number)

Superalloys	Forming
Deformation	Plastic Strain
Workability	Strain Rate Effects

20. ABSTRACT (Continue on reverse side if necessary and identify by block number)

A three year workability study of nickel-base superalloys has been completed. The objective was to study the high strain plastic flow behavior of high strength superalloys in the form of single crystals, rapidly solidified ingots and consolidated powder particles. The single crystal alloy studied was PWA 1444 (similar to Mar-M200) which had previously been well characterized at low strains. The flow characteristics of this alloy have now been documented out to 20% strain as a function of crystal orientation. The low to

DD FORM 1473 EDITION OF 1 NOV 65 IS OBSOLETE
1 JAN 73
S/N 0102-LF-014-6601

UNCLASSIFIED
SECURITY CLASSIFICATION OF THIS PAGE (When Data Entered)

#20. Cont'd

intermediate temperature flow stress has been measured after forming. Remark-
able strain hardening has been obtained at low strains for high modulus crystals
worked below the solvus temperature. Rapidly solidified and cooled ingots were
made by arc melting or electron beam skull melting or induction melting and
then "drip melting" into a cold copper mold. The compositions and heat treat-
ment were tailored to promote workability. Some of these buttons were heavily
deformed in uniaxial compression under isothermal conditions below the gamma
prime solvus temperature, and several were deformed in the single phase gamma
region. High strains were achieved under conditions of constant displacement
rate, true strain rate or energy input rate. These materials have been de-
formed to 90% reduction in height (true strain $\approx$-2.3) above the solvus without
cracking, although they are not truly superplastic. The strain dependence of
grain size has been investigated at 15% strain intervals during dynamic re-
crystallization. A fine grained structure has been created by cooling through
the gamma prime solvus temperature during the forming operation. The powder
base line material, PWA 1056 (IN-100) was confirmed to be superplastic by
strain rate sensitivity measurement using stress change experiments centered
around a strain rate of 0.2% s^{-1} (10% min^{-1}). The strain dependence of the
strain rate sensitivity has now been defined as well as the grain size depen-
dence. The strain rate was varied from 2 x 10^{-3}% s^{-1} to 1.5 x 10^{1}% s^{-1}, or
about four orders of magnitude.

UNITED TECHNOLOGIES RESEARCH CENTER

East Hartford, Connecticut 06108

R83-916100-1

Deformation Studies in
Workable Superalloys

Final Report
Contract F49620-82-C-0028

REPORTED BY _____
A. F. Giamei
Principal Investigator

APPROVED BY _____
E. R. Thompson, Manager of
Materials Sciences

DATE 5/31/83

NO. OF PAGES _____   COPY NO. _____

Deformation Studies in Workable Superalloys

TABLE OF CONTENTS

1.0 PROGRAM OVERVIEW

A program has been completed wherein a systematic study, from a fundamental point of view, was carried out on nickel base superalloy high temperature plastic flow behavior under carefully controlled experimental conditions in a variety of alloy chemistries and microstructures. This work relates to high performance applications for superalloy gas turbine disks made from materials without significant residual chemical macrosegregation. (These can be prepared by relatively high cooling rate techniques.) The object of this research was to define the physical and structural aspects of the large strain plastic flow behavior of homogeneous nickel alloys under precisely defined conditions of deformation temperature and energy input rate. The approach was to study the high strain plastic flow behavior of nickel base superalloys in three forms: single crystals, rapidly cooled ingot and consolidated powder product. The single crystal alloy was selected to be PWA 1444 (essentially Mar-M200), which is well characterized at low strains. Arc melted buttons and skull melts made by electron beam processing were made of several intermediate to high strength superalloys. The compositions and heat treatments were tailored to promote workability. Some of these buttons were heavily deformed in uniaxial compression under isothermal conditions below the gamma prime solvus temperature, and several were deformed in the single phase gamma region. Grain boundary cracking was normally limited to lower temperature deformation, unless incipient melting was encountered. High strains were achieved under conditions of constant displacement rate, true strain rate or energy input rate.

The powder alloy was selected to be PWA 1056 (IN-100) for a superplastic base line. Forming experiments were conducted under a wide variety of temperature and strain rate conditions below the gamma prime solvus temperature to stabilize the grain size. Stress change experiments were carried out to measure the strain rate sensitivity parameter over a wide range of strains. Deformation work was done with a computer controlled hydraulic testing frame. A program was derived to form at a constant rate of energy input. Microstructures were determined before and after forming. Yield strength measurements were made as a function of temperature for several classes of high strength superalloys both before and after forming.

2.0 INTRODUCTION

Improved performance in modern gas turbine engines has traditionally been achieved by greater turbine inlet temperature, or greater rotor speed, or both. These parameters increase the efficiency or thrust but place greater demands on the turbine blades, and therefore turbine disks. Substantial improvements in turbine blade performance are promised by directional solidification (DS) (Ref. 1) including single crystal components (SC) (Ref. 2), directional recrystalli-zation (DR), fiber reinforced superalloys (FRS) or eutectics (Ref. 3). The recent disk advances have centered around lowering density, cost and/or raw material utilization. With new requirements of higher disk alloy strengths, or longer lives, it will be necessary to gain a better understanding of nickel-base superalloy disk forming operations.

A brief review of superalloy disk working regimes as they relate to alloy composition and microstructure is in order. Alloys with low volume fraction of strengthening phase (Ni_3Ti, Ni_3Nb or Ni_3Al) are referred to as lean super-alloys, e.g. Waspaloy, and are normally cast as ingots, preheated to above the solvus temperature, and worked with relative ease. On the other hand, inter-mediate strength (and gamma prime volume fraction) superalloys, such as Astroloy, are again cast as ingots, but are worked just below the gamma prime solvus temperature with great care, particularly at low strain, to avoid grain boundary cracking (Ref. 4). Warm die forging is generally used with inter-mediate annealing.

The high strength superalloys represent a real challenge. These alloys can, on occasion, be cast as ingots, heat treated and worked successfully. However, these results are not reproducible from billet to billet, and alloys such as cast IN-100 or Mar-M200 are generally considered to be unworkable. It is known that these results are due, at least in part, to the influence of macrosegregation on the microstructure (Ref. 5). Substantial variations in the amount of aluminum and/or titanium lead to local differences in the amount of eutectic gamma prime, and therefore the local response to heat treatment. Residual microsegregation can lead to incipient melting at anomalously low temperatures.

It is unfortunate that the higher solute ("hardener") content superalloys are more prone to macrosegregation and seem to have a lower level of intrinsic grain boundary strength. This dilemma, as well as the promise of substantial improvements in the "fly/buy" ratio, fostered the advent of the powder metal-lurgy approach to making superalloy disks (Ref. 6). This method ensures the lack of substantial macrosegregation by the nature of the powder making process. The residual short wavelength microsegregation patterns are virtually eliminated

by consolidation steps such as hot isostatic pressing (HIP) or Gatorizing® or extrusion. The fine particle size (10-100μm) of the powder particles leads to superplastic flow in closed die isothermal forming (Ref. 7). The high ductility as well as the low flow stress are useful in making large complex shapes.

Further advances in powder metallurgy will require: tailoring the alloy to the processing methods to avoid both carbide precipitation at prior particle boundaries and incipient melting; minimization of inclusion content and size, leading to an extension of cyclic fatigue life; local grain size coarsening to enhance creep life; local thermo-mechanical strengthening (Ref. 8) to boost yield and/or ultimate tensile strength; and possibly local chemistry or particle size variations to achieve the desired level of creep resistance at the rim and fatigue resistance at the bore. We need more fundamental knowledge about these materials if these challenges are going to be met.

There may also be a path available to obtain substantial workability in cast high strength superalloys by combining the control of local composition and forming conditions. Some interesting experiments on model superalloys, and some of the supposedly unworkable alloys have now been completed. First, fine dendritic structures were obtained. This can be done over a short distance by using a water cooled copper chill surface, e.g., in an arc melted button, a drop casting or the lower end of a DS casting (Ref. 9). On a larger scale, drip melted ingots can be made in cold or cooled molds by clean melting techniques such as electric arc or electron beam. These techniques have the added advantage of avoiding ceramic contamination, and possibly reducing or volatilizing pre-existing inclusions. The ceramic contaminants tend to float and can be substantially reduced by skimming methods.

The primary and secondary dendrite arm spacings are related to cooling rate (Ref. 10) as follows:

$$S_1 \sim \left(\frac{\Delta T}{G \cdot R}\right)^p = \left(\frac{\Delta T}{\dot{T}}\right)^p, \quad p \approx 0.25 \tag{1}$$

$$S_2 \sim \left(\frac{\Delta T}{G \cdot R}\right)^n = \left(\frac{\Delta T}{\dot{T}}\right)^n, \quad 0.3 < n \leq 0.5 \tag{2}$$

where ΔT is the melting range of the alloy of interest, G is the thermal gradient perpendicular to the liquidus surface and R is the growth rate, the rate-gradient product is equal to the cooling rate, $\dot{T}$, as established below:

$$G \cdot R = \frac{\Delta T}{\Delta Z} \cdot \frac{\Delta Z}{\Delta t} = \frac{\Delta T}{\Delta t} = \dot{T} \qquad (3)$$

and G is related to the melting range and the mushy zone height, ΔZ, as follows:

$$G = \frac{\Delta T}{\Delta Z} = \frac{T_L - T_S}{Z_L - Z_S} \qquad (4)$$

where L and S represent the alloy liquidus and solidus temperatures, respectively.

The fine dendrite structures can now be wholly or partially eliminated according to the relationship (Refs. 11,12):

$$t_h \sim S_1^2 \qquad (5)$$

where t_h is the time required to obtain a given state of homogenization. Combining Eqs. (1) and (5), we have:

$$t_h \sim (\dot{T})^{-\frac{1}{2}} \qquad (6)$$

Based on observations with two Ni-Al-Ta alloys, the proportionality constant is approximately 10^5 when t is in seconds and $\dot{T}$ is in °C/sec. The implications of Eq. (6) for several alloy processing schemes are given in Table 2-1.

"Normal" DS might be typical of a microstructure found 3-5 cm from the chill plate. Actual DS structures range from this base line by about a factor of ten in cooling rate to either side if liquid metal cooling (LMC) is included (Ref. 13). The "thin zone" DS structure is simply an idealization of a drip melted ingot where cooling of each new layer is by conduction to the cold ingot below as well as radiation to the environs. Layerglazing is a process where an extremely thin melt layer is formed by surface melting of a cold ingot by using a laser pulse or scan. RSR is a rapid solidification rate powder making process. Low pressure plasma spray (LPPS) is a means of generating 98-99% dense material with little risk of oxidation or entrapment of gas. Many of the cooling rates are calculated rather than measured, but the potential advantages of rapid cooling (Ref. 14) are obvious.

The second key feature is the use of an intermediate strain rate isothermal forming process. This had been carried out in a model ternary alloy (Ni-Al-Ta) selected to simulate high γ' volume fraction superalloys. These alloys were

strained to 60% reduction in height in either a continuous or interrupted mode at nearly constant true strain rate <u>above</u> the solvus temperature. The significant aspect of the aforementioned deformation work was thought to be the excellent homogenizability afforded by high cooling rates during solidification combined with the high solidus temperatures of the model alloy (~1400°C). The flow stress curve below the solvus temperature in these alloys shows a high initial flow stress plus strain hardening, whereas the flow stress initiates and stays at a low level at temperatures above the solvus due to dynamic recrystallization. The relevant solvus temperatures are given in Table 2-2.

Mar-M200 and cast IN-100 have also been formed up to 60% engineering strain by isothermal forming at controlled true strain rate above the solvus temperature. Fine dendritic structures (capable of near homogenization in short times) were available in DS castings from 2-5 cm above the chill. Mar-M200 can be annealed at 1260°C without melting if a gradual approach to the high temperature is used. The following conditions can be used for homogenization: 1204°C/2 hr + 1232°C/2 hr + 1260°C/20 hr. This treatment almost completely eliminated dendritic segregation in PWA 664 at the 3 cm level (up from the chill). This material could be deformed in much the same manner as the modified IN-100 alloy, using a function generator and a hydraulic test frame.

Consistent with earlier observations, it was not possible to reproducibly work cast IN-100, cast + extruded, or cast ingots of the powder version. There are cases where high volume fraction gamma prime alloys could be consistently formed, namely Ni-Al-Ta model superalloys. Additionally, the intermediate volume fraction alloy Udimet 700 can also be readily worked above the solvus temperature to very high strains without cracking. These alloys had a gap between solidus and solvus, which is not the case for IN-100, nor most of its many modifications. Therefore, the most effective modification of the IN-100 alloy was to slightly decrease the solvus temperature by altering the gamma prime forming elements.

Thus IN-100 can sometimes be worked by an isothermal forming approach starting with extruded ingots or rapidly cooled arc melted buttons. It would appear that modified IN-100 can be prepared in large sizes without macrosegregation and with the high cooling rates essential for the elimination of most, if not all, microsegregation by electron beam melting of a stick, or ingot, and dripping into a chill mold. An 8 cm diameter ingot has been prepared as a preliminary demonstration that such a material can be homogenized and formed. There is still more to be done, but such an approach seems very promising. LPPS will also be examined as a high cooling rate alternative which may be easier to control on a fine scale. Both the drip melted material and its alternatives (Layerglaze or LPPS) would probably require a HIP or extrusion cycle.

Table 2-1

Approximate Theoretical Times to 80% Homogenization at
~1315°C for Tantalum in Nickel with Various Processes
(Assumes Only Microsegregation)

Process	$\dot{T}$ (°C/s)	$(\dot{T})^{\frac{1}{2}}$	$(\dot{T})^{-\frac{1}{2}}$	t_h (sec)	t_h (hr)
Large Ingot	10^{-2}	10^{-1}	10	10^6	∠78
Normal DS	1	1	1	10^5	∠8
Thin Zone DS	10^2	10	0.1	10^4	3
Drip Casting	10^3	32	0.03	3×10^3	0.83
Drop Casting or DISC	10^4	10^2	10^{-2}	10^3	0.28
Layerglaze, RSR or LPPS	10^6	10^3	10^{-3}	10^2	0.028

Table 2-2

Solvus Temperatures for $\gamma + \gamma'$ Supealloys

Alloy	$T\gamma'$ (°C)
U-700	1145
IN-100*	1180
MAR-M200	1185
PWA 1444	1260
Ni + 5 wt% Al + 13 wt% Ta	1290

*PWA 1056, 1058 or MOD IN-100

3.0 EXPERIMENTAL RESULTS

Superalloys have excellent high temperature properties due to the presence of the coherent ordered precipitate, gamma prime (γ'). From a workability point of view, we can separate such alloys into three main categories: low, intermediate and high strength (or hardener content or volume fraction γ') superalloys. The low strength alloys, e.g. Waspaloy, are easily hot worked above the γ' solvus temperature; the intermediate strength alloys, e.g. Astroloy, are worked (with some difficulty) below the γ' solvus; the high strength alloys such as IN-100 are generally considered unworkable in any condition other than as a consolidated (superplastic) powder metallurgy product (Refs. 15,16).

Previous fundamental alloy studies programs carried out at Pratt & Whitney Aircraft had suggested that good workability in alloys such as IN-100 and even Mar-M200 could be obtained even with a relatively coarse cast grain size and microstructure. The following are desirable factors for workability during high strain uniaxial isothermal compressive (hot upset) forming:

1) near elimination of residual microsegregation
2) isothermal conditions
3) approximately constant true strain rate, and
4) small amounts of carbide or eutectic γ' phases to act as nucleation sites for recrystallization.

Item 1 dictates a high cooling rate if the homogenization is to be done in a reasonable time. Item 2 is easily achieved in the kind of equipment available today. Item 3 was only crudely carried out in previous studies by combining several short strokes or by periodically adjusting the displacement rate based on prior calculations. This program has improved on these relatively crude techniques with the utilization of a process control computer. One objective was to control the rate of energy input rather than the load or displacement rate.

The general approach was to establish a powder metallurgy base line for the F100 first-stage turbine disk bill of material in terms of such variables as flow stress and strain rate sensitivity parameter. The flow characteristics were determined at several temperatures near, but below, the γ' solvus. Next, the high strain behavior was compared for rapidly cooled bulk alloys in between U-700 and IN-100 at temperatures above the solvus. Obviously, a gap between solvus and solidus is desirable for the maximum degree of flexibility in the control of microstructure. Another type of rapidly cooled bulk alloy (starting with arc or electron beam melted buttons) selected for this study was an equiaxed version of the single crystal alloy 444 (PWA 1444) which was selected because it represents a fully characterized alloy based on Pratt & Whitney Aircraft

and Air Force Office of Scientific Research sponsored work and because it allows the opportunity to deduce the effect of grain boundaries or to study the aniso-tropy effects or to simplify the analytical problem by the elimination of grain boundaries.

A rather complete characterization of the log stress-log strain relation-ship was completed for the powder base line. Nearly four decades of strain rate were covered. The strain rate sensitivity can now be accurately obtained as a function of both strain and strain rate. Some of the powder material was inten-tionally grain size coarsened to assess the importance of grain size on super-plasticity. TEM studies were carried out on the P/M material to establish the deformation mechanism.

The rapidly cooled cast structures were made in larger sizes so that post formed properties could be measured. It was decided to concentrate on a modi-fication of IN-100 which proved to be quite workable.

Single crystals of PWA 1444 were prepared in <001>, <110> and <111> orien-tations and work hardening studies were carried out to 20% strain at two tem-peratures below the solvus. Significant substructure strengthening was found.

The strain rate sensitivity of P/M superalloys is well in excess of the value of 0.3 which is generally regarded as the minimum value typical of super-plastic behavior. The rapidly cooled material generated in this program showed a strain rate sensitivity parameter, m, of 0.15-0.22, due to its coarser grain size (20-100μm vs 2-10μm for P/M material). Considerable effort was placed on raising m by using higher strain rate, variable strain rate cycles, lower defor-mation temperature and cooling during deformation. Although the rapidly chilled castings could easily be formed to high strains above the gamma prime solvus temperature, they could not be converted into truly superplastic materials by isothermal upset forming at low to moderate strain rates.

3.1 Consolidated Powder

The master test plan for PWA 1056 powder billet as well as the rapidly cooled multigrained materials and single crystals is given in Fig. 3-1. A large assembly of micrographs, macrographs, σ/ε curves and computer reduced data was obtained. Only the significant portions therefrom are reported here.

3.1.1 Strain Rate Sensitivity

Normally, the PWA 1056 powder billet was worked at 1080°C, which is below the γ' solvus temperature. The grain size is relatively stable at that tem-perature for 1-2 hrs. However, at temperatures in the range 1150-1200°C, the grain size coarsens rapidly. In the first year of this program, the strain rate

sensitivity, m, was determined to be 0.70 at 1070°C in the range 0.2 to 2% s^{-1}. The parameter m, or strain rate sensitivity is defined as follows:

$$\sigma = A \, \dot{\varepsilon}^{\,m} \tag{7}$$

$$\ln \sigma = \ln A + m \ln \dot{\varepsilon} \tag{8}$$

$$m = \frac{d \ln \sigma}{d \ln \dot{\varepsilon}} \tag{9}$$

The strain rate sensitivity can be determined from a stress change, or directly from a plot of $\ln \sigma$ vs $\ln \dot{\varepsilon}$. Such a plot was obtained for three grain size conditions in PWA 1056. The data were collected at 1080°C. The as-extruded material shows m = 0.68 in the strain rate range of 0.25 to 1.5% s^{-1}, while m drops to 0.36 (still superplastic) for powder material slightly coarsened by a 1150°C/4 hr/ AC treatment. The parameter m falls to 0.16 (out of the range of superplastic behavior) when the treatment is 1200°C/4 hr/AC. These observations were further substantiated by some cracking in the forming of 1200°C annealed material. The data were linear over the measured strain rate range. These data are considered to be quite valuable in that the coarsening effect is quite dramatic.

The grain size in the consolidated powder material could not be characterized by normal metallographic techniques at magnifications as high as 1600X. Several etchants were tried, but the grain size seemed to be too fine to resolve. There-fore, the base line extruded and grain coarsened materials were prepared for scanning electron microscopy (SEM). Again, the response of the material to several standard etchants was either poor or inconsistent. The best results were obtained with a Michigan "B" etch. The base line grain size can be seen to be about 1-2μm in Fig. 3-2. As shown in Fig. 3-3, 1150°C/4 hr coarsens the grain diameter to ~5μm and 1200°C/4 hr leads to a grain size of almost 10μm. The large blocky features in these micrographs are eutectic γ' with an occasional carbide or boride, as verified by Kevex analysis.

PWA 1056 production billet material was cut into small rectangular parallel-ipipeds with 2/1 aspect ratio and compressed 60% in height at 1202, 1190, 1150, 1110 and 1070°C at strain rates of from 0.05 to 0.50% sec^{-1}. Typical results for the case of constant true strain rate, both for engineering stress and approximate true stress (assuming constant volume and spatially constant cross section), are shown in Fig. 3-4. Note that for this case, the superplastic flow attributed to an extremely fine grain size is characterized by a nearly constant true stress. Figure 3-5 illustrates the strain rate effects of interest. Ob-viously this material is quite sensitive to the level of strain rate or to a step change in strain rate. This is typical of superplastic behavior. Note that there is very little "memory" in terms of strain rate dependent work hardening.

Figure 3-6 represents data acquired during the determination of a strain rate sensitivity parameter (m) at 1070°C in the range of strain rates from 0.24 to 2.18% sec^{-1}. The average m value after four sequential changes of 1/3X, 3X, 3X and 1/3X in strain rate was approximately 0.7, well above the 0.3 minimum value normally associated with superplastic flow. Note that the flow stress is in the range 20-60 MPa. The information presented in Fig. 3-7 represents a computerized determination of engineering strain, true strain, strain rate and true stress in various units as well as the four independent computed m values. Note the excellent quality of the data: m = 0.696 ± 0.024. It is possible that m is increasing slightly during the test.

A process control software package was written and debugged for forming at a constant rate of energy input. An application of this technology to the consolidated powder is compared to a constant displacement rate test in Fig. 3-8. The initial strain rate was selected to be 0.17% sec^{-1} in both cases (10% min^{-1}, as in Pratt and Whitney Aircraft Gatorizing[R]). Note that the constant energy input rate gives a more nearly constant true stress.

The temperature dependence of the high strain plastic flow behavior of the as-extruded 1056 billet material is illustrated in Fig. 3-9 for a strain rate of 0.50% sec^{-1} (30% min^{-1}). Note as the temperature is increased, the flow stress first drops, as expected, and then increases, most likely due to grain coarsening at 1150°C, only 40°C below the gamma prime solvus temperature.

A series of experiments was carried out to determine the effect of strain on the strain rate sensitivity parameter and to broaden the data over a wider range of strain rates to search for the sigmoidal shape typical of other materials (Ref. 17). A subset of the overall strain rate sensitivity expanded test plan is shown in Fig. 3-10. It was immediately obvious that there were both strain and strain rate effects. Previously only three flow stresses were available over one decade of strain rate (and four m values). Now, using four specimens and four decades of strain rate, 24 flow stresses (with repeats at higher strains) are available as well as 44 m values. The step changes were carefully planned to jump up as well as down, with large as well as small changes (but all within one decade on one sample).

There were several conclusions. Previous attempts to generate such data using multiple specimens had failed due to a strain dependence. With much more data, it could be seen that the flow stress decreased slightly with strain at the high strain rates. This effect was quite pronounced in the grain coarsened material. This would strongly suggest that grain size refinement is occurring during superplastic forming in these alloys, even though the deformation temperature is below the solvus by 110°C. Figures 3-11 through 3-14 show the data for $\varepsilon()$ = 10 ± 5, 25 ± 5, 40 ± 5 and 55 ± 5, respectively. These latter figures include the as-extruded base line and the 1050°C/4 hr coarsened material.

Careful examination of the full range of data indicates that since the sigmoidal character of strain rate response was found, the behavior of the 1150°C coarsened material can be matched to that of the as-extruded base line by a shift of approximately one decade in strain rates; i.e., the coarsened material is superplastic, but at an order of magnitude lower strain rate. (On such plots, the 1050 and 1150°C coarsened materials would be nearly identical.) The data are generally very well behaved when taken in ϵ intervals of no more than 10%. Otherwise, changes of up to 20 MPa at a given strain rate may give the appearance of scatter.

Another approach is to average the flow stress values measured at various strains at a given strain rate and plot $\bar{\sigma}$ vs $\dot{\epsilon}$ as in Fig. 3-15. The smooth curve drawn through this master plot leads to Fig. 3-16, a plot of the strain rate densitivity parameter, m, as a function of strain rate for the as-extruded powder. Now it can be seen that for superplasticity ($m \geq .3$), the allowable strain rate range for as-extruded PWA 1056 is from 2.5×10^{-2} to 5% s^{-1} or 1.5 to 300% min^{-1}. This is consistent with industrial practice which is generally in the range 3% to 40% min^{-1}. Coarser grain sizes than 1-2μm would mean a shift to lower strain rates (~0.1X in strain rate for ~3X in grain size).

3.1.2 Closed Die Forming

In the manufacture of Gatorized[R] superalloy disks closed dies are used in order to achieve near net shape turbine disks. The Gatorizing[R] process utilized the superplastic forming capabilities of the fine powder IN-100 alloy PWA 1056. This concept was attempted under laboratory conditions. A set of closed dies of Vistal[*] were machined. A drawing of the die is given in Fig. 3-17. Two specimens 0.8 cm x 0.8 cm x 1.76 cm (.313" x .313" x .694") were compressively formed in this closed die apparatus. Both tests were run at 1080°C at a constant engineering strain rate of $\dot{e}$ = 0.17 min^{-1}. The first specimen T/512 was run with no lubricant and cracked the die at an undetermined point. A second attempt was made at closed die forging using a fine powder of Pyrex glass as a lubricant between the die and the specimen. The true stress strain plot is given in Fig. 3-18. After a steady stress of 12.8 MPa was achieved, the flow stress began increasing at ϵ_T ~-100%. At this point the metal was coming in contact with the die walls. When the stress reached ~16 MPa the specimen was cooled and examined to confirm that the die had not broken. At this point the metal had flowed to the die walls and was in contact throughout the circumference, but had not totally filled the die. As testing resumed, the load increased steadily until a stress of ~20 MPa was achieved, at which time the die fractured and the stress dropped rapidly. Examination of the specimen revealed it to have filled the die cavity completely but when deformation required the flash to be forged outside the die cavity the die walls fractured.

*A trademark of Coors Procelain Co, Golden, CO.

Figure 3-19 illustrates the polished and etched cross-section of the
closed die formed specimen. A uniform grain structure is observed throughout
the specimen with faint streamline flow lines observed in one-half of the
sample. The shape did not exactly conform to the original cavity shape due to
failures at the die walls. It has been recognized that this risk was present
due to the thin ceramic rim on the die. This problem can be circumvented by
less aggressive die design or by working with TZM dies in vacuum or inert gas
atmosphere. The grain size appears coarsened from the starting condition.
This is probably attributable to the very low strain rate which was selected
for these forming trials. A strain rate of 0.17% sec^{-1} (10% min^{-1}) would have
been closer to commercial practice.

3.2 Rapidly Solidified Structures

3.2.1 Alloy Studies

Arc melted buttons were prepared in a partial pressure of argon and grad-
ually solidified over a 1-3 min period from bottom to top to avoid shrinkage.
These buttons are made from 50-400g and contain fine microstructures which are
relatively easily homogenized. The degree of microstructural uniformity in the
consolidated powder alloy is truly remarkable, particularly after heat treat-
ment. Similar structures can be developed in cast alloys. Figure 3-20 shows
the presence of only precipitated gamma prime and monocrystal carbides and the
complete absence of any microsegregation in a cast button of PWA 1056 after
exposure to 1204°C/24 hr followed by 870°C/32 hr. This thermal history was
applied to all cast arc melted buttons in preparation for yield strength measure-
ment vs temperature to obtain a comparison with other cast alloys on an equal
basis. The normal preparation sequence was to homogenize and "Fast Furnace
Cool" in a vacuum furnace with a low heat capacitance, solutionize and air
cool, and finally precipitation age and air cool.

Forming specimens were then cut out either parallel or transverse to the
columnar grain growth pattern with an aspect ratio of 2:1 for height:width.
For repeated compressive yield strength measurement, an aspect ratio of from
3:1 to 4:1 was used. This gave stability to the forming specimen, and led to a
finite zone without major end effects for yield stress measurements.

The as cast material was homogenized for the wrought U-700 (Astroloy)
composition and for a modified IN-100 alloy (no vanadium). A dramatic improve-
ment in microstructural uniformity was noted in both cases. Such structures
deform easily based on prior experience. The homogenized U-700 was fully heat
treated according to specifications and two specimens were prepared for repeated
yielding. Data showed excellent reproducibility at a strain rate of 5% min^{-1}.
The microstructure of fully heat treated wrought U-700 showed a high frequency
of annealing twins. This would be indicative of a low stacking fault energy in
this intermediate strength and volume fraction gamma prime alloy.

The cast arc melted button version of PWA 1056 mentioned previously was
sectioned, ground, heat treated and prepared for constant energy rate forming.
The grains coarsened significantly after homogenization at 1204°C/24 hrs. This
same material was formed at 1204°C at 0.0115 MPa/sec to a strain level of -60%
or a true strain of -0.92. The resultant grain diameter (after furnace cool)
was about 0.3 mm. The microstructure is extremely uniform.

It was known at the start of this program that wrought or cast U-700 (35
vol% γ') could be worked above the gamma prime solvus temperature, but alloys
such as IN-100 and Mar M-200 (~65 vol% γ') could not, at least not on a con-
sistent basis. Therefore, a threefold approach was taken to obtaining work-
ability in a cast high strength superalloy solidified at a high cooling rate.
First, modify the IN-100 (1058) to remove the vanadium. This element is easily
oxidized and can thus introduce inclusions, has no obvious technical merit in
the alloy at the small level present, causes alloy degradation in aggressive
high temperature environments, depresses the incipient melting point signifi-
cantly and decreases scrap value since it is only found in the IN-100 family.
Second, blend the workable low carbon U-700 (1013) with the higher strength
modified 1058 in 50/50 proportions. This might give a workable alloy with a
50 vol% γ' microstructure. Careful heat treatment and/or working might pro-
vide enough strength for a modern turbine disk application. Third, modify the
cobalt free version of Mar M-200 (1444) to provide grain boundary ductility by
adding hafnium, carbon and boron and also decrease the aluminum to provide a
wider gap between solidus and solvus temperatures. The actual target chemis-
tries are delineated in Table 3-1.

Figure 3-21 illustrates that the four cast alloys U-700 (wrought alloy
composition), 50/50 blended 1013/1058, IN-100 (1056 with aluminum, titanium
and vanadium at the low end of the allowable specification range) and MOD 1058
(no vanadium) all can be worked above the gamma prime solvus temperature with-
out any trace of external edge cracking or internal grain boundary cavitation.
These tests were done to a true strain of -0.92% under conditions of constant
energy input rate of 0.01-0.02 MPa/sec. These results are truly remarkable,
when one considers that they were obtained from 2/1 aspect ratio square cross
section compression specimens without lateral constraint. Figure 3-22 shows
the etched views of the MOD 1058 specimen before and after forming as a typical
example from this series. Note the post-formed microstructural uniformity and
the extensive degree of dynamic recrystallization (possibly coarsened slightly
by a slow furnace cool after forming).

The modified polycrystalline versions of PWA 1444 at 4.0, 4.5 and 5.0 wt%
Al presented a serious challenge. To begin with, the 5.0 Al alloy probably has
too much eutectic gamma prime to be useful as a disk alloy. At the 4.5 Al
level, under the normal condition of constant displacement rate forming, minor

14

edge cracking was observed. Even at the 4.0 Al level, there were internal cracks forming at grain boundaries. This alloy may contain too much hafnium for the small amount of gamma prime which remains at high temperature. The hafnium thus segregates to the grain boundaries and causes cracking. Figure 3-23 shows that this class of materials can be formed to a high strain level without any trace of external or internal cracking (or incipient melting) at a forming temperature of 1225°C by means of constant energy rate forming. Higher temperatures result in internal cracking, probably associated with the complete dissolution of gamma prime and the segregation of hafnium to grain boundaries. The use of constant true strain rate resulted in minor edge cracking. Thus the Constant Energy Rate Forming does seem to provide a definite benefit. The workability window may be opened at the 4.5 Al level by lowering the hafnium content.

With these apparent successes, the next goal was to measure the yield stress versus temperature curve for formed material. The typical 200 gram arc melted button yielded several forming specimens with a typical weight of 3 grams each and lateral dimensions which were too small to allow for the preparation of a proper compressive yield strength specimen. A series of 400 gram arc melted buttons was prepared which allowed several 20 gram specimens at 2/1 aspect ratio to be sectioned for forming. The subsequent lateral dimensions, following a 60% reduction in height, were large enough to obtain at least one compressive yield specimen with 3/1 aspect ratio, approximately 14 mm x 4 mm x 4 mm. Examples of such specimens are shown in Fig. 3-24 and the post formed yielding behavior is illustrated in Fig. 3-25. The temperature range of interest for a disk would be below 750°C. With this in mind, note that the forming operation significantly enhances the yield strength, and that a further gain is achieved by a short or partial solution heat treatment and typical gamma prime precipitation and carbide stabilization heat treatments. The worked consolidated powders show the highest strength levels due to their fine grain size. However, the cast alloy strengths are high and may be increased by more strain, higher strain rate, faster cooling after forming, decreasing temperature during working or improved heat treatments.

A significant step forward was made in obtaining more massive high cooling rate cast alloys when it was demonstrated that 1200-1600 gram buttons could be obtained by a skull melting technique using electron beam processing. Three to four 400 gram buttons can be made by conventional arc processing, and these can be combined into one large button using electron beam melting. These large buttons were melted twice to ensure chemical homogeneity. A gradual power down (1-3 min) was used after the melting cycle to minimize any residual porosity and to maximize the opportunity for the flotation of oxide inclusions. The ingot structure was fine columnar grained, as illustrated in Fig. 3-26 and was fully workable in the form of a 70 gram 2/1 aspect ratio specimen under heat treatment and working conditions established for 200-400 gram buttons. The 3,

20 and 70 gram formed specimens are compared in Fig. 3-27. It is highly encouraging that a 23X scale-up in weight and volume was obtained in MOD 1058 and the 1013-1058 blended alloy without difficulty.

3.2.2 Very High Strain Deformation

If turbine disks are ever to be made by isothermally forming homogenized cast superalloys above the solvus temperature, local strains larger than those typical of a 60% reduction in height may be required. In fact, higher strains may also lead to higher strength levels. The modified 1058 alloy looked the most promising to attempt a 90% reduction in height. Figure 3-28 indicates that a "quarter" sized specimen can be produced without any trace of edge cracking. The corresponding true stress versus true strain curve was essentially constant out to a true strain of -1.0, Fig. 3-29, indicating no significant frictional effects at engineering strains of up to 70% in compression without any platen lubrication. (Translucent alumina platens were used at the faces of high strength fully dense alumina rams in all the forming experiments.) All of the elements are present to extend this forming method to large bodies. All forming tests done to date have been in air or impure flowing argon. Larger specimens could be done in evacuated tight chambers and this would give cleaner surfaces.

3.2.3 Parametric Studies

A modification of IN-100 (no vanadium) was cast (buttons) and homogenized prior to forming. This alloy was the focus of an extension of the strain rate sensitivity testing which had been completed for the consolidated powder. The results are shown in Fig. 3-30. The data are truly remarkable in that they are very well behaved (with little strain dependence) over four decades of strain rate, and are decidedly linear. The m value is 0.22. This is very close to the critical value of 0.3 for superplasticity. Additionally, no cracking was observed during the strain rate sensitivity testing out to 60% reduction in height at 1204°C.

The effect of strain rate on dynamically recrystallized grain size is clearly shown in Figs. 3-31 and 3-32 where the grain size is seen to gradually be refined as the average strain rate is increased from 0.006% s^{-1} to 6% s^{-1}. A factor of 10^3 increase in strain rate brings about a factor of 10 decrease in grain diameter, namely from 1 mm to 0.1 mm. These results seem to indicate little static recrystallization or grain growth after forming during a furnace cool; otherwise the grain size differences might not be so pronounced.

The lack of a dependence of flow stress on strain level and the lack of any nonlinearities in the ℓn σ vs ℓn ε plot for the columnar grained arc melted buttons of modified PWA 1058 (IN-100) must be a consequence of the fact that the material is constantly dynamically recrystallizing above the solvus temperature.

This is in direct contrast to the powder work below the solvus, where grain size changes, although they occur to some degree, are not significant in the overall deformation behavior.

The true flow stress vs true strain is plotted in Fig. 3-33 for buttons of modified PWA 1058 (IN-100) at various strain rates. Note the steady character of these flow curves. A peak in true stress below a strain of 10% would indicate the onset of dynamic recrystallization at relatively low strain levels. The evolution of the recrystallized grain structure was monitored for the exact conditions set forth in Fig. 3-33 at strain levels of 15, 30, 45 and 60%. These results are shown in Figs. 3-34 through 3-37. Note that the dynamically recrystallized grain structure is considerably finer at 12.5% s^{-1} vs 5 x 10^{-3}% s^{-1} and that the recrystallization process has just barely begun at 15% strain at 5 x 10^{-3} % s^{-1}, whereas it has progressed considerably further at the same 15% strain level at the selected strain rate of 12.5% s^{-1}. Although the grain refinement is remarkable, the data of Fig. 3-33 are entirely consistent with those of Fig. 3-30, namely m $\simeq$ 0.22. Further grain size refinement is apparently required for superplasticity. The grain size of about 50μm in Fig. 3-37 may still be 5X to 10X too coarse for true superplasticity (Ref. 18).

3.2.4 Grain Size Refinement

Starting with a columnar grained arc melted button of modified 1058, an attempt was made to significantly impact the grain size by cooling through the gamma prime solvus temperature during forming. The rams, buttons and forming specimen were soaked at 1204°C to obtain initial isothermal conditions. Forming was initiated at 0.33% s^{-1} (20% min^{-1}). At that rate 60% strain only takes about 4.4 min (due to a slowdown to maintain constant true strain rate). After 1 min, the furnace was turned off. The temperature declined almost immediately and dropped at about the rate of 20°C/min. After 2.5 min into the deformation cycle (40% strain, see Fig. 3-38), the temperature dropped below the gamma prime solvus.

Figures 3-39 and 3-40 show how the stress varied with strain and with temperature. Figure 3-40 shows an undercooling of about 28°C before the flow stress truly escalates. The experiment seemed to work as planned. No cracking occurred. Without preconditioning the microstructure by straining above the solvus, the specimen would have surely cracked below the solvus at a 20% min^{-1} strain rate. Note the outstanding grain size refinement indicated in Fig. 3-41. The initial grain structure can still be seen in the dead zone near the Lucalox loading platens (no lubrication was used in these experiments). The final grain size is in the range 20-50μm. Further refinement seemed possible at higher cooling rates combined with higher strain rates.

Recognizing that a fine equiaxed grain structure is necessary to obtain superplasticity below the γ' solvus temperature and that the highly desirable low oxygen concentrations are regularly achieved in superalloy castings, the following experiments were devised in order to form fine grained material from a cast structure.

In order to achieve finer grain size, arc melted columnar grain Mod PWA 1058 was compressively deformed under various conditions above the γ' solvus temperature, $T\gamma'$, where it has previously been shown during this study that this structure is formable, but not superplastically due to its inherent large grain size. During this high temperature deformation the temperature was reduced to below $T\gamma'$ with the desire of locking in a fine grain size that would be deform-able superplastically. A summary of these experiments is given in Table 3-2 where T_i is the initial deformation temperature ($T_i > T\gamma'$), T_f is the final deformation temperature ($T_f < T\gamma'$), $\dot{\epsilon}_i$ is the true strain rate, ϵ_i is the strain to which the specimen was deformed at $T > T\gamma'$, ϵ_f is the cumulative true strain to which the specimen was deformed prior to the m determination and m is the strain rate sensitivity parameter defined previously. Specimens T/308, 311 and 324 were deformed initially at 1204°C (2200°F, $T\gamma'$ +40°F) to high strains at varying initial strain rates, $\dot{\epsilon}_i$, in order to achieve a homogeneously deformed structure with various grain sizes. During deformation the temperature was dropped to 1149°C (2100°F, $T\gamma'$ -60°F) and m determined immediately. It can be seen that initial strain rate, $\dot{\epsilon}_i$, only marginally affected the strain rate sensitivity parameter below the γ' solvus temperature where the formability was always below superplastic limits. Table 3-2 shows that greater deformation rates above the γ' solvus, $\dot{\epsilon}_i$ increase the strain rate sensitivity parameter. This indirectly points to a decrease in steady state grain size above $T\gamma'$ with increasing strain rate, confirming metallographic results. To study the effects of T_f on the formability of cast alloys, specimens T/312 and T/313 were tested in compression at a true strain rate of 3% min^{-1} at 1204°C (2200°F) to a true strain of 48%, cooled, resquared and tested again at T_f = 1127°C (2060°F, $T\gamma'$- 100°F) and 1071°C (1960°F, $T\gamma'$ -200°F). No effect of T_f was observed in the strain rate sensitivity parameter which was constant at m = 0.160.

A slow temperature cool during forming from $T\gamma'$ +20°F to $T\gamma'$ -20°F was con-ducted on specimen T/315 after deformation at $\dot{\epsilon}_i$ = 10% min^{-1} to ϵ_i = 30%. The slow cool down was completed during deformation at a true strain of ϵ_f = 50% at which time m was determined to be .207, the highest value achieved below the γ' solvus temperature.

It has previously been shown that slow to moderate rates of deformation above $T\gamma'$ result in grain sizes too large to be formable under superplastic conditions. By forming below the γ' solvus temperature and then heating with final deformation occurring above $T\gamma'$, the deformation process may store a

sufficient amount of strain energy in the material to reduce the grain size so that superplastic deformation may occur. To conduct this experiment, specimen T/323 was initially deformed at $T_\gamma' +11°C$ ($T_\gamma' +20°F$) to $\varepsilon_i = 17\%$ at $\dot{\varepsilon}_i = 10\%$ min^{-1}. The temperature was then dropped to $T_\gamma' -11°C$ ($T_\gamma' -20°F$) and deformation continued to $\varepsilon_f = 34\%$ after which the temperature was again raised to T_γ' $+20°F$ and m determined to be .204 showing no increase due to the final temperature increment.

3.2.5 Dual Ramp Rate

A dual strain rate program was developed in order to form superalloys above the γ' solvus temperature. Under these forming conditions a specimen can be deformed to a predetermined strain ε' at an initial strain rate $\dot{\varepsilon}_0$. A dual ramp function then continually cycles the strain rate from $\dot{\varepsilon}_i$ to $\dot{\varepsilon}_2$ in an appropriate time ratio to yield an average strain rate $\dot{\varepsilon}_3$.

The required time ratio can be defined as:

$$\phi = \frac{\Delta t_2}{\Delta t_1} = \frac{\dot{\varepsilon}_1 - \dot{\varepsilon}_3}{\dot{\varepsilon}_3 - \dot{\varepsilon}_2} \qquad (10)$$

We can calculate Δt_1 as follows:

$$\Delta t_1 = \frac{\varepsilon'' - \varepsilon'}{n} \left[\dot{\varepsilon}_2 \phi + \dot{\varepsilon}_1 \right]^{-1} \qquad (11)$$

and the other required time interval is then computed as:

$$\Delta t_2 = \Delta t_1 \phi \qquad (12)$$

The dual strain rate is carried out to a strain ε''. This dual strain rate test is depicted in Fig. 3-42. The initial strain rate is used to develop a steady state grain size indicative of $\dot{\varepsilon}_0$ and T. The high strain rate, $\dot{\varepsilon}_1$, is used to increase the strain energy input into the alloy causing strain hardening which is followed by deformation at $\dot{\varepsilon}_2$, which will allow recovery and strain softening to occur.

A Mod 1058 specimen was tested at 1204°C using this program and the parameters $\dot{\varepsilon}_0 = 10\% \ min^{-1}$, $\dot{\varepsilon}_1 = 30\% \ min^{-1}$, $\dot{\varepsilon}_2 = 3.3\% \ min^{-1}$, $\dot{\varepsilon}_3 = 10\% \ min^{-1}$, $\varepsilon' = 30\%$ and $\varepsilon'' = 60\%$. At 47% true strain, at the maximum strain rate $\dot{\varepsilon}_1$, of 30% min^{-1}, a true stress of 31.4 MPa was required to sustain deformation. This can be compared with the constant true strain rate tests given in Fig. 3-33 where the stresses were seen to be comparable, thereby yielding no apparent benefit in terms of a reduction in grain size. No edge cracking was detected after this deformation program.

19

3.2.6 RST Processing

An initial attempt was made to prepare some material by drip melting. A vacuum induction melt was prepared by heating drop cast bars of modified IN-100 in a recrystallized Al_2O_3 crucible. A recrystallized Al_2O_3 protection tube with a 1.0 mm internal diameter served as an orifice and was held in place with high purity alumina cement. A frequency of 350 k Hz was used to heat a tantalum susceptor around the charge. Fibrous zirconia was used to separate the hot zone from the cold zone, where a water cooled copper mold was positioned. At a vacuum of 10^{-4} Torr, the mold was rapidly heated from 1300 to 1500°C. The entire melt dripped out in about 4 min. The crucible and the as-cast ingot are shown in Fig. 3-43. The copper mold was 5 cm in diameter by 10 cm in length with a 1.2 cm diameter tapered hole. The temperature rise in the copper mold was only 60°C. A ceramic shell mold with an orifice of 1.5 mm (dia.) produced about the same result.

The dendrites were extremely fine, as indicated in Fig. 3-44. The primary spacing at the center is consistent with a cooling rate of 10^3°C/s. This had been estimated previously in Table 2-1 for a structure similar to a drop casting. The dendrite size did not vary markedly with location in the ingot from bottom to center. The ingots did not appear to have surface connected porosity, so an attempt was made to Hot Isostatically Press (HIP) one without "canning". The conditions used were 1120°C/100 MPa/2 hr. The resulting microstructures are shown in Fig. 3-45. The as-HIP grain size is 0.3 mm; that is to be compared with an initial grain size in the columnar grained homogenized arc melted buttons of 5 mm x 0.5 mm dia. In fact, the initial grain size will now be comparable to that obtained after forming of the arc melted buttons above the solvus temperature. Careful metallographic examination showed the lack of any trace of dendrites through most of the ingot and a small bit of residual porosity. Apparently this was surface connected. The "canning" approach (evacuated and degassed stainless steel) was successfully used for a second ingot, where the HIP conditions used were 1200°C/103 MPa/3 hr.

A considerable effort was made to assess the formability of the drip melted product. The temperature strain rate combinations attempted are shown in Fig. 3-46. The temperatures range from 1175 to 1200°C and the strain rates attempted were 0.05% s^{-1} to 15% s^{-1}. None of these specimens were cracked externally, but internal flaws were noted in all but the 1175°C case. (This was quite repeatable.) This is not considered to be a useful condition due to the lack of recrystallization, see Fig. 3-47. The initial large and nonuniform grain size is undesirable. Higher strain rates may be required to break down the initial grain structure.

The presence of only internal cracking can be a sign of inadequate initial breakdown. Therefore the test was repeated at 1200°C with an initial strain rate of only 1% min^{-1} (vs 3% min^{-1} previously). As shown in Fig. 3-48, after

20% engineering strain, the strain rate was stepped up to 10% min^{-1}, and again after an engineering strain of 40% had been reached, the strain rate was jumped to 100% min^{-1}. The specimen showed no signs of internal or external cracking.

The grain size is shown in Fig. 3-49 to be unremarkable (50-100μm). The flow stress data of Fig. 3-48 are entirely consistent with Fig. 3-30. The drip cast material behaves the same as the arc melted buttons. Both can be formed above the solvus, if one is careful about initial breakdown. The stress requirements are close to, but not quite representative of superplastic behavior.

These ingots appeared to be reasonably sound in about 50% of the attempts to drip melt. Most of the problems could be avoided by slight modifications in the process. Further experimentation is required to find the optimum combination of parameters to assure a reproducible process. The most significant problem seems to be a nonuniformity in as-cast grain size. This is due to a lack of a constant fill rate, which in turn is dependent upon heating rate, changes in metallostatic head pressure and the geometry relationship between orifice and chill mold. Other processes, such as the use of a uniformly heated melt, dripping from an arc melt, or LPPS should also be investigated as alternatives to transient drip melting.

A rapid solidification technique that will yield a low oxygen content alloy is the Droplet In-Situ Collection (DISC) process, developed under UTRC internal funds. The DISC process is carried out in vacuum at 10^{-4} to 10^{-5} Torr. A reasonably sound centerless ground bar of feedstock is held in a variable speed motor (up to 40,000 RPM) and heated from above by an electron beam. As the top layer becomes liquid, a fine spray of liquid droplets is generated. These are collected on a metallic ring, e.g. copper. A rapidly cooled deposit is formed with >95% collection efficiency and $\geq$95% of theoretical density. It is estimated that the splats cool at least at 10^{4}°C/s. The material can easily be canned in vacuum and consolidated by HIP. Two DISC specimens of Mod 1058 were produced under internal funding and HIP'd at 1204°C (2200°F) for 2 hrs at 105 MPa (15 ksi) pressure. These specimens were deformed in compression to determine the strain rate sensitivity exponent. Specimen T/306 was tested at 1204°C, 20°C above Tγ' while specimen T/307 was tested at 1180°C, the γ' solvus temperature. The former yielded m = 0.2 with no observed surface cracks while the latter gave m = 0.17 with severe surface cracking. Figure 3-50 shows a cross section of a DISC ring having a grain size of ~0.5 mm after HIP. The supersolvus specimen is shown in cross section after deformation in Fig. 3-51. The cracking observed in the sample deformed at the γ' solvus temperature was indicative of its relatively large grain size. The specimen deformed above the solvus showed no signs of cracking and showed excellent formability, although not in a superplastic mode.

3.3 Dynamic Recrystallization: P/M and Cast Alloy Comparison

It has been shown both here and by other investigators (Refs. 19-22) that superplastic deformation in Ni-base superalloys occurs by a dynamic recrystallization process in which the steady state grain size is a function of temperature

and true strain rate. Before a steady state grain size is achieved the flow stress goes through a transient phase either at higher or lower levels than the steady state case at which time the grain size is changing in the approach to a steady state condition. Since appreciable deformation occurs during the transient phase, the initiation mechanism of recrystallization becomes the critical step. If the initiation mechanism is understood, the deformation process can be modified to the material requirements.

Study of the recrystallization process was carried out in two separate experiments. Mod PWA 1058 was arc melted into buttons and solidified into columnar grains. Specimens .51 x .51 x 1.02 cm (.2 x .2 x .4") were cut with their length parallel to the columnar grain structure. The material was homogenized and compressively deformed at a true strain rate of 5×10^{-3} % sec^{-1} to true strains of 2, 5, 10 and 15% at T_γ' +22°C (+40°F). Another set of identical specimens was deformed at the same temperature at strain rates of .035, .25 and 1.25 sec^{-1} to a true strain of 5% which resulted in the test matrix given in Table 3-3.

Macroscopic photographs of the compression specimens T/316 through T/319 are given in Fig. 3-52. This figure illustrates the initial grain size changes with true strain in a cast structure. At 2% strain no change has occurred in the grain structure from the as-cast and homogenized case. The strain energy to this point has been absorbed by the grains or relieved by recovery processes. The onset of recrystallization has begun at 5% strain as shown in Fig. 3-52b. The large grain to one side of the micrograph is an example of strain annealing to produce very large crystals. This is a well known effect in which rapid grain growth resulting from a few widely separated nucleation sites occurs. During deformation these large grains would not be expected to occur since continued deformation would nucleate more recrystallization events and a competitive process should initiate. In this case, however, deformation was stopped at temperature before cooling commenced which allowed ample time for this type of rapid grain growth.

Figure 3-52c illustrates continued strain anneal effects at ϵ = 10% with one crystal dominating half of the test specimens. Note that this crystal appears to be twin free. The remaining grain structure shows refinement when compared to Fig. 3-52a and is approaching an equiaxed state. Many smaller grains containing annealing twins are observed in Fig. 3-52d and the grain structure is seen to be nearly equiaxed in nature at ϵ = 15%.

The results of these experiments have shown that the recrystallization event first occurs at strains between 2 and 5% for a strain rate of 0.005 % sec^{-1}. At .17% s^{-1}, it had previously been assumed that recrystallization set in at about 10% strain as indicated by a noticeable drop in true stress. At approximately 15% strain an equiaxed structure is formed from the original columnar structure.

The onset of recrystallization should be a function of true strain rate since recrystallization will occur when the strain energy imparted into the grains accumulates to a critical stored energy. The stored energy will then be the difference between the strain energy input rate minus the recovery rate integrated over the time of deformation. If it is assumed that the recovery rate at appreciable strains is constant with constant temperature, the stored energy input rate is directly proportional to the strain rate for a perfectly plastic material of which this is an excellent example. One may then conclude that recrystallization will be enhanced at higher strain rates.

Figure 3-53 illustrates the recrystallization effect as a function of strain rate at a constant deformed strain of 5%. The strain rate as shown here has a second order effect on grain size and recrystallization with respect to strain. (This study did show finer g.s. at higher $\dot{\varepsilon}$ at high ε levels, see Figs. 3-31 - 3-32). Close examination of Fig. 3-53 reveals that the columnar grain boundaries become more irregular with increasing strain rate. This is shown more clearly in Fig. 3-54 in which specimen T/322 is shown at a greater magnification. Since recrystallization is expected to nucleate at slip band-grain boundary intersections these grain boundary irregularities are expected to be nucleation sites. It should be pointed out that during the course of these tests, the specimens deformed at lower strain rates were kept at temperature for longer periods of time, therefore allowing rapid grain growth to occur. This explains the lack of large strain annealed grains in the higher strain rate specimens, namely T/320, 321 and 322.

To understand the mechanisms which lead to recrystallization in both powder PWA 1056 and cast Mod PWA 1058 a thin foil TEM study was conducted on deformed material. The test matrix is summarized in Table 3-4. The 1056 alloy, which was shown to be formable under superplastic conditions, was deformed at 1080°C to a true strain of 60% at strain rates of 0.06, 0.6 and 6.0% sec^{-1} which have been shown from Fig. 3-16 to have strain rate sensitivity coefficients of 0.35, 0.6 and 0.4 respectively. The cast Mod 1058 alloy was formed at the same strain rates as above at $T_{\gamma}' +20°C$.

Thin foil micrographs of the 1056 alloy are given in Fig. 3-55. Two features of significance are observed immediately aside from the small grain size. These are the fine subgrain (cell) structures being developed in many of the grains denoted by the letter A and the large featureless grains showing no signs of γ' precipitation denoted as B. The misorientation of the subgrains was studied in some detail and was found to be within 10° in most cases. An example of one of these cell walls developing in specimen T/328 is given in Fig. 3-56. It was concluded that because of the wide range of subgrain misorientations and the fact that at some points it was hard to distinguish

between subgrain boundaries and grain boundaries that the recrystallization
event occurs through the constant recovery of strain energy through the accumu-
lation of dislocations in cell walls. These cell walls absorb dislocations
until their misorientation becomes so large as to make them individual grain
boundaries. The new smaller strain free grains are able to grow in size at the
expense of neighboring highly stressed grains until enough strain is accumulated
within them to form new cell walls and the process continues.

Selected area diffraction patterns (SADP) of the large featureless grains
revealed them to be γ' grains, an example of which is given in Fig.3-57. The
<001> zone SADP of Fig. 3-57a shows the characteristic (100) and (011) spots
which are extinct in random FCC alloys. Figure 3-57b illustrates a centered
dark field photo of Fig. 3-57a using a (100) spot. Referring back to Fig. 3-55
most of the observed subgrain boundaries exist between γ' and $\gamma + \gamma'$ regions or
within γ' grains alone. Since all of the deformation occurred here below the γ'
solvus it is expected that the γ' is much more deformable than the precipitation
hardened $\gamma + \gamma'$. It is therefore theorized that a significant portion of the
plastic deformation and continual recrystallization occurs in the large γ'
grains. It is also suspected that the γ' grains are continuously precipitating
and redissolving into the $\gamma + \gamma'$ grains. This is seen in Fig. 3-58 for specimen
T/328 where two $(\gamma')-(\gamma + \gamma')$ cell walls are observed. The large precipitated
γ' (A in Fig. 3-58a) is seen not to be tilted with respect to the γ matrix while
the two large islands of γ' separated by cell walls (B in Fig. 3-58a) do not
appear in the centered dark field photograph, Fig. 3-58b. Some of these struc-
tures are comparable to the results of Menzies et al. (Ref. 23).

The cast Mod 1058 alloy was never observed to deform superplastically. It
was therefore expected that its mode of deformation would be much different than
for the 1056 alloy. Formability of Mod 1058 was previously achieved above the
γ' solvus, so appreciable dislocation recovery should be expected during the
specimen cool down after the termination of the test. Figure 3-59 illustrates
the microstructure of specimens T/325 and 327. At a strain rate of 0.06 sec^{-1}
no dislocations were observed and no direct sign of deformation is apparent.
The higher strain rate, however, produced more intense slip bands which did not
anneal out. Figure 3-59b illustrates the beginnings of an intense slip band
composed of paired dislocations. This deformation mechanism should not lead to
a rapid recrystallization by cell wall formation as in the powder material.
Instead, grain boundary irregularities form at the slip-band grain boundary
intersections. Recrystallization events then nucleate at the grain boundaries.
These results substantiate the earlier speculation that a small amount of free
γ' plays a key role in the overall high strain deformation process.

3.4 Single Crystals

PWA 1444 was selected as a reasonably well understood model high strength single crystal alloy. The composition of this alloy as well as others used in this phase of the program is given in Table 3-1. The room temperature and 700°C yield behavior is shown in Fig. 3-60. Virgin material frequently shows $\sigma_{.02}$ significantly lower than $\sigma_{.2}$, evidence for preyield microstrain. Yielding is characteristically smooth at room temperature and exhibits jerky flow at 700°C. The initial objective was to impose 10% strain below the solvus temperature to avoid dynamic recrystallization and to assess the influence of the stored energy on subsequent plastic flow properties. Up to 10% strain was introduced at 1190°C without difficulty. It was observed that a slight drop in yield strength at room temperature occurred after forming, possibly due to the significantly coarsened precipitated γ'. An attempt to resolution at 1245°C could not be done reproducibly without recrystallization. Partial resolutioning at 1235°C did result in a small volume fraction of coarse γ' which prevented any recrystallization. Rapid cooling preserved the bulk of the fine secondary γ' structure and resulted in a room temperature yield strength of 1000 MPa vs a base line of 965 MPa.

It has been noted that as little as 10% prestrain before a high temperature heat treatment can lead to recrystallization in the single phase γ regions which can occur due to a temperature in excess of the bulk γ' solvus, or even the local γ' solvus temperature within the dendrite cores. These regions are lower in aluminum and titanium due to microsegregation. It may be desirable to homogenize rather than simply solutionize such alloys to generate a more nearly uniform response to high temperature heat treatment. The degree of residual microsegregation after a 4 hr solution heat treatment at 1288°C has a pronounced effect on the gamma prime particle size distribution. Increasing the time to 24 hrs almost eliminates the variable precipitate morphology, and a full 72 hrs in this tungsten bearing alloy is required to fully homogenize crystals grown at 150°C/cm and 25 cm/hr. This may be an important treatment prior to working and resolutioning for optimum strength.

Another, perhaps simpler approach for obtaining substructure strengthening in high strength superalloys was to attempt the introduction of 5 to 10% plastic strain significantly below the γ' solvus temperature. If this could be done without buckling or kinking, substructure might be introduced without significant γ' particle size coarsening, thus obviating the need for a resolutioning heat treatment and the risk of recrystallization. As indicated in Table 3-5, this approach has led to significant improvements in post formed yield strength at both 20°C and the important temperature of 595°C (typical root attachment or disk rim temperature).

These studies were carried out to 5 and 10% plastic strain at both 890 and 990°C in the three high symmetry orientations: <001>, <110> and <111>. The results are rather remarkable. Note that the base line yield strengths are reproducible to at least ±1.8%. At the 890°C condition, even 5% strain leads to a 26% improvement in <100> and a 57% increase in <111> yield strength at 595°C. The 10% strain values are again improved (except for <110>) relative to the 5 increments. In every case up to 10% strain, working led to substructure strengthening. (This had not been the case at 1190°C.) The 10% strain experiment at 890°C did result in a kink for the <111> crystal. At 890°C the hardening in <110> does not appear to be monotonic with strain.

Testing was extended to 15% prestrain in all three orientations. As indicated in Table 3-5, further strengthening occurred in <111>, almost no change in <001> and a drop (due to specimen failure) in the <011> orientation. The <111> strengthening is quite impressive with a 37% improvement in yield strength at room temperature and an 80% improvement in compressive yield strength at 595°C.

The true stress true strain characteristics of PWA 1444 are shown in Figs. 3-61 through 3-69 for the cases of <001>, <011> and <111> tested in 100°C increments from 890 to 1190°C. The flow stress increases markedly with increasing temperature for the cases of <100> and <111>, with the <011> nearly constant from 1190 to 1090°C. None of these materials is recrystallizing over this range of temperatures as shown in Fig. 3-70, and yet the true flow stress generally decreases with increasing strain from 2 to 20% true strain. It is generally accepted that this situation comes about due to the coarse nature of slip in superalloys and the large amount of damage which is typically left behind in the γ' on an active slip plane (Ref. 24). In addition, there may have been some γ' particle size coarsening during the test. The debris can be in the form of vacancies, loops, jogs, etc. and generally leads to a certain degree of disorder. The damage cannot be annealed out rapidly enough as the strain continues, and the material work softens. Apparently the same debris leads to substructure strengthening at lower temperatures such as 20 or 595°C, see Table 3-5. Apparently the γ' completely reorders on a cool to room temperature and the dislocation debris can now act to work harden, disperse slip and thereby lead to a higher flow stress.

The actual work softening rate is generally quite small. There was one case of work hardening observed at temperature, namely <111> deformed to 15% true strain at 890°C and 0.5% sec⁻¹. It turns out that this prestrain condition led to the most effective strengthening at 595°C, see Table 3-5. The <111> specimen at 890°C may have been in the transition between low temperature octahedral slip and high temperature cube slip (Ref. 25) and this could lead to significant intersecting slip and less intense shear bands and therefore isothermal work hardening rather than the usual work softening.

Table 3-1

Nominal Cast Nickel Alloy Button Chemistries
for Workability Studies (wt%)

Type	Al	Ti	Cr	Co	Mo	V	Zr	C	B	W	Cb	Hf
U-700	4.3	3.3	15	18.5	5.0	-	-	0.07	0.03	-	-	-
1056 or 1058	5.0	4.3	12	18.0	3.2	0.8	0.06	0.07	0.02	-	-	-
1013-1058*	4.5	3.9	13.7	17.8	4.1	-	0.03	0.07	0.015	-	-	-
Mod 1058	5.0	4.3	12.4	18.5	3.2	-	0.03	0.07	0.015	-	-	-
1444	5	2.00	9.0	-	-	-	-	0.005	-	12.0	1.0	-
Mod 1444	4-5	1.75	9.0	-	-	-	-	0.05	0.03	11.0	1.0	0.8

*Blend at 50/50 with no vanadium

Table 3-2

Summary of Grain Refinement Experiments in
a Cast Nickel-Base Superalloy

Spec. No.	T_i (°C, °F)	$\dot{\varepsilon}_i$ (%min^{-1})	ε_i (%)	T_f (°C, °F)	m
T/324	1204,2200	30	60	1149,2100	.180
T/308	1204,2200	20	60	1149,2100	.157
T/311	1204,2200	15	45	1149,2100	.153
T/312	1204,2200	3	48	1127,2050	.160
T/313	1204,2200	3	48	1071,1960	.160
T/315	1193,2180	10	30	1171,2140	.207
T/323	1193,2180	10	17	{1171,2140 1193,2180}	.204

Table 3-3

Experimental Outline for Recrystallization Study
(Cast Mod PWA 1058)

Spec. No.	True Strain Rate (% sec^{-1})	True Strain (%)
T/316	0.005	2
T/317	0.005	5
T/318	0.005	10
T/319	0.005	15
T/320	0.250	5
T/321	0.035	5
T/322	12.500	5

Table 3-4

Experimental Outline for TEM Recrystallization Study
(Cast Mod PWA 1058)

Spec. No.	Materials	Strain Rate ($\%$ sec^{-1})	Temp. (°C)	m
T/325	Mod 1058	0.06	1204	0.22
T/326	Mod 1058	0.60	1204	0.22
T/327	Mod 1058	6.00	1204	0.22
T/328	1056	0.06	1080	0.35
T/329	1056	0.60	1080	0.60
T/330	1056	6.00	1080	0.40

Table 3-5

Substructure Strengthening in Hot Worked PWA 1444 Crystals

Orient.	Starting Condition* 0.2% YS (ksi)		Def. Cycle		After Deformation 0.2% YS (ksi)		YS Increase (%)	
	20°C	595°C	Strain (%)	Temp (°C)	20°C	595°C	20°C	595°C
[001]	140.6	131.3	5	990	155.2	150.4	10.4	14.5
"	138.8	131.7	10	990	160.0	154.7	15.3	17.5
"	138.1	131.6	5	890	174.9	166.0	26.6	26.1
"	143.5	136.2	10	890	187.7	177.3	30.8	30.2
"	141.3	132.0	15	890	179.4	168.4	27.0	27.6
[011]	159.8	139.5	5	990	174.5	175.0	9.2	25.4
"	159.1	137.9	10	990	169.1	172.0	6.3	24.7
"	160.2	141.1	5	890	197.6	193.5	23.3	37.1
"	157.0	136.4	10	890	177.7	179.2	13.2	31.4
"	164.2	144.2	13+	890	120.3	101.2	(-)	(-)
[111]	166.1	115.0	5	990	209.2	167.1	26.0	45.0
"	164.2	112.5	10	990	221.6	182.5	35.0	62.2
"	165.4	116.0	5	890	222.5	182.6	34.5	57.4
"	162.7	112.0	10	890	208.0	192.2	27.8	71.6
"	160.9	114.1	15	890	219.8	205.6	36.9	80.2

*1288°C/4 hr/AC + 1080°C/4 hr/AC + 870°C/32 hr/AC; Aspect Ratio = 2:1

+ test planned for 15% strain discontinued due to onset of failure

4.0 SUMMARY AND CONCLUSIONS

This was a complex research program with many facets. Formability of superalloys was evaluated for various initial grain sizes and shapes, from 1μm grain size P/M product to single crystals. The parameters investigated included preconditioning, forming temperature, strain, strain rate and strain rate sensitivity. The temperature was normally held isothermal throughout the deformation cycle with the exception of a few special experiments wherein the temperature was gradually reduced in a controlled manner during the deformation process. The strain rate was variously applied in such manner as to establish a constant engineering strain rate, true strain rate or energy input rate. Another special set of experiments was done with multiple strain rates so as to encourage recrystallization. Special attention was paid to microstructure for all deformation cycles. Microstructural analysis included optical and electron microscopy. The deformation cycles were of the upset forming variety, with and without forming dies. The compressive strain was delivered by a servohydraulic MTS system which was operated either in a data acquisition/reduction mode or in a full computer control mode.

PWA 1056 powder was shown to have a 1 to 5μm grain size which could be coarsened by a brief exposure above 1100°C. The fine grained material is super-plastic at moderate strain rates, but coarsening the grain size to 10μm drops the strain rate sensitivity by a factor of four and leads to a nonsuperplastic condition. The material responded well to strain rate changes with steady state flow typically reestablished within a few percent strain. Strain rate jumps of up to 10X were accomplished. All testing was done with ceramic rams in air. A computer controlled isothermal forming process was developed wherein the displacement rate was adjusted in a manner to hold the true strain rate a constant. A program was developed with input parameters of total strain and strain rate as well as reduced data output, e.g. true stress.

A computerized analysis for strain rate sensitivity was developed. A computer controlled method of constant energy rate forming was derived and used with excellent results in terms of reducing the tendency toward edge cracking in marginally workable situations.

A detailed strain rate sensitivity study was done for PWA 1056. Two grain sizes were studied over four decades of strain rate as a function of strain. These data indicated that the PWA 1056 material at 1080°C is superplastic over at least two decades of strain rate centered at 0.17% sec^{-1}, or 10% min^{-1} which is consistent with the commercial Gatorizing[TM] process. Closed die forming trials indicated the advantage of using a lubricant at high strains.

Several cast alloys were investigated for workability characteristics. After rapid solidification and dendritic homogenization at least four super-alloys were defined which could be upset to a true strain of -0.9 above their respective gamma prime solvus temperatures by Constant Energy Rate Forming (CERF). These alloys were significantly reduced in grain size during forming. Based on flow curves and microstructural analysis, it was concluded that the material was dynamically recrystallizing during forming (as in the case of pure Ni, Ref. 26). This was confirmed by immediate withdrawal of the specimen from the hot zone after forming and by the observed effect of increased strain rate on final grain size. The kinetics of static recrystallization are apparently sufficiently slow that it does not play a key role in the overall deformation process.

Methods were found to make rapidly cooled buttons of substantial size (1200 to 1600 g) using electron beam rather than arc melting. This allowed a 23X "scaleup" in the weight of a forming specimen. Using these large buttons, equiaxed test specimens were cut from dynamically recrystallized columnar grained alloys for the determination of post formed properties. After heat treatment to yield equivalent gamma prime particle size, the post formed properties were at least equal to those of the undeformed material. In some cases, evidence for substructure strengthening at low to intermediate temperature was found in the determination of yield strength following an upset strain of 60%.

Cast and homogenized buttons could be routinely upset 60% (true strain = -0.92 and in some cases to 90% (true strain = -2.27) above the solvus temperature without any signs of internal or external cracking. True stress/true strain analysis indicated that frictional effects were insignificant at upsets of 60% using ground Lucalox buttons as the loading faces.

Strain rate sensitivity analysis indicated that the homogenized rapidly solidified cast material had a parameter, m = 0.22, somewhat short of the 0.3 value generally accepted for superplasticity (as a minimum). This measurement, above the solvus temperature, persisted over four decades of strain rate and the cast material did not exhibit the classic three regions of strain rate sensitivity that the same material did in a consolidated P/M condition.

The recrystallized grain size of the cast and homogenized alloys was clearly shown to decrease with increasing strain rate. The flow curves and the microstructures indicated that recrystallization was initiated between 2 and 5% strain, and that a reasonably steady state grain size was reached between 15 and 30% strain. Microstructural analysis indicated that recovery played more of a role at the lower strain rates and delayed the initiation of recrystallization. A 1000X increase in strain rate decreases the grain size by less than 10X.

The greatest success in reducing the grain size of a cast material was associated with the continuous cooling of the specimen during deformation, thereby forming gamma prime precipitates to pin the grain boundaries. This reduced the grain size of a modified IN-100 alloy to $50\mu m$. However, this material was still not superplastic above or below the gamma prime solvus temperature. Dual or triple strain rate forming to attempt to encourage the production of more grain nuclei in stages did not appear to make a significant difference in ultimate grain size. Drip melting did produce a fine grain size; however, this "ballooned" during a supersolvus anneal, and the grain size was nonuniform which led to localized flow and poor workability.

Another rapid solidification technique known as Droplet In-Situ collection (DISC) was attempted to refine the initial grain size. Again these fine grains were enlarged during the hot isostatic pressing operation and led to about the same strain rate sensitivity as the cast material.

Experiments at low strain at various strain rates above the gamma prime solvus showed irregular grain boundaries due to coarse slip. The material deformed at the higher strain rates showed more irregularities. Since the initial nucleation sites for the recrystallized grains seem to be at the grain boundaries, this would give a mechanism to explain the strain rate effect on recrystallized grain size.

TEM analysis of P/M material deformed below the gamma prime solvus and the same basic alloy in the cast + homogenized condition upset formed above the solvus temperature indicated that the P/M product deformed by accommodating strain in large deformable islands of gamma prime and subboundary (cell) formation with gradual rotation into a new grain to retain an extremely fine grain size, whereas the cast material appeared to be largely strain free with an occasional slip band. The former mechanism is somewhat different than the usual grain boundary sliding accepted for most superplastic materials (Refs. 27-29), while the latter is entirely consistent with the dynamic recrystallization process.

Single crystal PWA 1444 (a modification of MAR-M200) was shown to be capable of large strain in compression (up to 20%) without recrystallization when deformed below the solvus temperature at 0.5% sec^{-1} (30% min^{-1}). These large strain flows were normally accompanied by a small amount of work softening in all orientations studied, except for the <111> at 890°C. This work softening was associated with a small amount of local disorder in the gamma prime in the vicinity of intense slip bands and some γ' coarsening. Upon cooling to room temperature or about 600°C, the dislocation debris associated with the hot working led to substructure strengthening. This strengthening was a function of

orientation and was appreciable for very low prior strains. <111> Crystals showed yield strength increases of up to 80%. The <011> appeared to be the least stable orientation from a hot working point of view, with frequent kinking or buckling. This orientation must have very coarse slip at intermediate temperature as evidenced by extremely jerky flow after yielding.

5.0 ACKNOWLEDGEMENT

6.0 REFERENCES

1. F. L. VerSnyder and R. W. Guard, Trans. ASM, 52, 485 (1960).

2. F. L. VerSnyder and M. E. Shank, Mat. Sci. Eng., 6, 213 (1970).

3. E. R. Thompson, F. D. George and E. M. Breinan, Proc. on the Conf. on In-Situ Composites, NMAB 308-2, 1972.

4. E. W. Kelley, Met. Eng. Q., 10, Feb. 1971.

5. A. R. Knott and C. H. Symonds, Metals Tech., 370, Aug. 1976.

6. J. B. Moore and R. L. Athey, Design News, 17, Jan. 1970.

7. A. F. Giamei and F. L. VerSnyder, Grain Boundaries in Engineering Materials, Claitor's, Baton Rouge, 1975.

8. J. C. Uy, Metals/Materials Today, March 1976.

9. A. F. Giamei, E. H. Kraft and F. D. Lemkey, New Trends in Materials Processing, ASM, 1976.

10. T. Z. Kattamis, J. Coughlin and M. C. Flemings, Trans. TMS-AIME, 239, 1504 (1967).

11. M. C. Flemings and R. Mehrabian, Solidification, ASM, 1971.

12. M. C. Flemings, Solidification Processing, McGraw Hill, New York, 1974.

13. A. F. Giamei and J. G. Tschinkel, Met. Trans. A, Sept. 1976.

14. C. P. Sullivan, A. F. Giamei and F. L. VerSnyder, Proc. 5th Int'l. Symp. on Special Melting, 525, Carnegie-Mellon, Pittsburgh, PA, 1975.

15. S. Fulop and H. F. McQueen, Superalloys - Processing, MCIC #72-10, 1972.

16. B. H. Kear, J. M. Oblak and W. A. Owczarski, J. Met. 24, 25 (1972).

17. J. W. Edington, Metals Technology, p 138, March 1976.

18. "Superplastic Forming of Structural Alloys", N. E. Paton and C. H. Hamilton, ed., AIME (1982).

19. J-P A. Immarigeon, G. Van Drunen and W. Wallace, Proc. 3rd Int. Conf. Superalloys, Seven Springs, p 464, Claitor's (1976).

20. J-P. A. Immarigeon and P. H. Floyd, Met. Trans., 12A, 1177 (1981).

21. R. G. Menzies, J. W. Edington and G. J. Davies, Metal Science, 210 (May 1981).

22. R. G. Menzies, G. J. Davies and J. W. Edington, Metal Science, 16, 483 (1982).

23. R. G. Menzies, G. J. Davies and J. W. Edington, Metal Science, 15 (May 1981).

24. G. R. Leverant, M. Gell and S. W. Hopkins, Mat. Sci. Eng., 8, 125 (1971).

25. E. Kuramoto and D. Pope, Acta Met., 26, 207 (1978).

26. M. J. Luton and C. M. Sellars, Acta Met., 17, 1033 (1969).

27. M. F. Ashby and R. A. Verrall, Acta Met., 21, 149 (1973).

28. J. W. Edington, Met. Trans. 13A, 703 (1982).

29. A. Arieli and A. K. Mukherjee, ibid., p 717.

7.0 PUBLICATIONS AND PRESENTATIONS FROM
AFOSR SPONSORED WORK

A presentation on the orientation dependence of creep rates was made in the Fall Meeting of TMS-AIME, Milwaukee, WI in October 1979.

A presentation of the effects of Re on superalloy deformation was made at the Fall Meeting of TMS-AIME in Milwaukee, WI in October 1979.

A paper entitled "Rhenium Effect on Creep Behavior of Ni-base Superalloys" was presented at the annual EMSA meeting in Reno, Nevada, August 1980.

The above paper was published in the Proceedings of the 38th Annual Meeting, EMSA, p 330, Claitor's Publ. Div., Baton Rouge, LA, 1980.

A paper entitled "Workability of High Strength Superalloys" was presented at the International Symposium on Superplasticity and Forming in San Diego, CA, June 20-24, 1982.

The above paper was published in the symposium proceesings "Superplastic Forming of Structural Alloys", N. E. Paton and C. H. Hamilton, eds., p 225, AIME (1982).

A manuscript entitled "Dynamic Recrystallization during Supersolvus Forming of Nickel Base Superalloys" by A. F. Giamei and D. L. Anton is being prepared for submittal to Metallurgical Transactions (A).

MASTER TEST PLAN

```
┌─────────────────────────────────────────────────────────────┐
│  INPUT      ⎧ PWA 1056 EXTRUDED BILLET                        │
│  MATERIALS  ⎨ WROUGHT U-700                                   │
│             ⎪ CAST 1056                                       │
│             ⎪ CAST U-700 + MOD. 1058                          │
│             ⎪ CAST MOD. 1058                                  │
│             ⎪ CAST MOD. 1444 – EQUIAXED OR COLUMNAR GRAIN     │
│             ⎩ CAST 1444 – SINGLE CRYSTAL                      │
└─────────────────────────────────────────────────────────────┘
        │                                    │
        ▼                                    ▼
┌────────────────────┐           ┌────────────────────┐
│  AS RECEIVED        │           │  HEAT TREATMENT     │
│  MICROSTRUCTURE     │           │                     │
└────────────────────┘           └────────────────────┘
        │                                    │
        ▼                                    ▼
┌────────────────────┐           ┌────────────────────┐
│  SOLVUS TEMPERATURE │           │  HEAT TREATED       │
│  DETERMINATION      │           │  MICROSTRUCTURE     │
└────────────────────┘           └────────────────────┘
                                             │
                                             ▼
┌────────────────────┐     ┌──────────────────────────┐     ┌──────────────────┐
│  ETCH AND PHOTOGRAPH│ ◄── │  SECTION, GRIND, HEAT     │ ──► │  REPEATED         │
│  SIDE FACES AND ENDS│     │  TREAT COMPRESSION        │     │  YIELD            │
└────────────────────┘     │  SPECIMENS                │     │  STRENGTH         │
                           └──────────────────────────┘     │  MEASUREMENT      │
                                             │               │  VS. TEMPERATURE  │
                                             ▼               └──────────────────┘
┌────────────────────┐     ┌──────────────────────────┐
│  PHOTOGRAPH         │ ◄── │  FORMING TESTS FOR        │
│  AS FORMED          │     │  SEVERAL STRAINS, STRAIN  │
└────────────────────┘     │  RATES, STRAIN RATE       │
        │                  │  CONTROL SCHEMES AND      │
        ▼                  │  TEMPERATURES             │
┌────────────────────┐     └──────────────────────────┘
│  LONGITUDINAL       │                     │
│  SECTION, ETCH AND  │                     ▼
│  PHOTOGRAPH         │     ┌──────────────────────────┐
└────────────────────┘     │  SECTION, GRIND, HEAT     │
        │                  │  TREAT FORMED SPECIMENS   │
        ▼                  └──────────────────────────┘
┌────────────────────┐                     │
│  TRANSVERSE SECTION,│                     ▼
│  POLISH, ETCH AND   │     ┌──────────────────────────┐
│  PHOTOGRAPH         │     │  REPEATED YIELD STRENGTH  │
└────────────────────┘     │  VS. TEMPERATURE OF       │
                           │  FORMED MATERIAL          │
                           └──────────────────────────┘
```

FIG. 3-2

SEM PHOTOS SHOWING GRAIN SIZE IN AS EXTRUDED PWA 1056

a)

2μm

b)

1μm

81-12-8-10
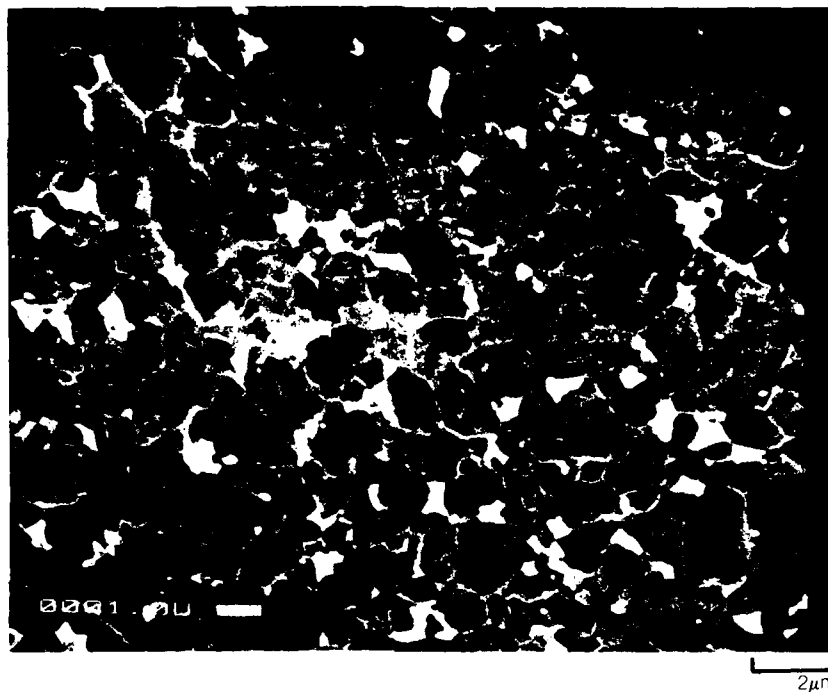
SEM PHOTOS SHOWING GRAIN SIZE IN HEAT TREATED PWA 1056

a) 1150C/4 hr/AIR COOL, 1200 C/4 hr/AIR COOL

2µm
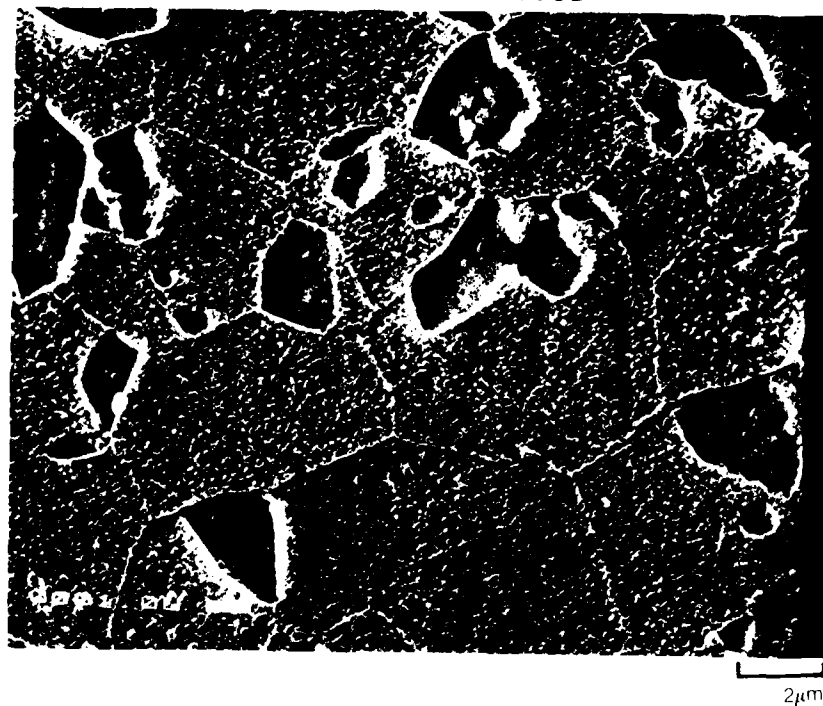
b) 1200C/4 hr/AIR COOL

2µm

81-12-8-11
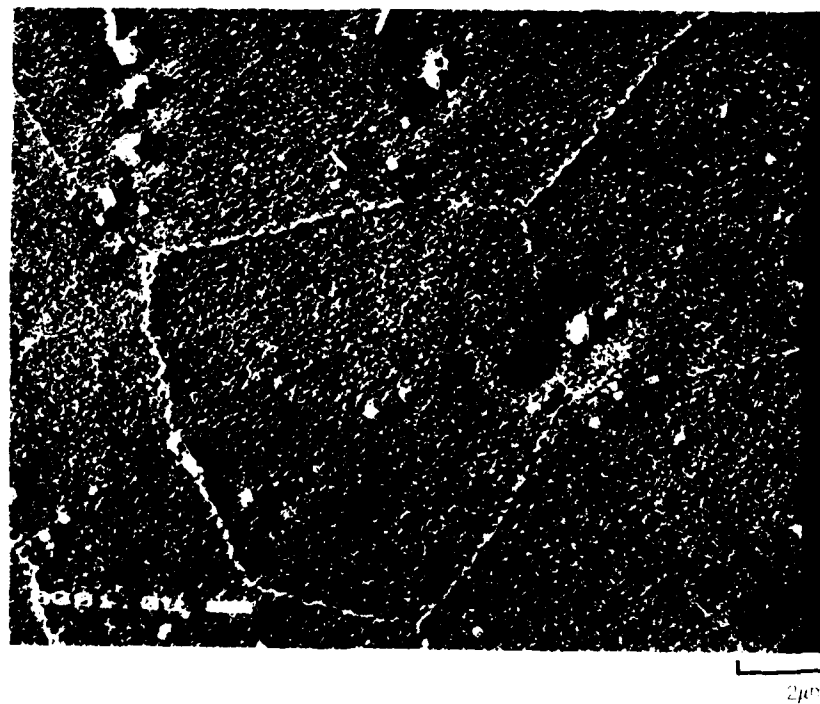
PWA 1056 — AS EXTRUDED BILLET

FORMING TEMPERATURE = 1070°C

$\dot{\epsilon}_c = 0.05\%/sec$

FIG 3-5
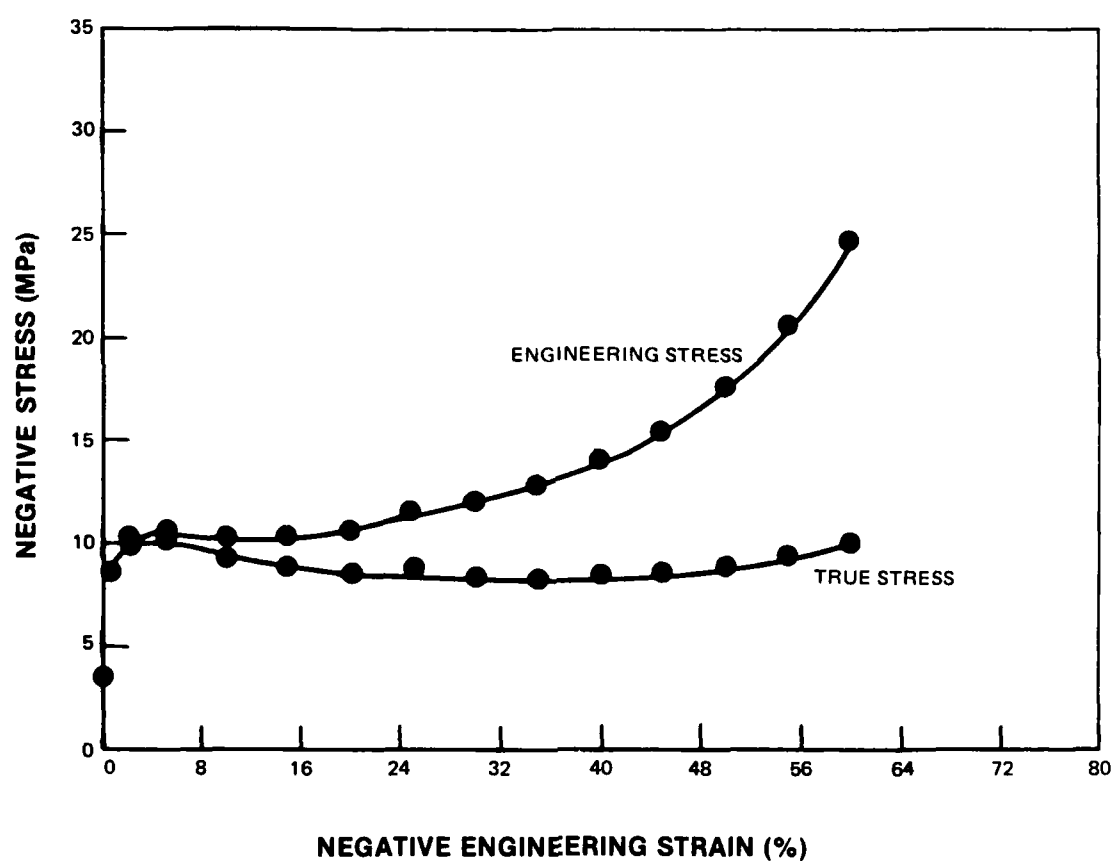
PWA 1056 — AS EXTRUDED BILLET

FORMING TEMPERATURE = 1150°C

FIG. 3-6
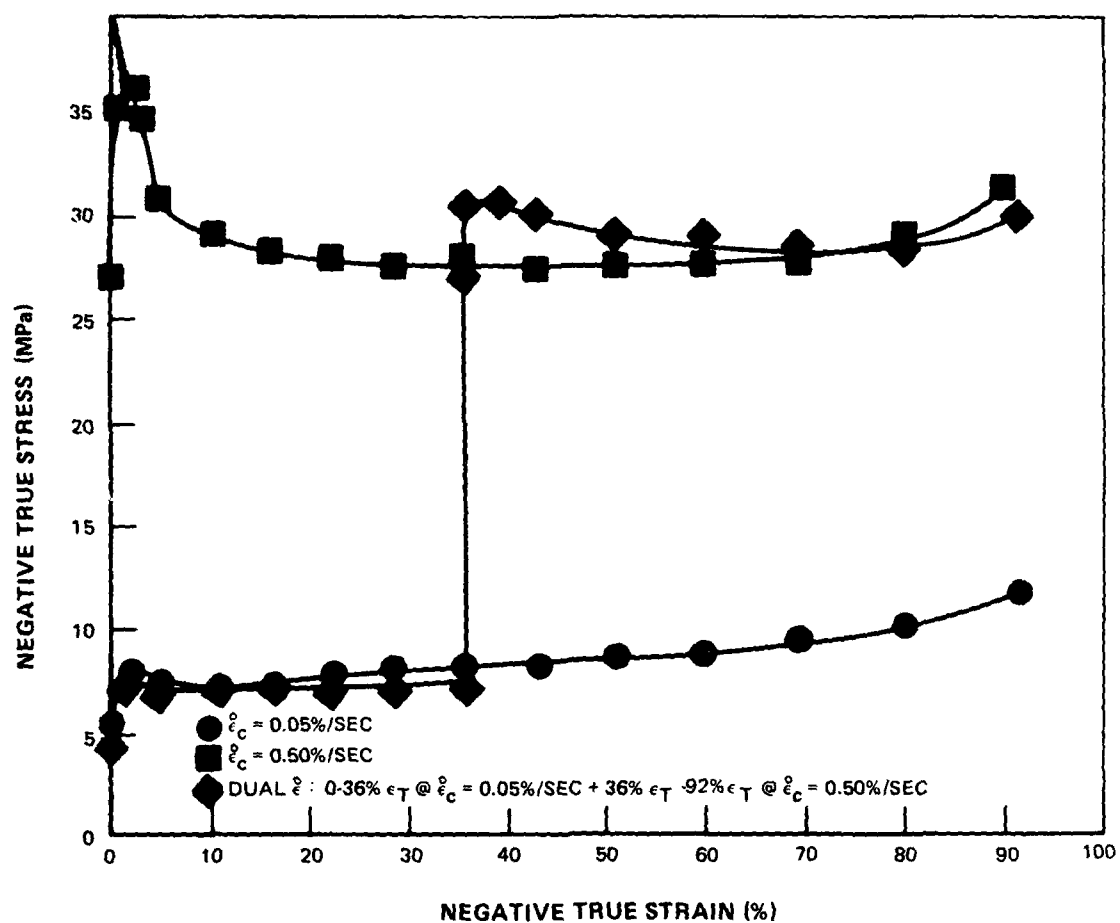
PWA 1056 — AS EXTRUDED BILLET

FORMING TEMPERATURE = 1070 °C
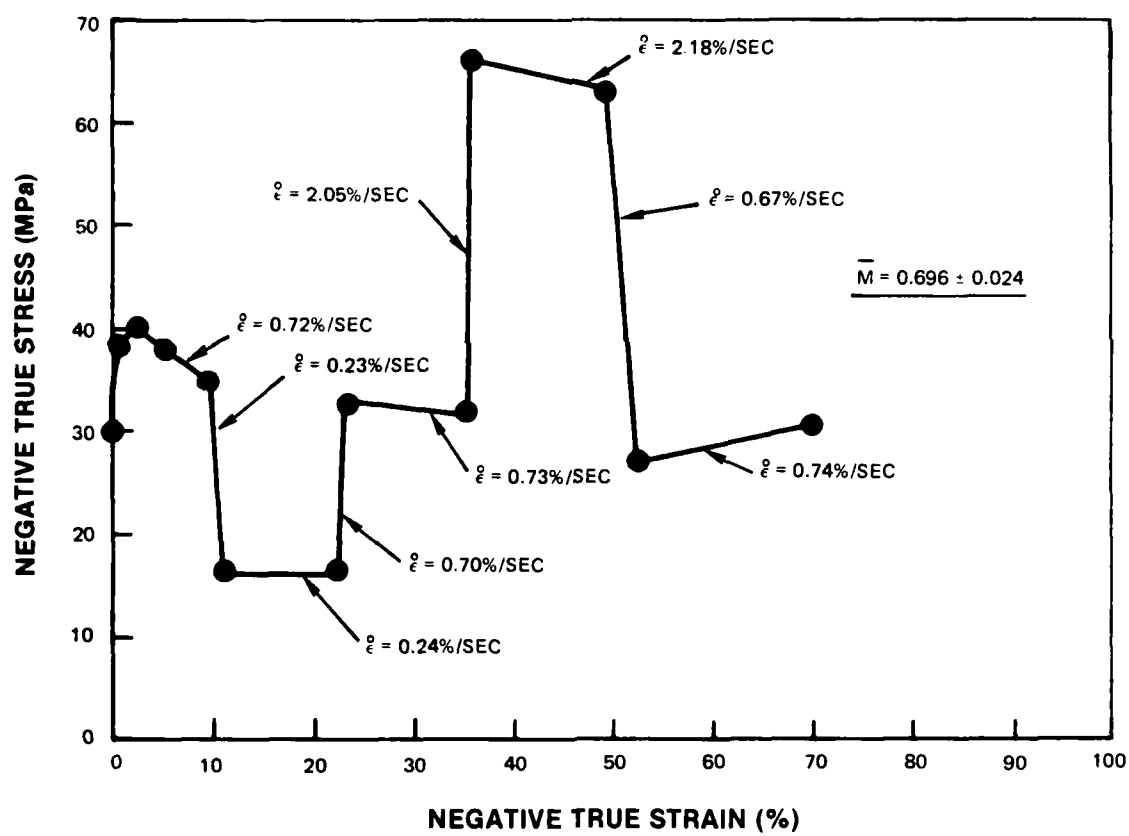
MTS PROCESS CONTROL COMPUTER OUTPUT: DETERMINATION OF STRAIN RATE SENSITIVITY PARAMETER

PWA 1055 BILLET H 1023 N 1 T/159 "M" DETERMINATION @ 1070 C

INDEX	ENG. STRAIN %	TRUE STRAIN %	STRAIN RATE %/SEC	TRUE STRESS MPa
0	0	0	.69	29.97
1	-9.28	-9.74	.72	31.74
2	-10.26	-10.83	.23	16.14
3	-19.97	-22.28	.24	15.99
4	-20.71	-23.21	.7	33.01
5	-29.81	-35.39	.73	31.56
6	-30.11	-35.83	2.05	66.1
7	-38.96	-49.37	2.18	63.21
8	-40.74	-52.33	.67	27.03
9	-50.02	-69.36	.74	30.62

INDEX	ENG. STRAIN %	TRUE STRAIN %	STRAIN RATE %/MIN	TRUE STRESS KSI
0	0	0	41.68	4.35
1	-9.28	-9.74	43.19	5.04
2	-10.26	-10.83	13.7	2.34
3	-19.97	-22.28	14.55	2.32
4	-20.71	-23.21	41.85	4.79
5	-29.81	-35.39	43.78	4.58
6	-30.11	-35.83	123.11	9.59
7	-38.96	-49.37	130.89	9.17
8	-40.74	-52.33	40.45	3.92
9	-50.02	-69.36	44.27	4.44

THE VALUE OF "M" BETWEEN -9.28 % STRAIN @ .72 %/SEC AND -10.26 % STRAIN @ .23 %/SEC IS .672

THE VALUE OF "M" BETWEEN -19.97 % STRAIN @ .24 %/SEC AND -20.71 % STRAIN @ .7 %/SEC IS .677

THE VALUE OF "M" BETWEEN -29.81 % STRAIN @ .73 %/SEC AND -30.11 % STRAIN @ 2.05 %/SEC IS .716

THE VALUE OF "M" BETWEEN -38.96 % STRAIN @ 2.18 %/SEC AND -40.74 % STRAIN @ .67 %/SEC IS .72

READY

PWA 1056 — AS EXTRUDED BILLET

FORMING TEMPERATURE = 1070°C

Chart axes:
- Y-axis: NEGATIVE TRUE STRESS (MPa), 0 to 30
- X-axis: NEGATIVE TRUE STRAIN (%), 0 to 100

60% REDUCTION IN HEIGHT

▲ CONSTANT ENERGY FORMING RATE = 0.039 MPA/SEC; $\dot{\epsilon}_o$= 0.17%/SEC

X CONSTANT DISPLACEMENT RATE = 6.84 × 10^{-4} INCH/SEC; $\dot{\epsilon}_o$= 0.17%/SEC; $\dot{\epsilon}_{60}$ = 0.42%/SEC
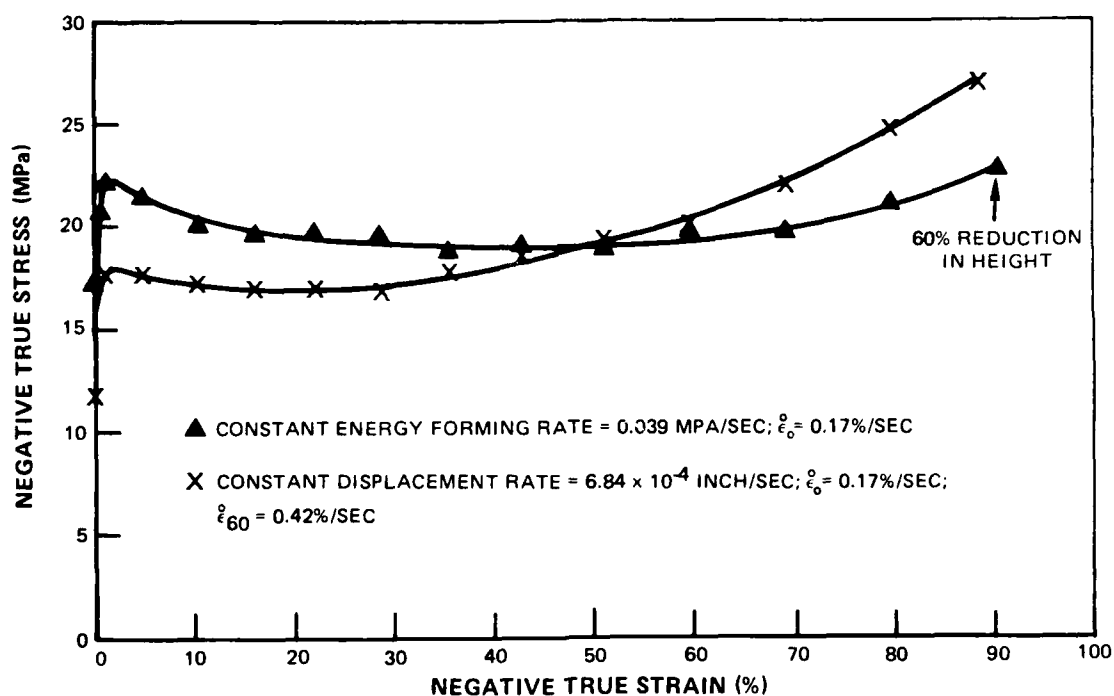
PWA 1056 — AS EXTRUDED BILLET

CONSTANT FORMING RATE = 0.5% s⁻¹
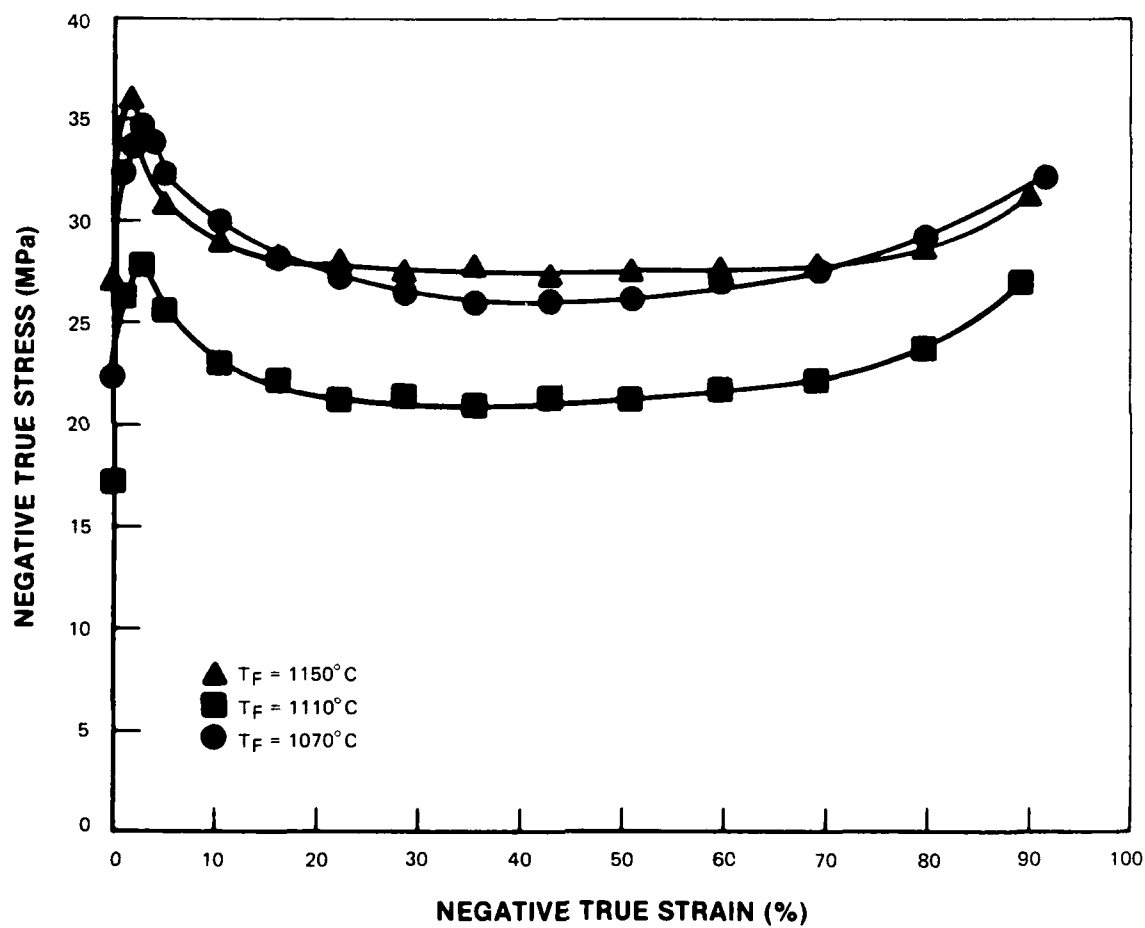
DETAILED PLAN AND EXAMPLE OF STRAIN RATE SCHEDULE FOR THE RANGE $\dot{\varepsilon} = 0.25$ TO 1.5% S^{-1}

$T_F = 1204°C$

$1204°C/24$ hr/HC

ε	0-5	5-10	10-15	15-20	20-25	25-30	30-35	35-40	40-45	45-50	50-55	55-60	(%)
$\dot{\varepsilon}$	0.7	1.5	0.25	0.5	1.0	0.35	0.7	1.5	0.25	0.5	1.0	0.35	(% S^{-1})
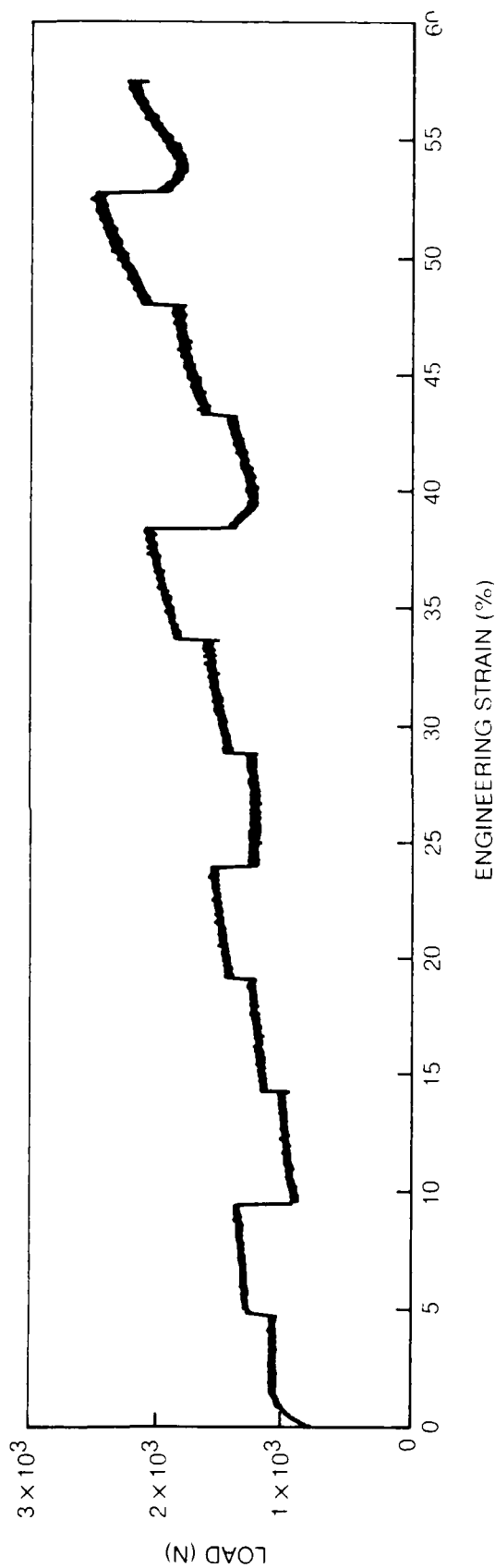
LOAD (N) vs ENGINEERING STRAIN (%)

R1-8-3-6

FIG. 3-11

Ln STRESS vs ln STRAIN RATE PLOT WITH EXTENDED STRAIN RATE RANGE FOR PWA 1056 EXTRUDED BILLET; TAKEN FOR e = 10 ± 5%

STRAIN RATE (%/sec)

STRESS (MPa)

□ AS EXTRUDED + 1150°C/4 hr/AC
○ AS EXTRUDED

FIG. 3-12

Ln STRESS vs ln STRAIN RATE PLOT WITH EXTENDED STRAIN RATE RANGE FOR PWA 1056 EXTRUDED BILLET; TAKEN FOR e = 25 ± 5%

□ AS EXTRUDED + 1150°C/4 hr/AC
O AS EXTRUDED

FIG. 3-13

Ln STRESS vs ln STRAIN RATE PLOT WITH EXTENDED STRAIN RATE RANGE FOR PWA 1056 EXTRUDED BILLET; TAKEN FOR e = 40 ± 5%

81-8-3-4

FIG. 3-14
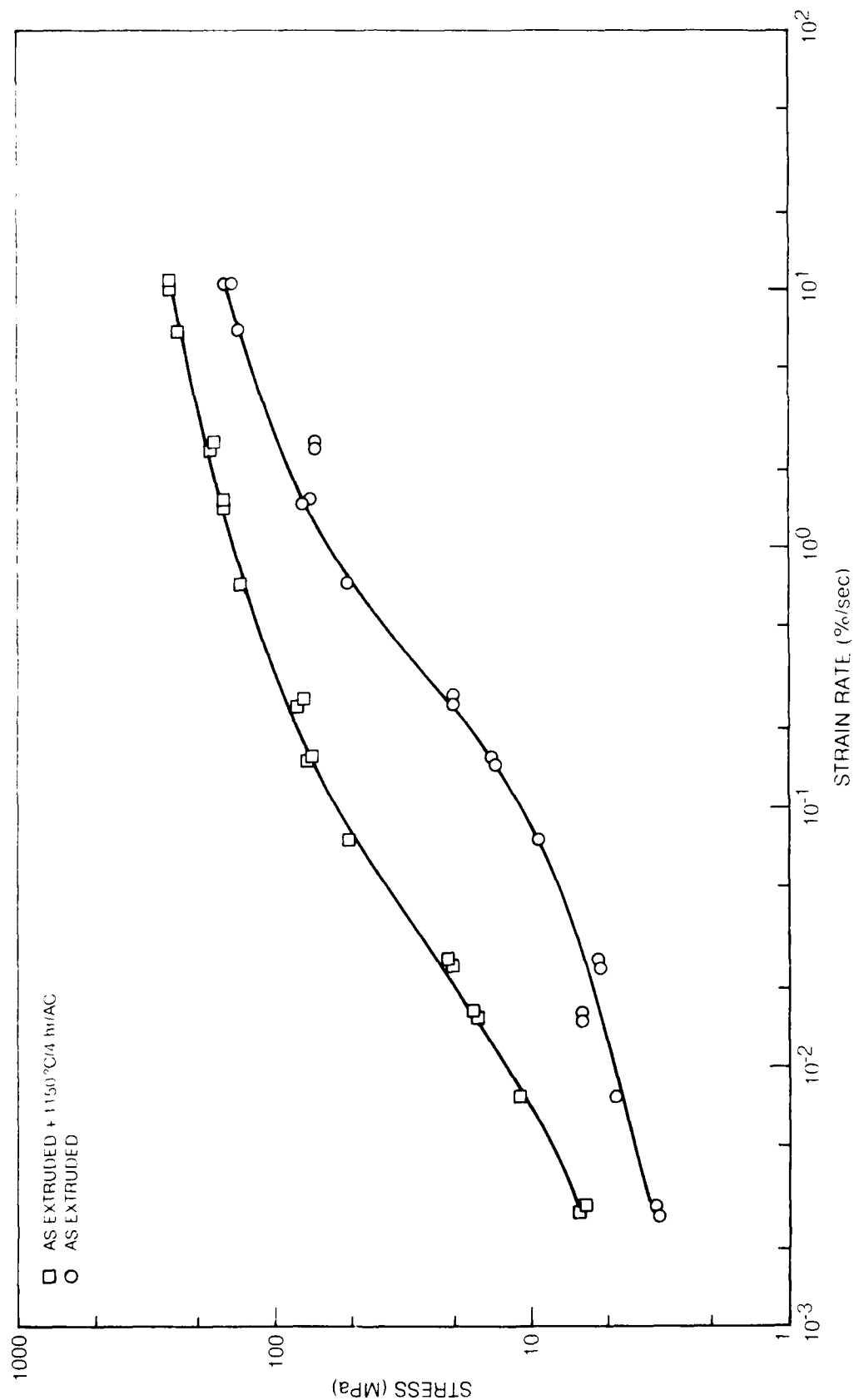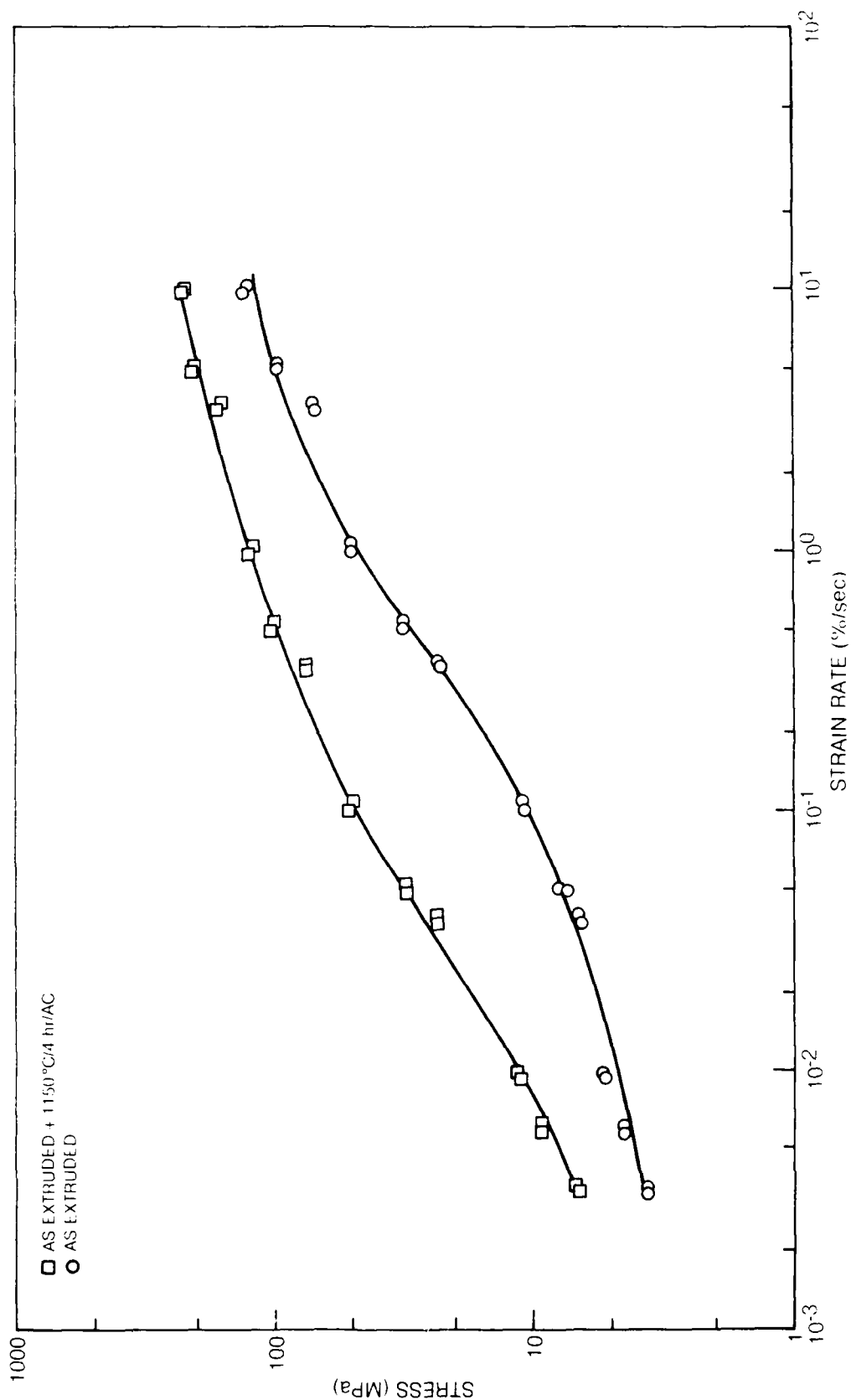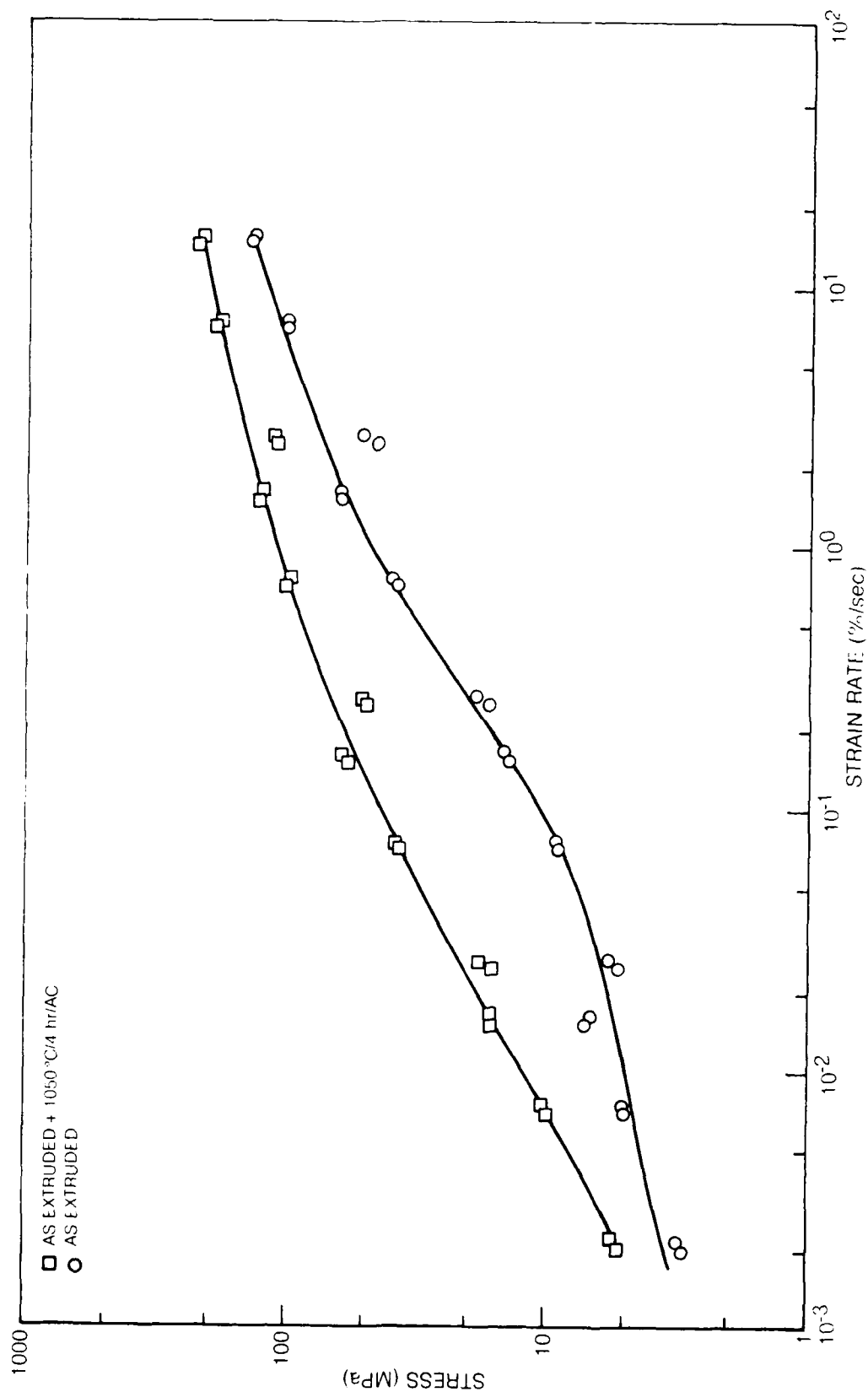
Ln STRESS vs ln STRAIN RATE PLOT WITH EXTENDED STRAIN RATE RANGE FOR PWA 1056 EXTRUDED BILLET; TAKEN FOR e = 55 ± 5%

81-8-3-5
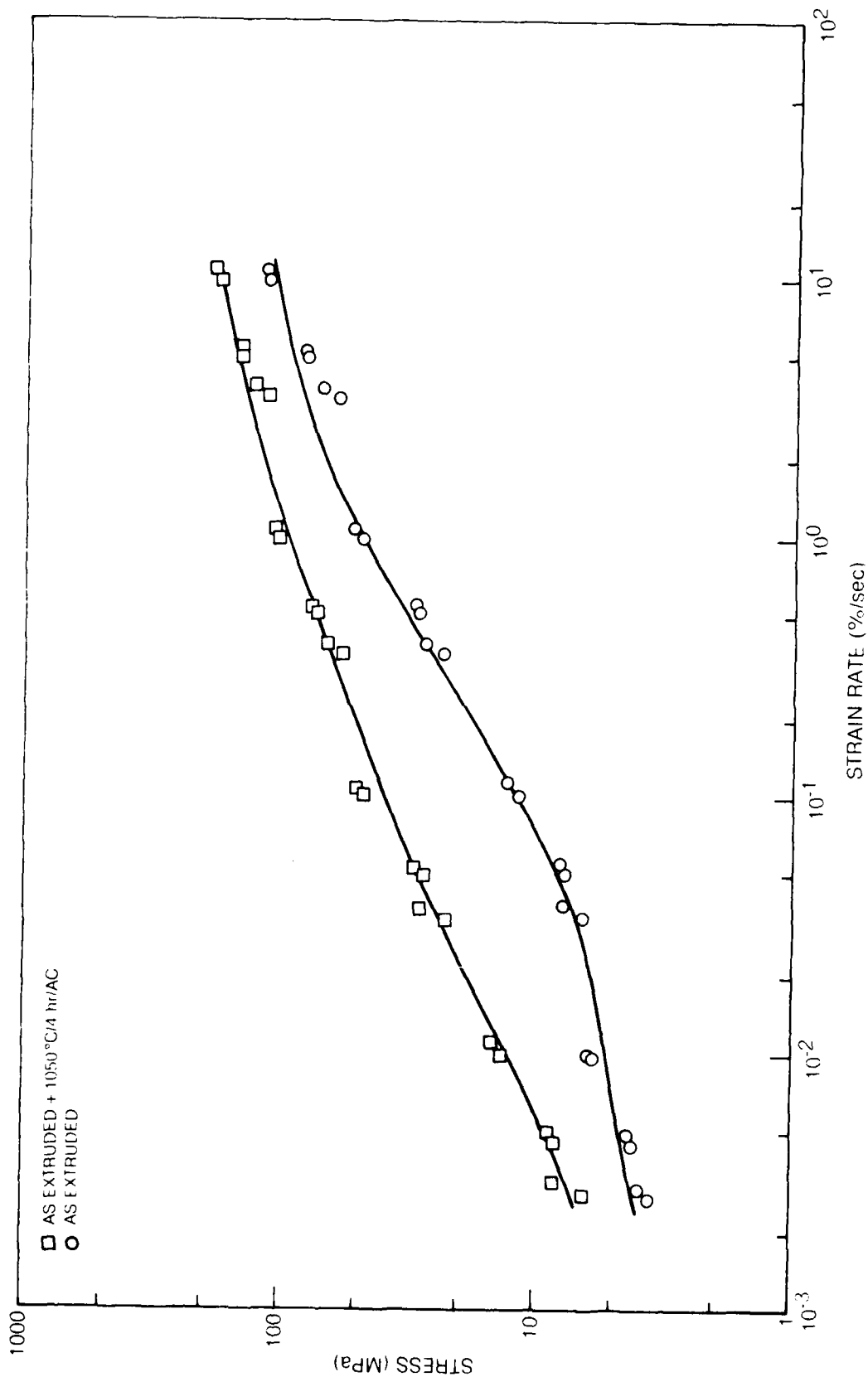
LN STRESS VS LN STRAIN RATE WITH TRUE FLOW STRESS AVERAGED AT VARIOUS STRAIN LEVELS

EXTRUDED POWDER BILLET — PWA 1046 T_F — 1080°C

AVERAGE COMPRESSIVE FLOW STRESS ($\bar{\sigma}$, MPa, 10% < e < 55%)

COMPRESSIVE STRAIN RATE ($-\dot{\epsilon}$, % sec^{-1})
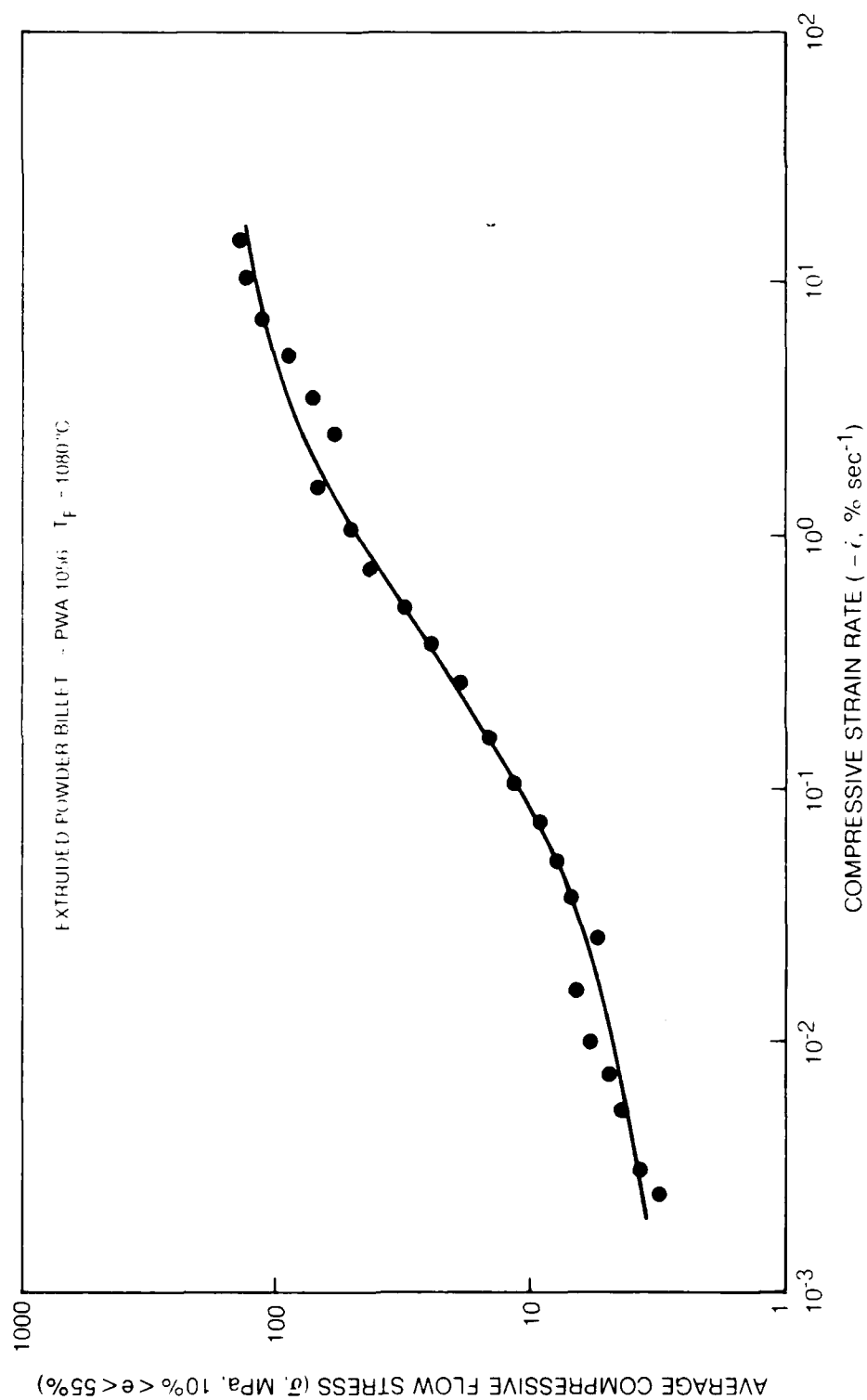
FIG. 3-16

STRAIN RATE SENSITIVITY PARAMETER, m, AS DETERMINED FROM THE SMOOTH CURVE IN FIG. 3-15 VS LN STRAIN RATE

PWA 1056 EXT POWDER BILLET   T   1080°C

81-12-8-3

FIG. 3-17
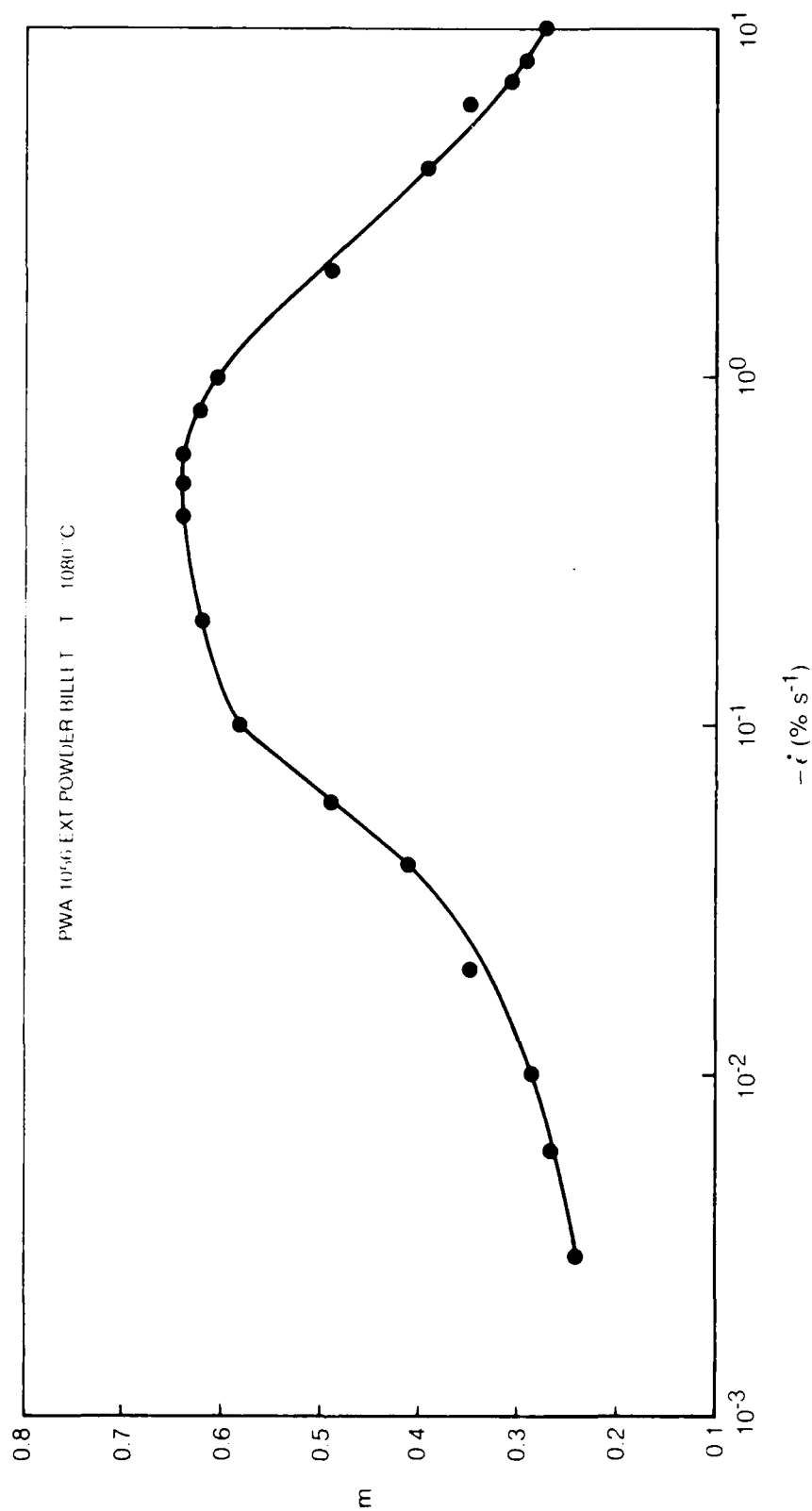
SUPERALLOY FORGING DIES

2.54 cm
(1.00 in.)

1.9 cm
(0.75 in.)

10°

1.27 cm
(0.50 in.)

0.318 cm
(0.125 in)

83-5-102-22
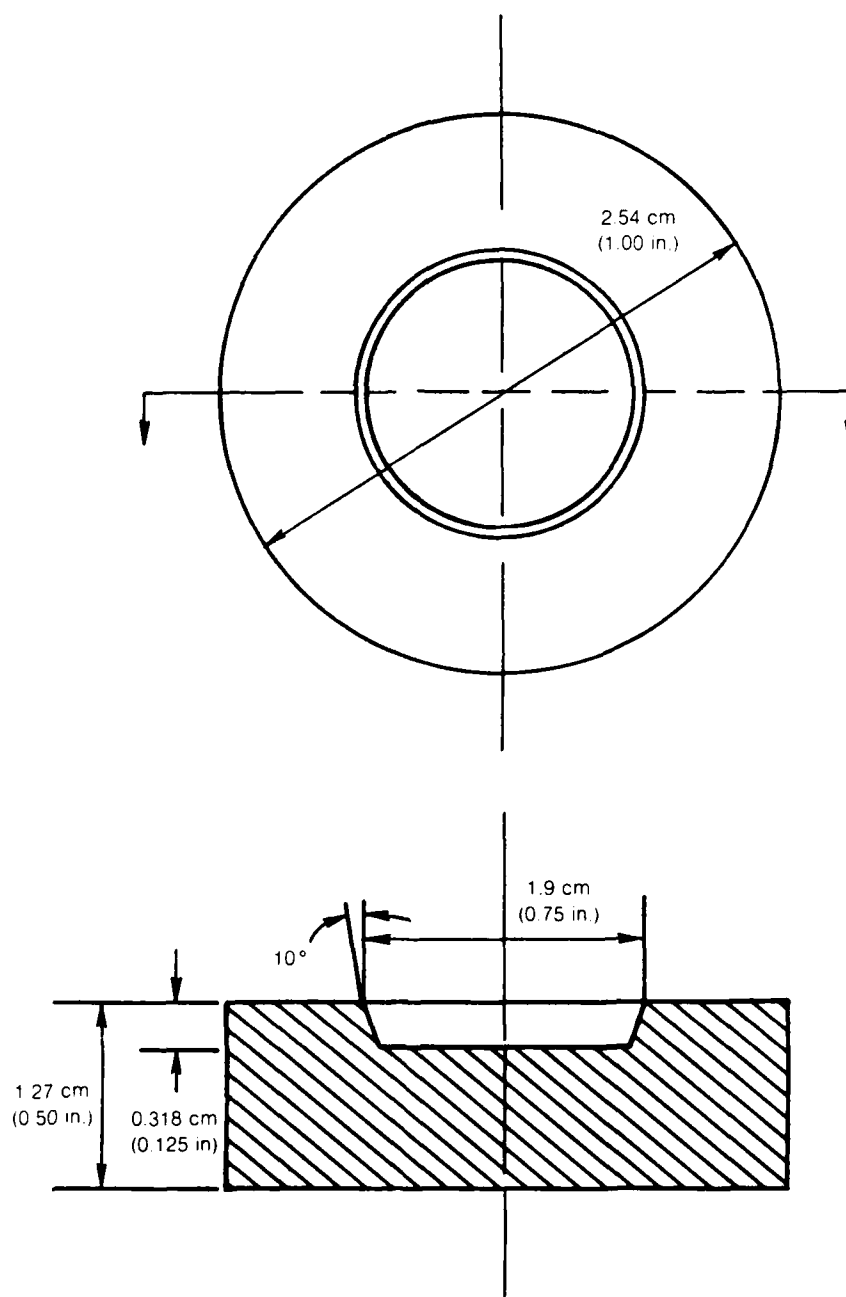
CLOSED DIE FORMING OF PWA 1056 AT 1093°C

$\dot{\epsilon} = 0.17 \, min^{-1}$

DIE FRACTURED

FIRST TEST ENDED

$-\sigma_T$ (MPa)

$-\epsilon_T$

R83-916100-1

FIG. 3-18

83-5-102-23
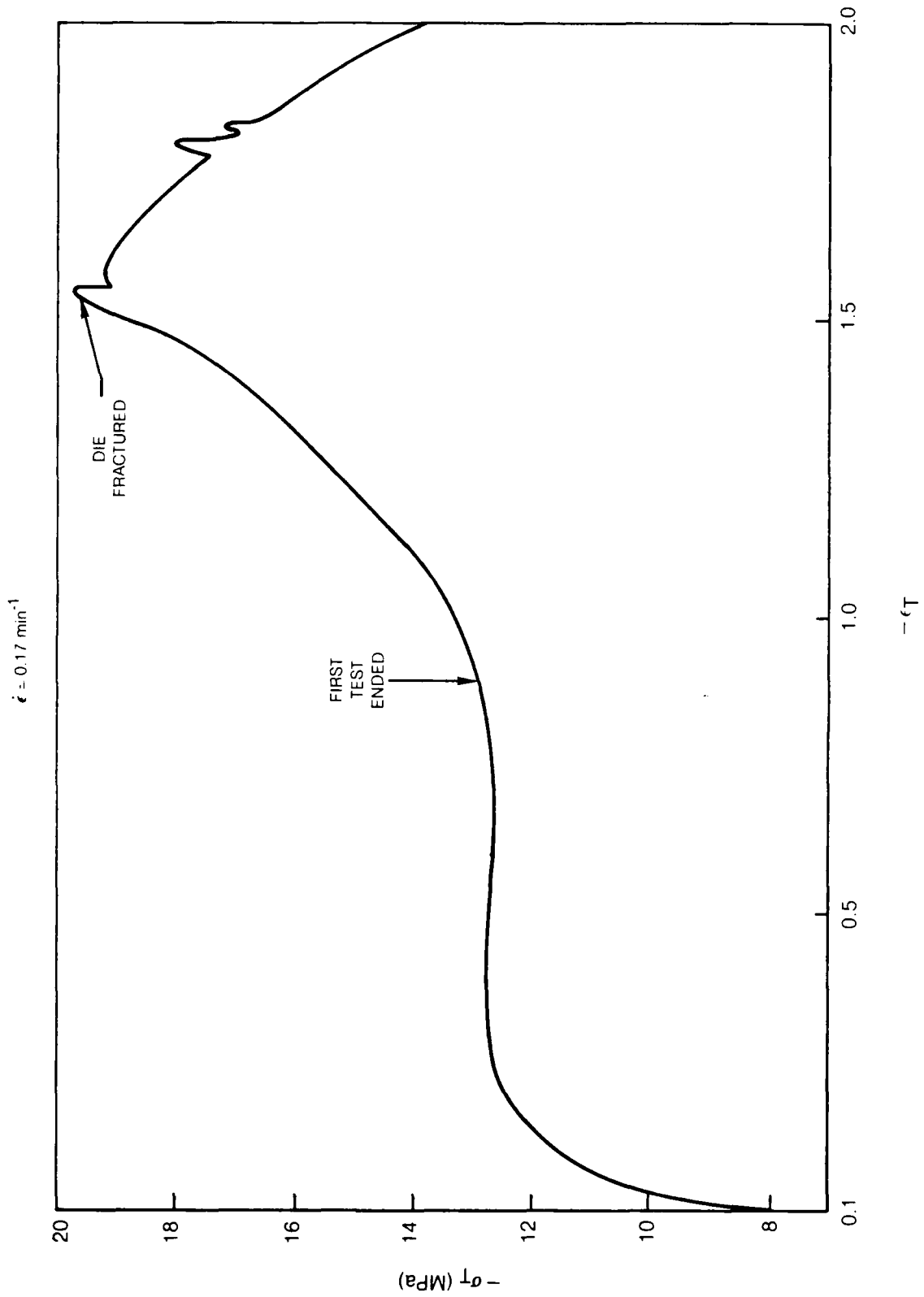
CLOSED DIE FORMED SPECIMEN

1 mm

83-5-102-31

PWA 1056 CAST BUTTON

1204 °C/24 hr FFC + 1204 °C 1 hr AC + 870 °C 32 hr AC
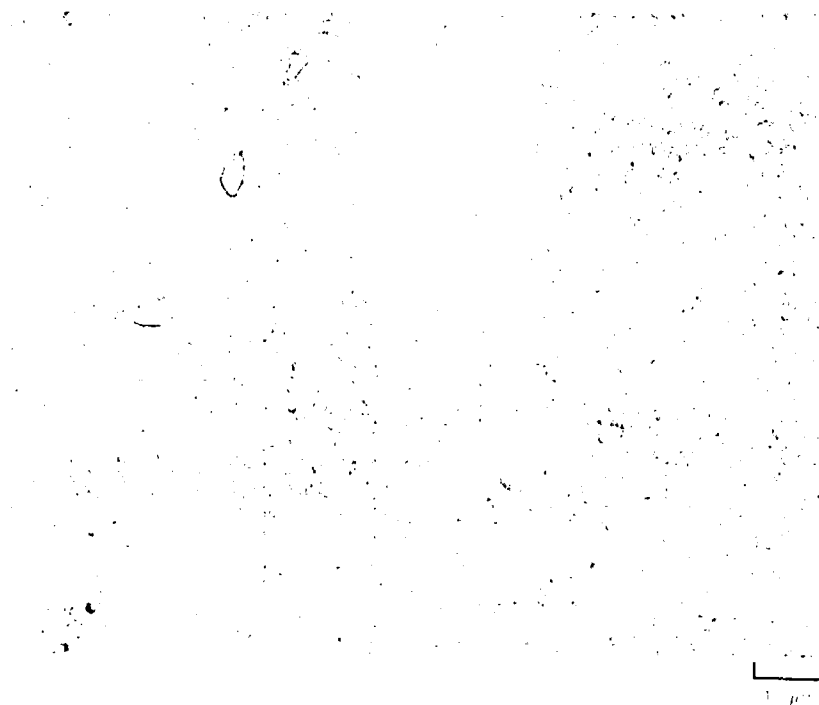
CONSTANT ENERGY RATE FORMING CURVES
HOMOGENIZED RAPIDLY COOLED BUTTONS

	TEMP °C	$\dot{E}_c$ MPa/sec
● U-700	1177	0.0166
▲ MOD 1013-1058	1204	0.0116
■ 1056 – CAST	1204	0.0115
✕ MOD 1058	1204	0.0096

83–5–102–8
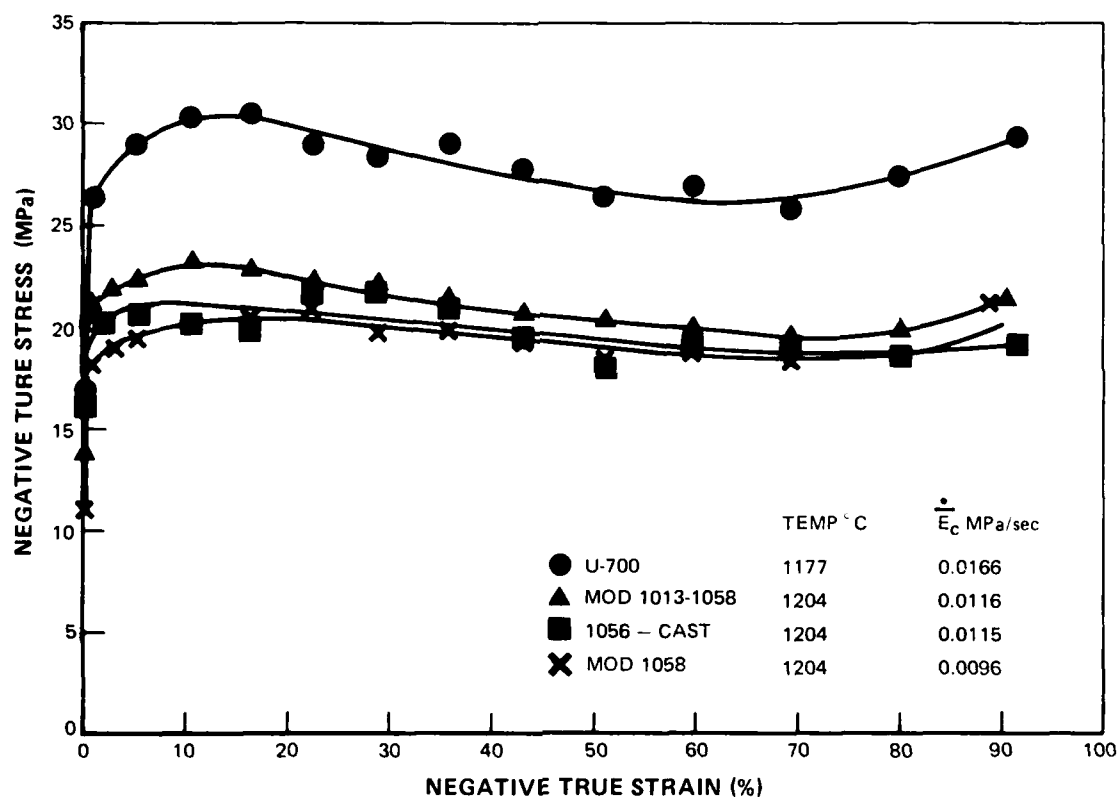
MODIFIED PWA 1058 AFTER RAPID COOLING
HOMOGENIZATION AND CONSTANT ENERGY RATE FORMING AT 1204°C AND 0.01 MPa/sec

SIDE VIEW OF
FORMING SPECIMEN.   0.13 cm
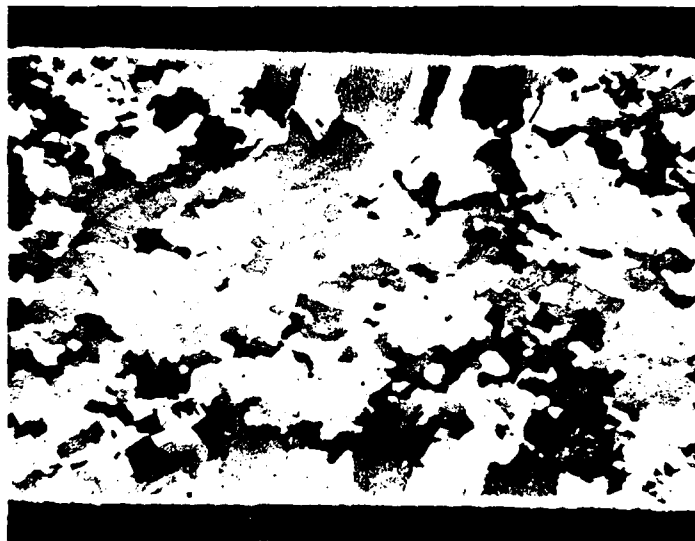
LONGITUDINAL SECTION AFTER 60%
REDUCTION IN HEIGHT.   0.08 cm
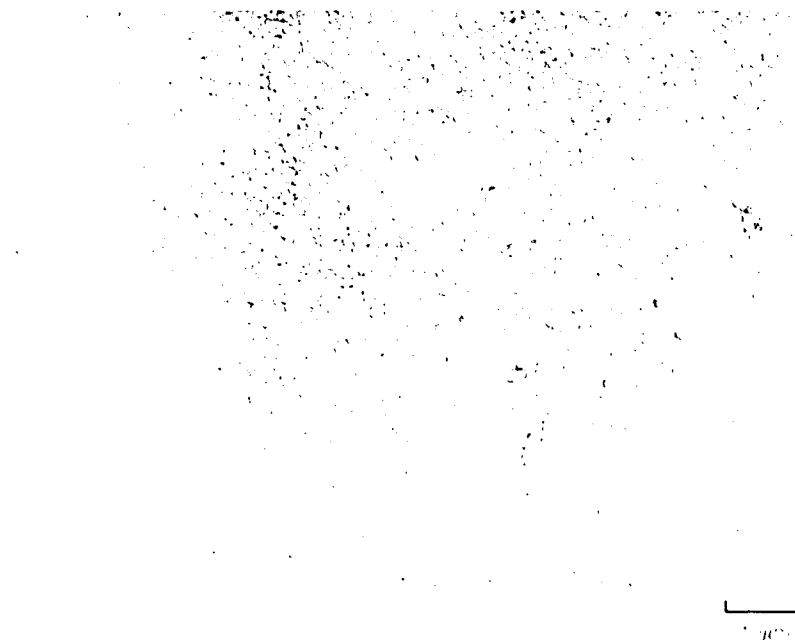
MICROSTRUCTURE FROM TRANSVERSE SECTION AFTER FORMING.

83-5-102-9

FIG. 3-23

4.5 wt% MODIFICATION OF POLYCRYSTALLINE 1444

HOMOGENIZED AT 1225°C/24 hr/FFC

FORMING TEMP.	STRAIN RATE	CONSTANT ENERGY RATE	CRACKING
● 1225°C	0.05%/SEC		MINOR
▲ 1225°C		0.0117 MPa/SEC	NONE
◆ 1235°C	0.05%/SEC		SEVERE
■ 1240°C	0.05%/SEC		MODERATE

NEGATIVE TRUE STRESS (MPa)

NEGATIVE TRUE STRAIN (%)

83-5-102-10
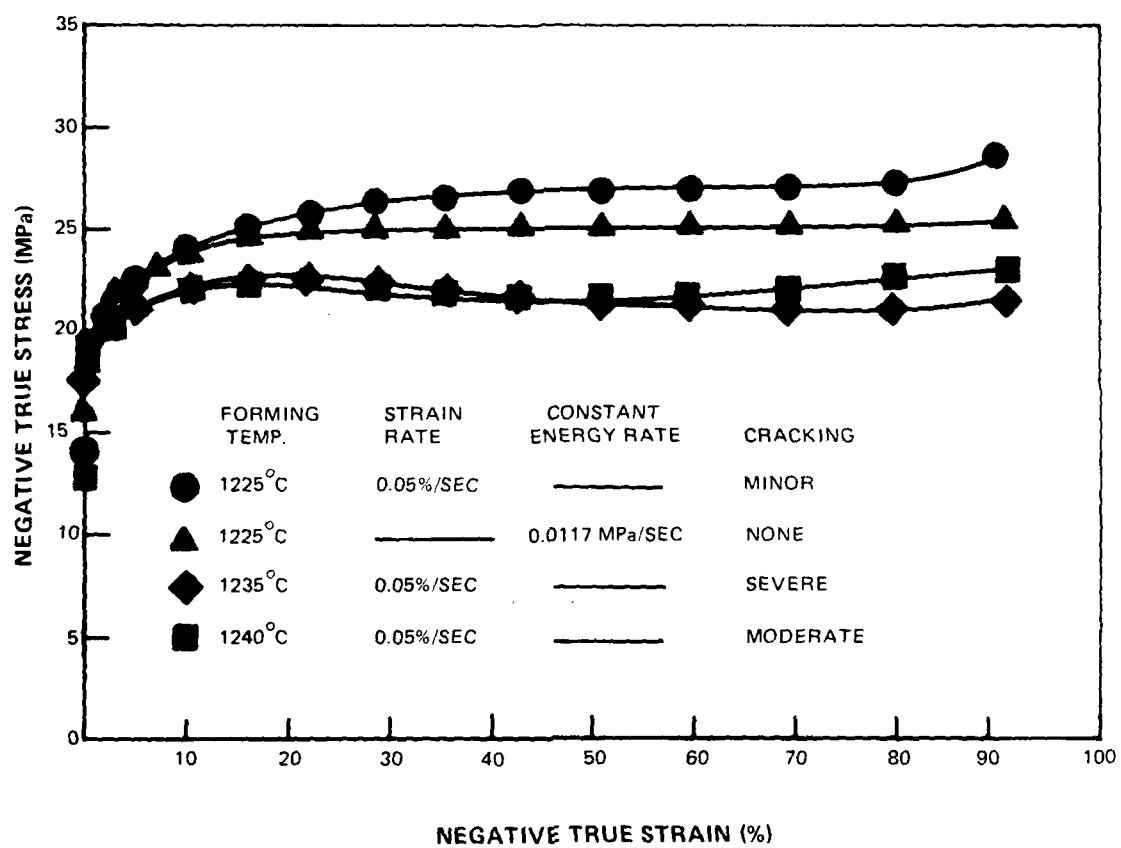
COMPRESSIVE YIELD SPECIMENS TAKEN FROM ALLOYS FORMED TO 60% REDUCTION
IN HEIGHT AT A CONSTANT TRUE STRAIN RATE OF 0.05% sec^{-1}
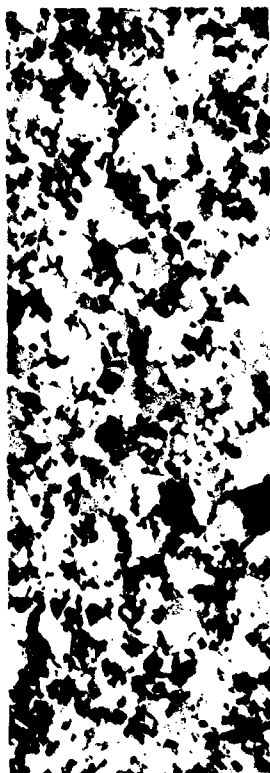
CAST U-700 HOMOGENIZED AND FORMED
AT 1177 C.

CAST MOD 1058 HOMOGENIZED AND
FORMED AT 1204 C.

83-5-102-11

YIELD STRENGTH VS TEMPERATURE FOR CAST 50/50 BLEND OF PWA 1013 AND 1058
(MINUS VANADIUM)

83-5-102-12

FIG. 3-26
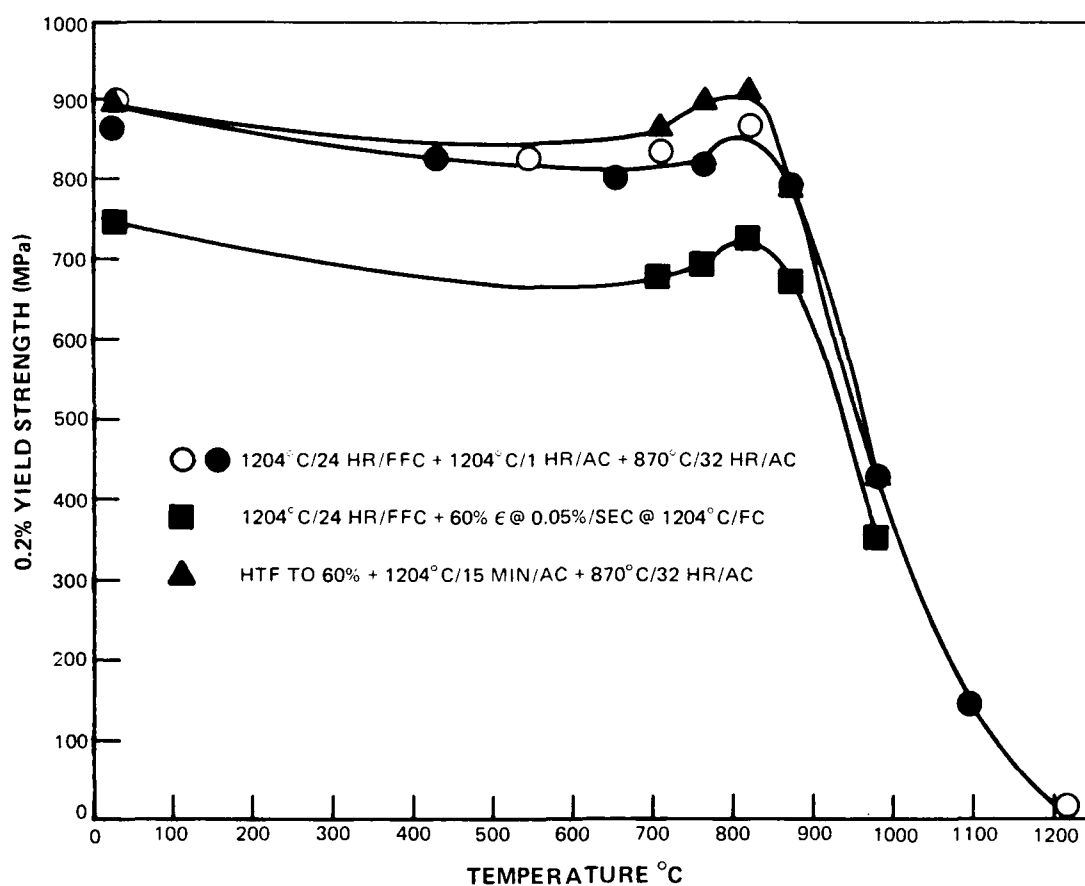
MOD 1058 70g FORMING SPECIMEN TAKEN FROM ELECTRON BEAM SKULL MELT

TOP VIEW
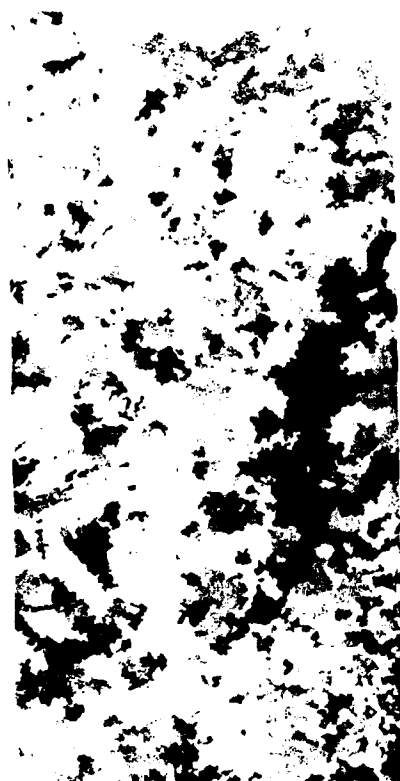
FRONT VIEW

SIDE VIEW

FIG. 3-27
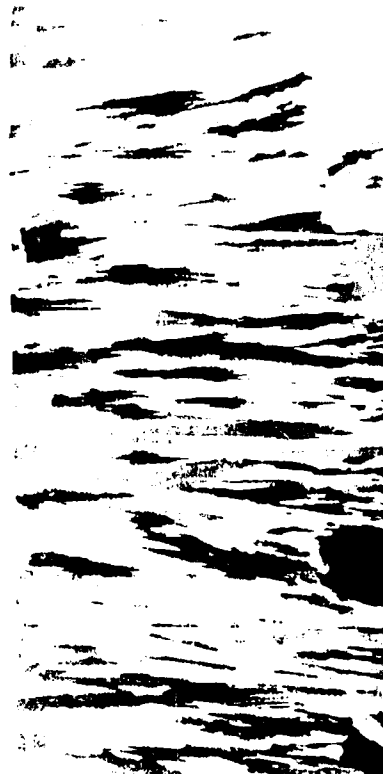
TOP EXTERNAL VIEWS OF 3, 20 AND 70g ISOTHERMALLY FORMED SPECIMENS OF CAST + HOMOGENIZED MOD 1058

FIG. 3-28

MODIFIED 1058 BUTTON AFTER 1204°/24 hr HOMOGENIZATION PLUS ISOTHERMAL FORMING TO 90% REDUCTION IN HEIGHT

CONSTANT TRUE STRAIN RATE = 0.05% sec^{-1}

AFTER   BEFORE

OBLIQUE VIEW   └─────┘
6 mm

NORMAL VIEW OF FORMED SPECIMEN └───┘

83 5 102 15

FIG. 3-29

MOD 1058 BUTTON HOMOGENIZED AT 1204°C/24 hr/FFC + ISOTHERMALLY FORMED AT 1204°C AT $\dot{\epsilon}_c = 0.05\%$/sec

83−5−102−16
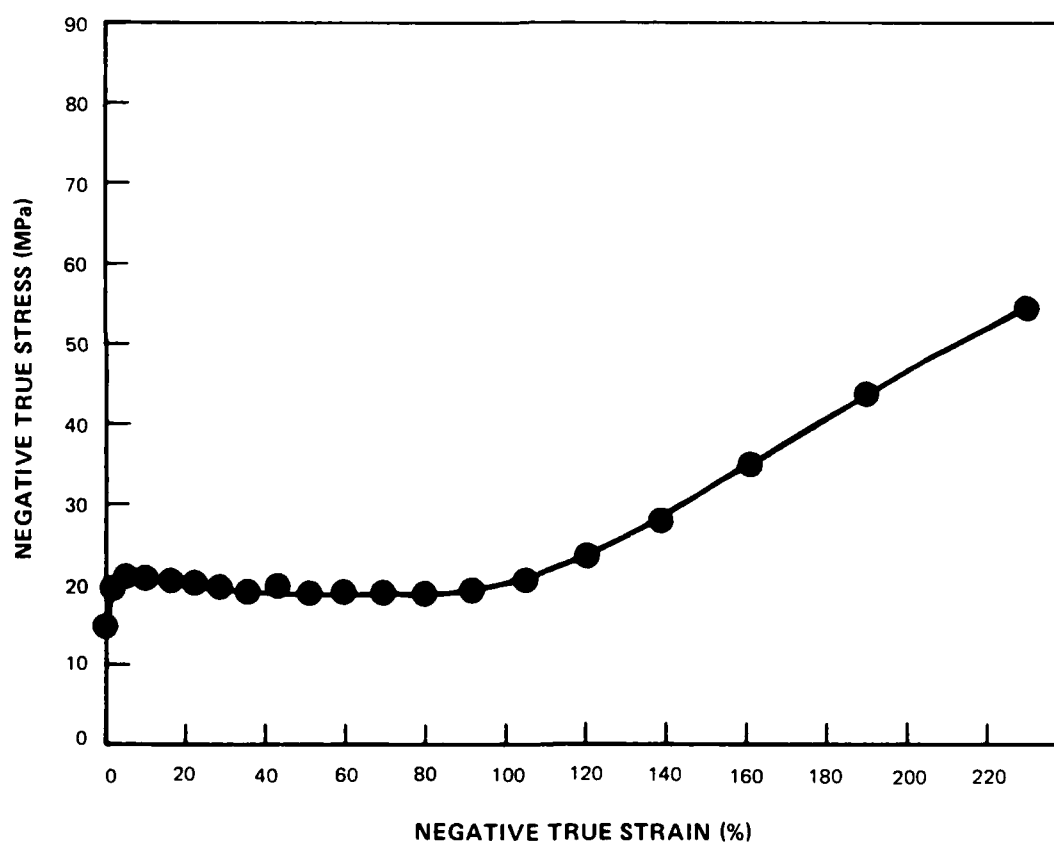
Ln STRESS vs ln STRAIN RATE PLOT WITH EXTENDED STRAIN RATE RANGE FOR MODIFIED IN100

81-8-3-7
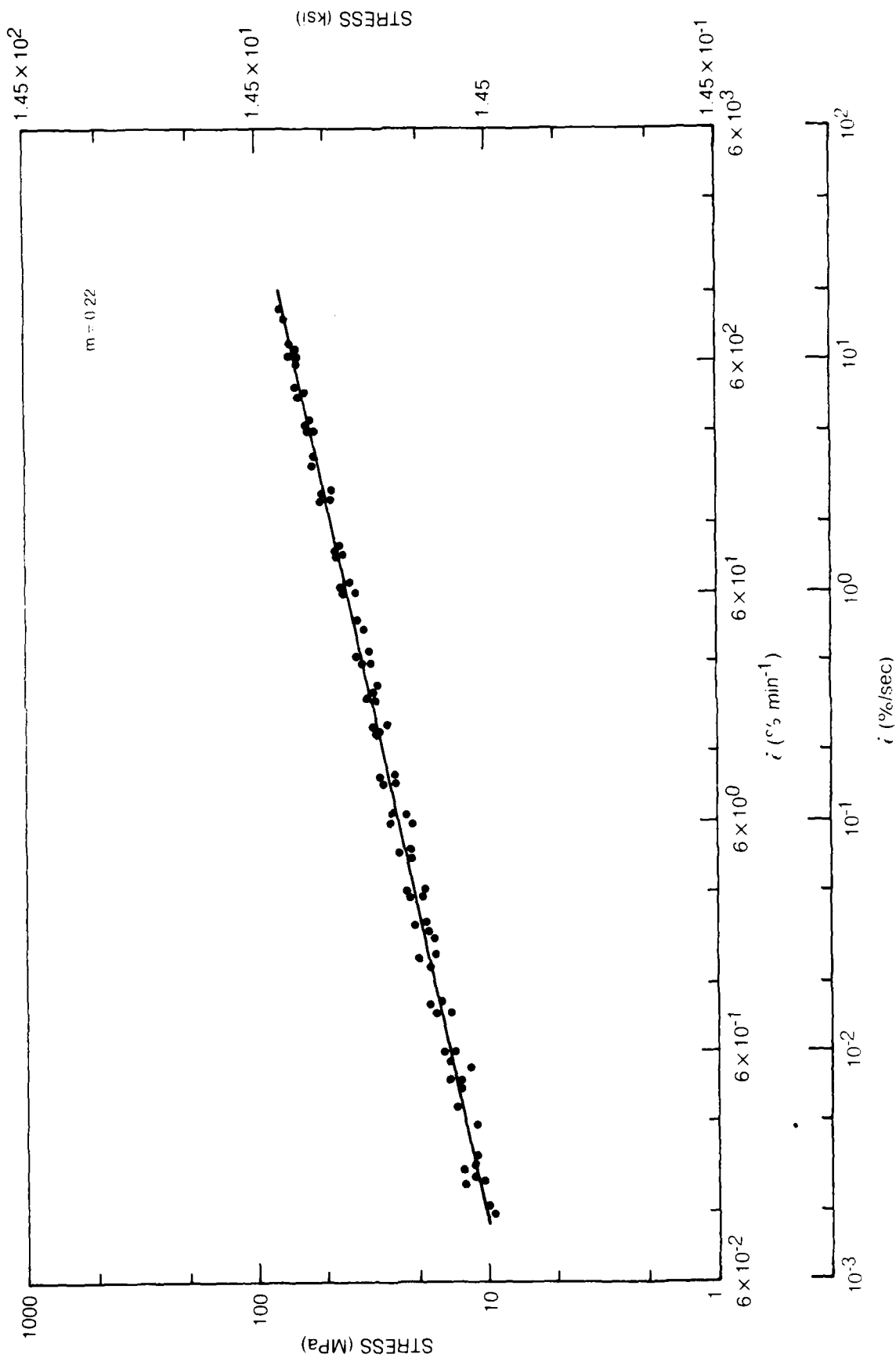
FIG. 3-31A

MODIFIED IN100 UPSET TO 60% REDUCTION AT $<\dot{\epsilon}> = 0.006\%$ S^{-1}

1000μ
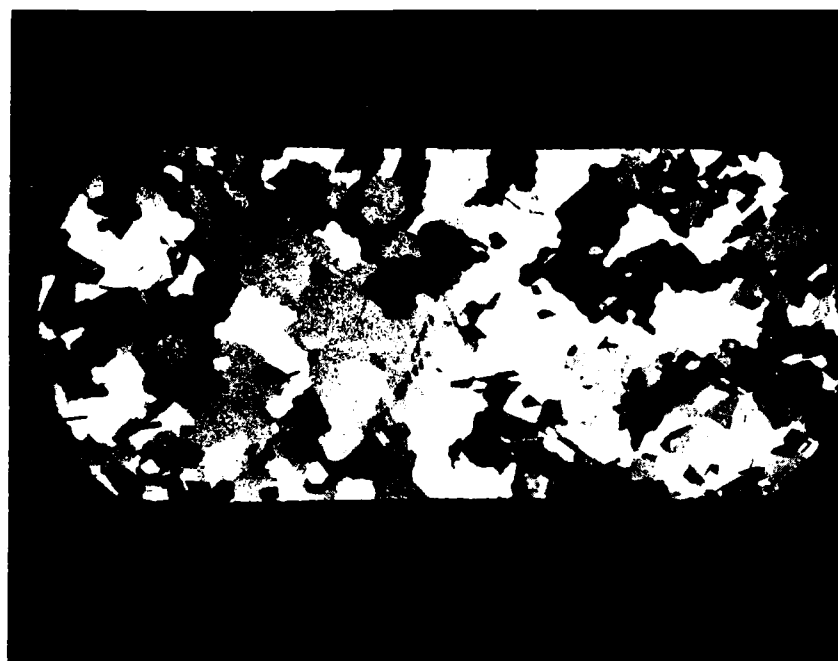
FIG. 3-31B

MODIFIED IN100 UPSET TO 60% REDUCTION AT $<\dot{\epsilon}> = 0.06\%$ S^{-1}

1000μ

81—8—3—8

FIG. 3-32A

MODIFIED IN100 UPSET TO 60% REDUCTION AT $<\dot{\epsilon}> = 0.6\%$ S^{-1}

1000μ

FIG. 3-32B

MODIFIED IN100 UPSET TO 60% REDUCTION AT $<\dot{\epsilon}> = 6.0\%$ S^{-1}

FIG 3-33
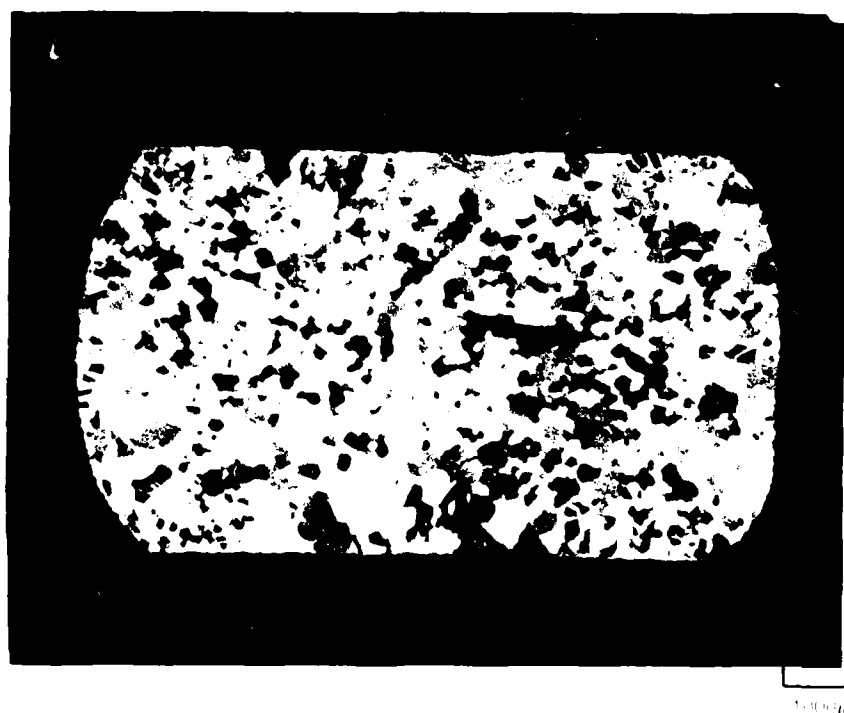
MODIFIED PWA 1058 BUTTONS FORMED AT $T_F = 1204°C$ AT VARIOUS STRAIN RATES

81-12-8-4
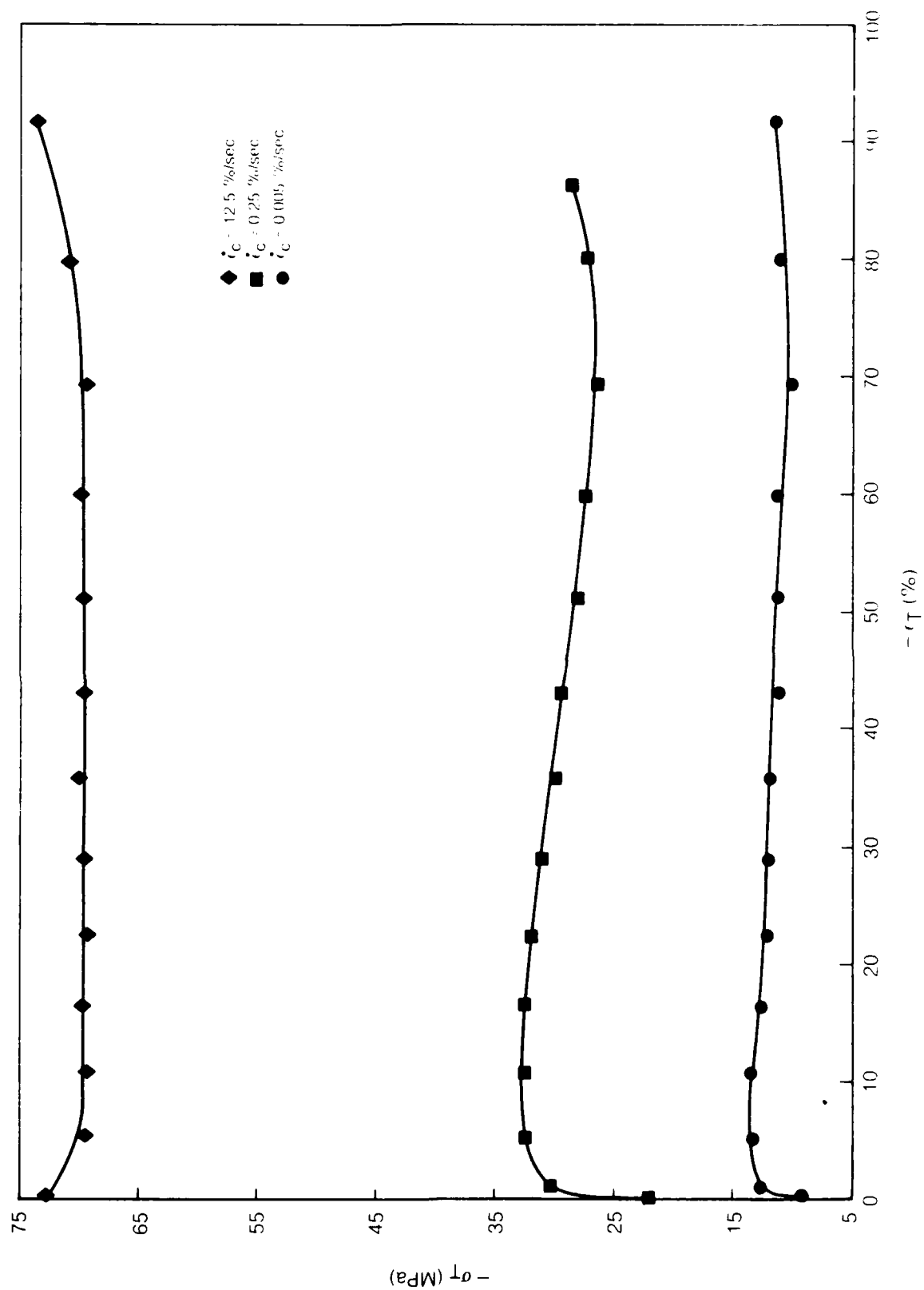
LONGITUDINAL SECTIONS OF MODIFIED IN100 FORMED AT 1204°C AT 5×10^{-3} % s^{-1} TO THE INDICATED STRAIN LEVELS

(a) 15%

1000μm

(b) 60%

LONGITUDINAL SECTIONS OF MODIFIED IN100 FORMED AT 1204°C AT 2.5×10^{-1} % s^{-1} TO THE INDICATED STRAIN LEVELS

(a) 15%

1000μm

(b) 60%

1000μm

81-12-8-14

LONGITUDINAL SECTIONS OF MODIFIED IN100 FORMED AT 1204°C AT 12.5% s⁻¹ (750% min⁻¹) TO THE INDICATED STRAIN LEVELS

(a) 15%

1000μm

(b) 30%

1000μm

81-12-8-15

FIG. 3-37

LONGITUDINAL SECTIONS OF MODIFIED IN100 FORMED AT 1204°C AT 12.5% s⁻¹ (750% min⁻¹) TO THE INDICATED STRAIN LEVELS

(a) 45%

1000μm

(b) 60%

1000μm

81-12-8-16

FIG. 3-38
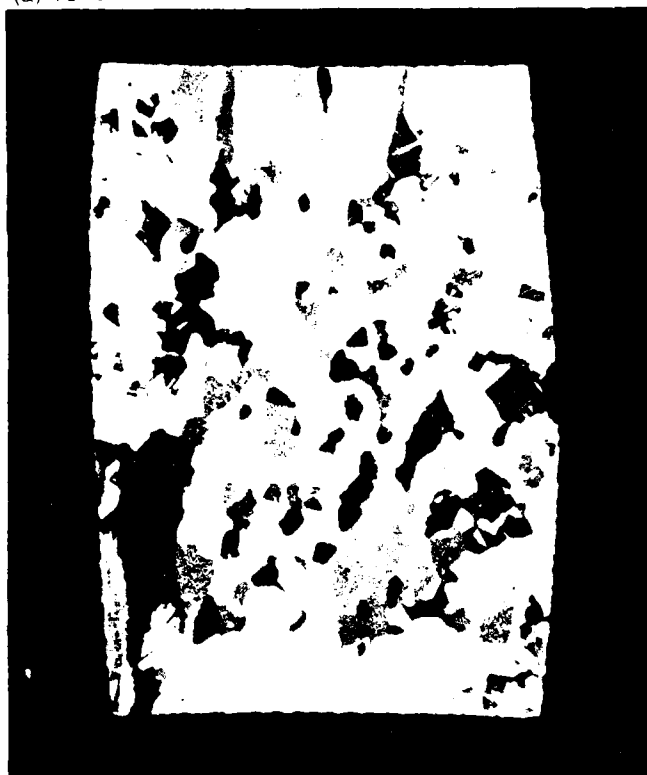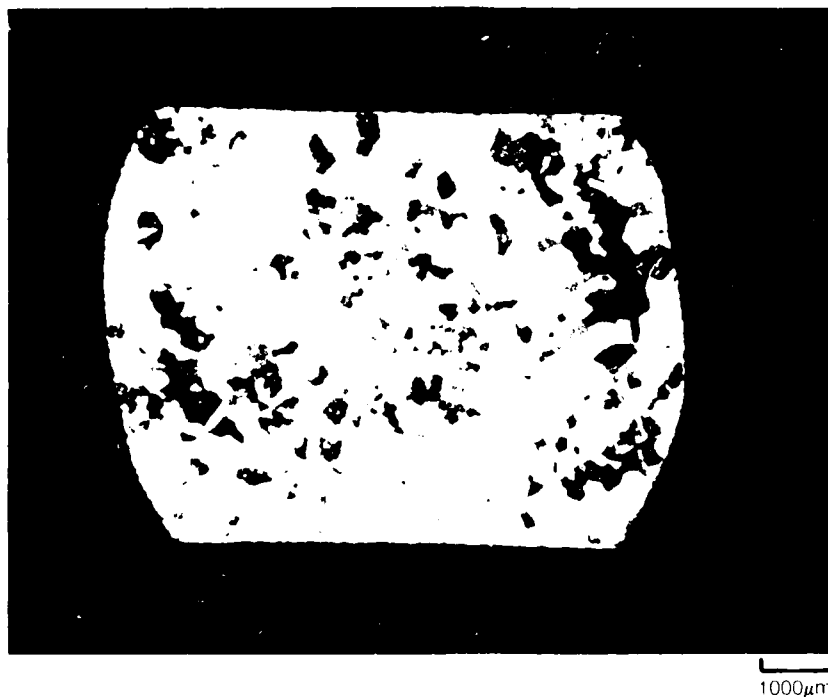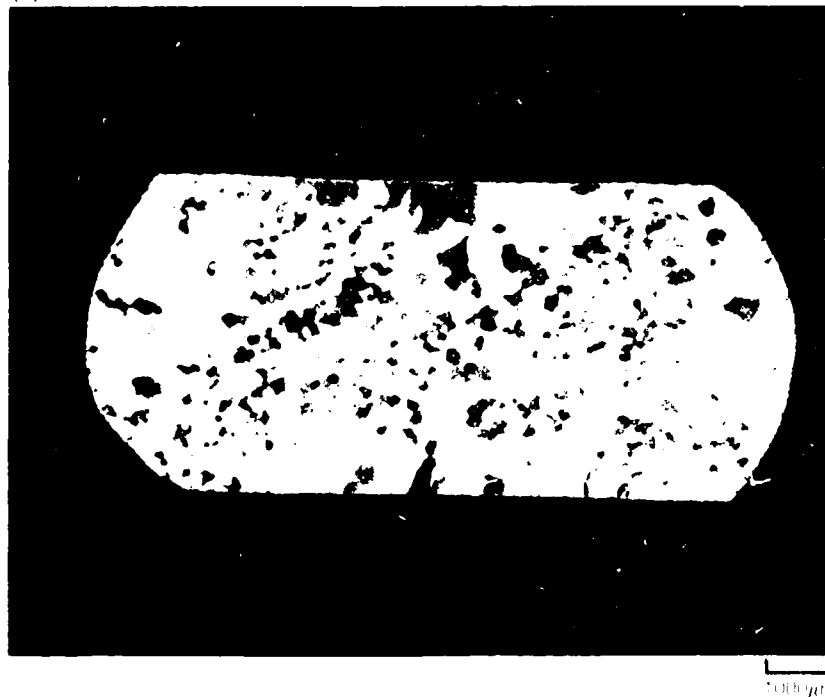
CONTINUOUS COOLING FORMING EXPERIMENT: TEMPERATURE AND STRAIN VS TIME

81-12-8-5

FIG 3-39
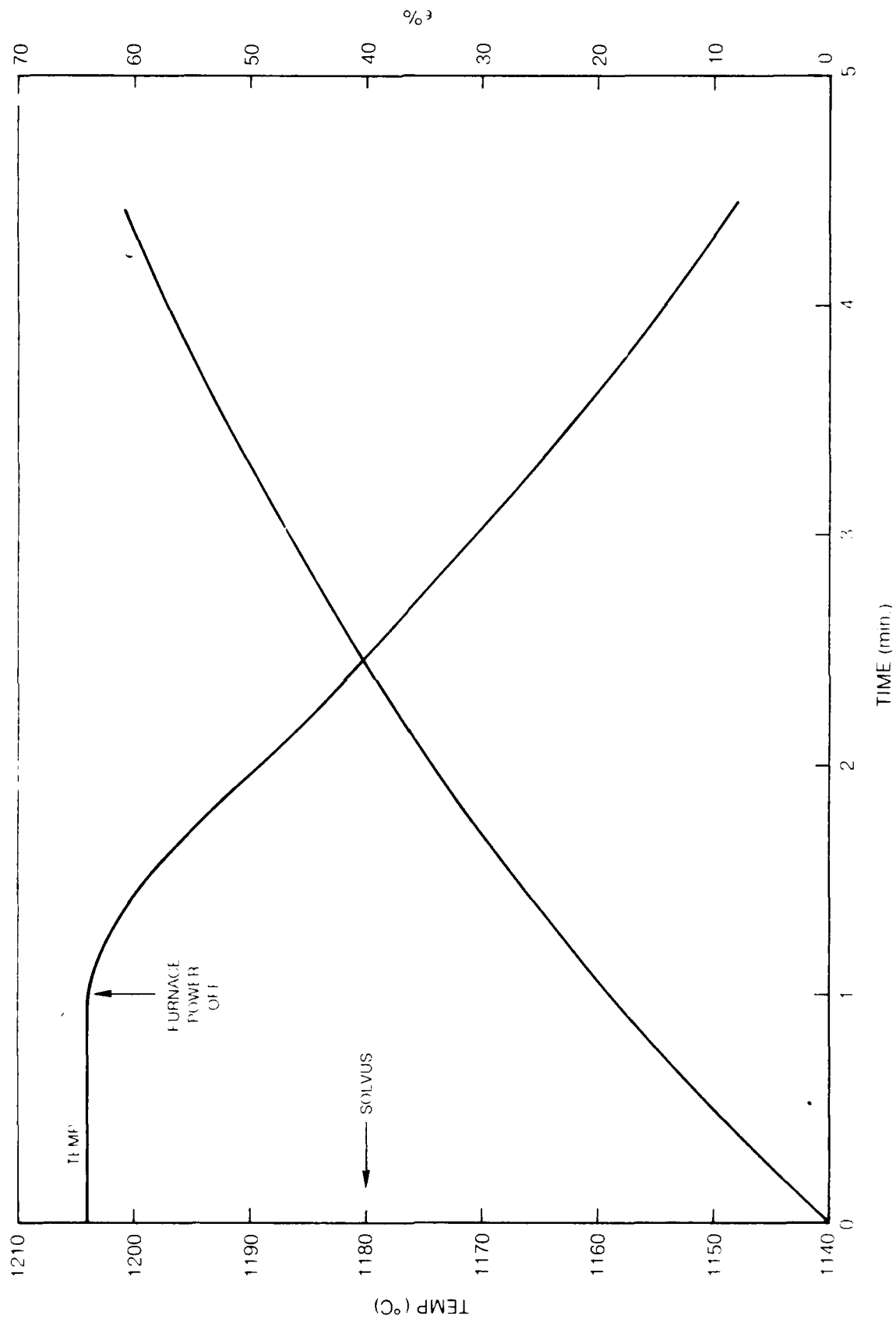
CONTINUOUS COOLING FORMING EXPERIMENT: TEMPERATURE AND TRUE STRESS VS TRUE STRAIN

FIG. 3-40
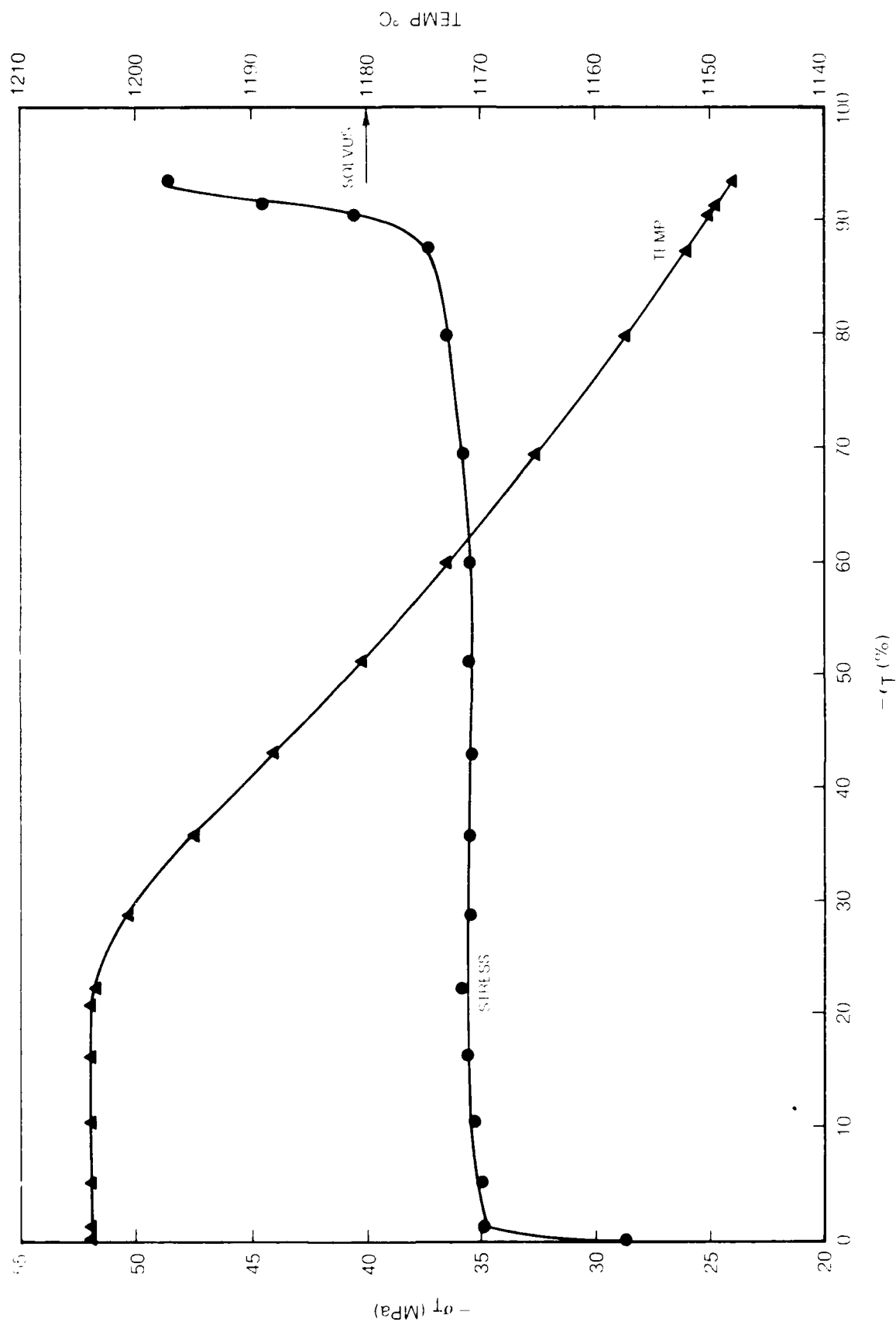
CONTINUOUS COOLING FORMING EXPERIMENT: CROSS-PLOT OF TRUE STRESS VS TEMPERATURE

81−12−8−7
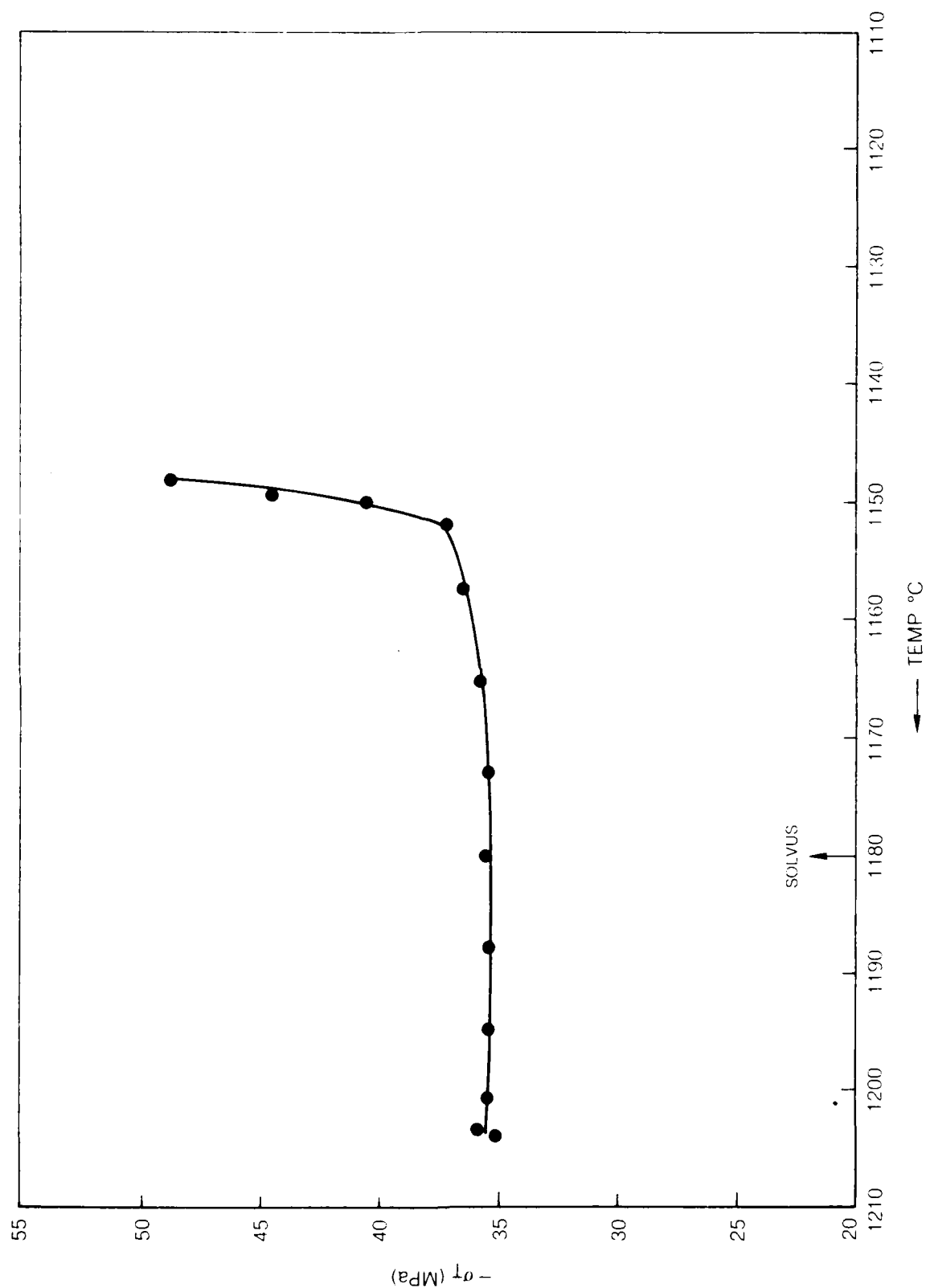
LONGITUDINAL SECTION AT 60% STRAIN FROM MODIFIED IN-100 CONTINUOUS COOLING
FORMING EXPERIMENT

1000μm

FIG. 3-42

DUAL STRAIN RATE TESTING PROCEDURE

STRAIN

TIME
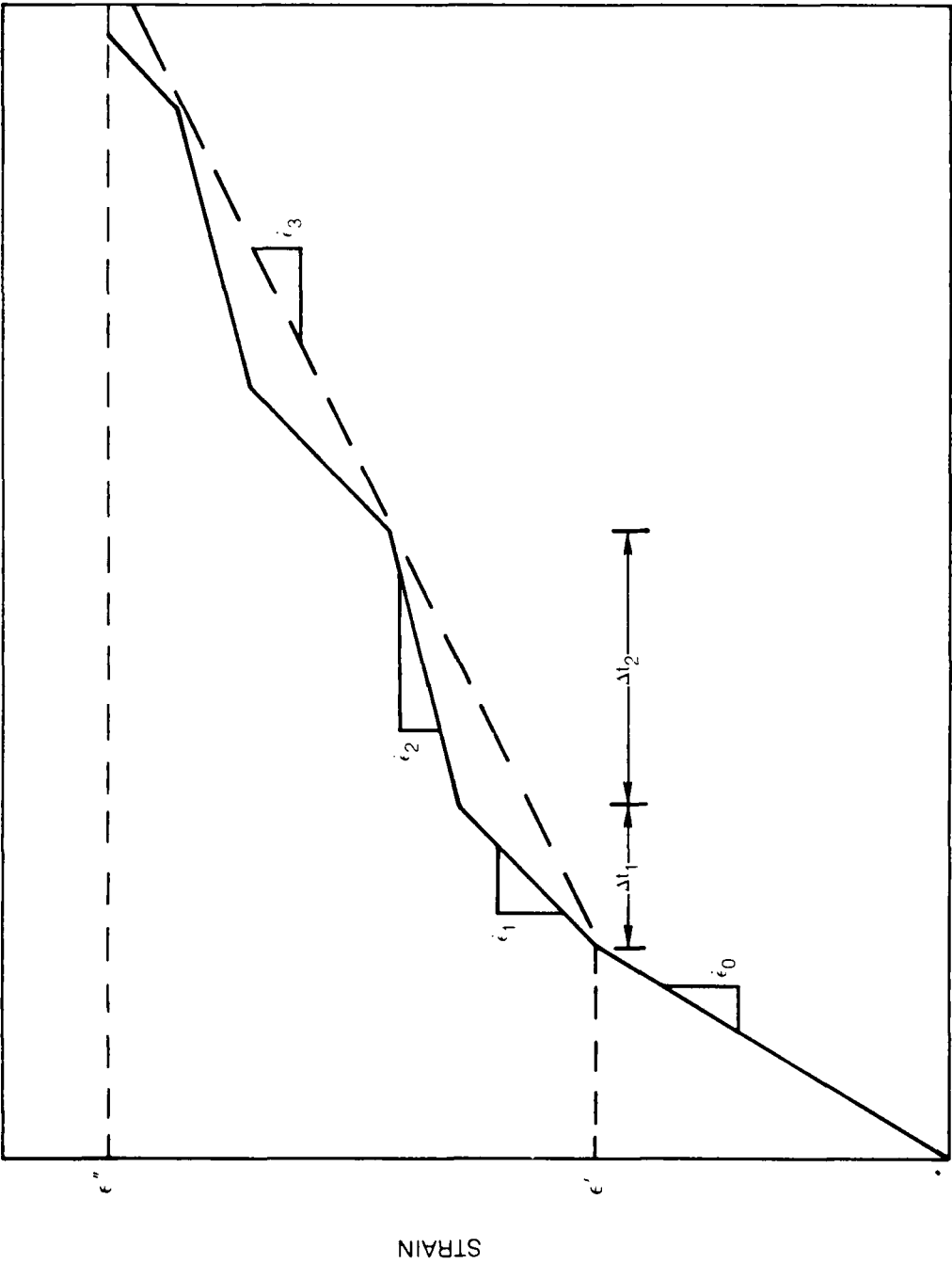
FIG 3-43A

DRIP MELTING CRUCIBLE AND ORIFICE
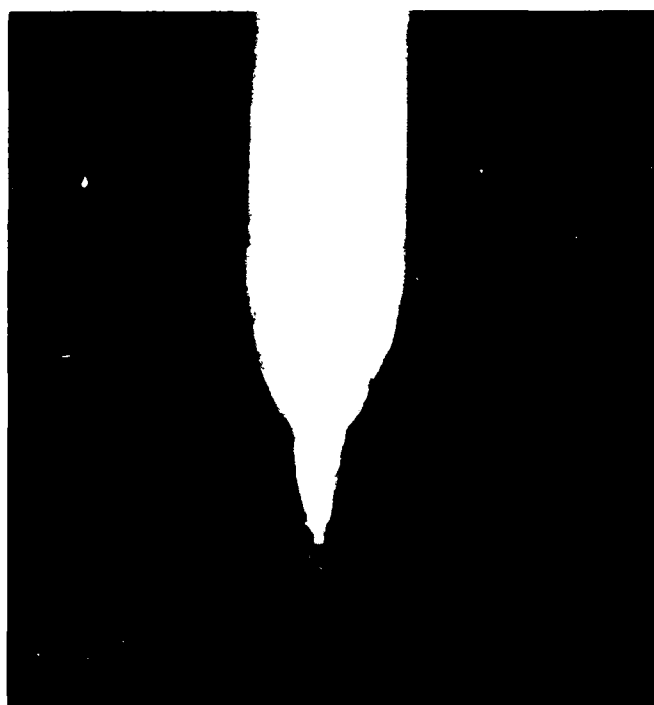
1 cm

FIG 3-43B

1 cm

DRIP MELTED INGOT TAKEN FROM COPPER MOLD

81—8—3—10

FIG. 3-44A

BOTTOM SECTION OF DRIP MELTED MODIFIED IN100
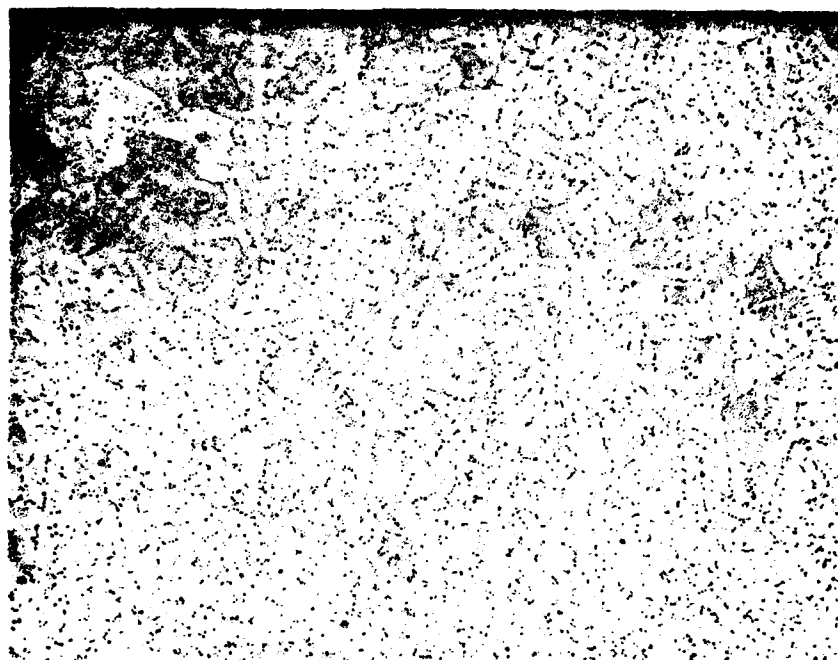
100µ

FIG. 3-44B

CENTER SECTION OF DRIP MELTED MODIFIED IN100

100µ

81-8-3-11
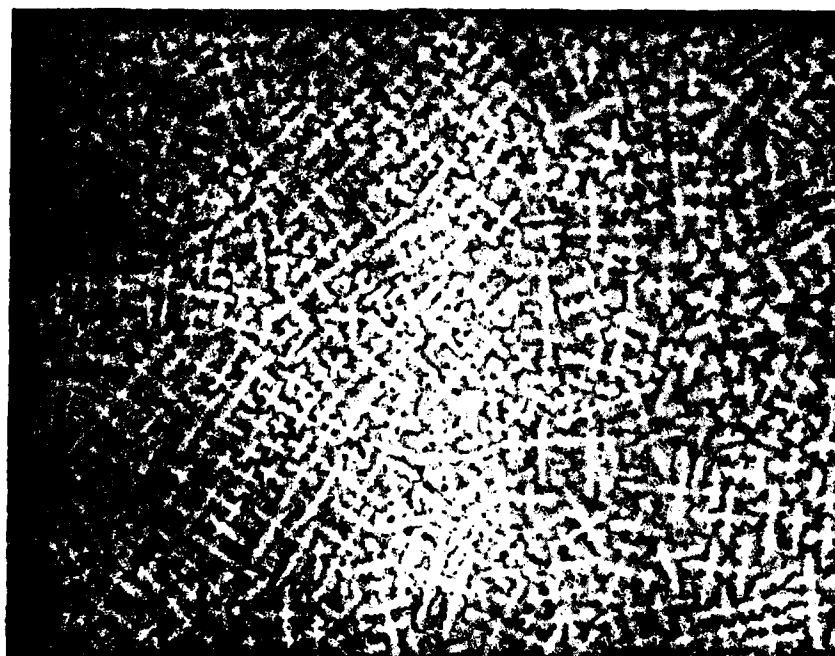
FIG. 3-45A

GRAINS IN DRIP MELTED MODIFIED IN100 AFTER HIP CYCLE

700μ

FIG. 3-45B

γ/γ′ IN DRIP MELTED MODIFIED IN100 AFTER HIP CYCLE

10μ

81−8−3−13
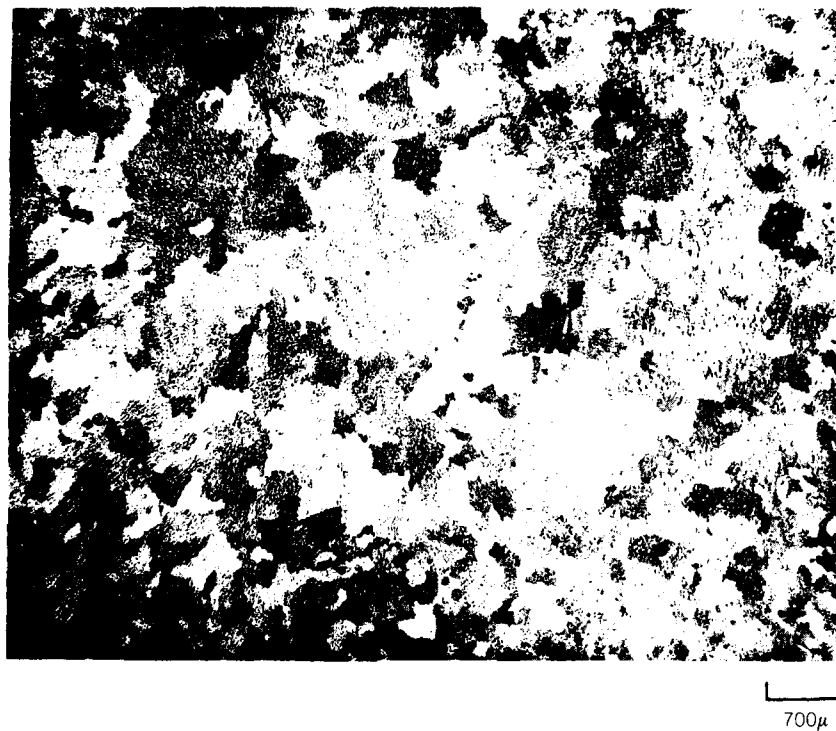
FIG. 3-46
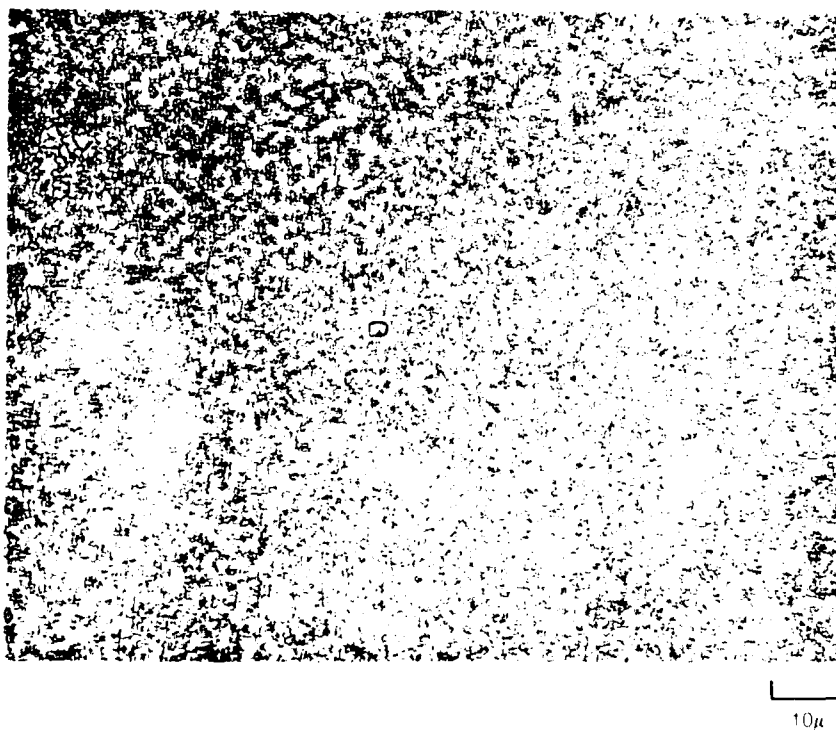
FORMING CURVES FOR DRIP CAST IN-100

FIG. 3-47
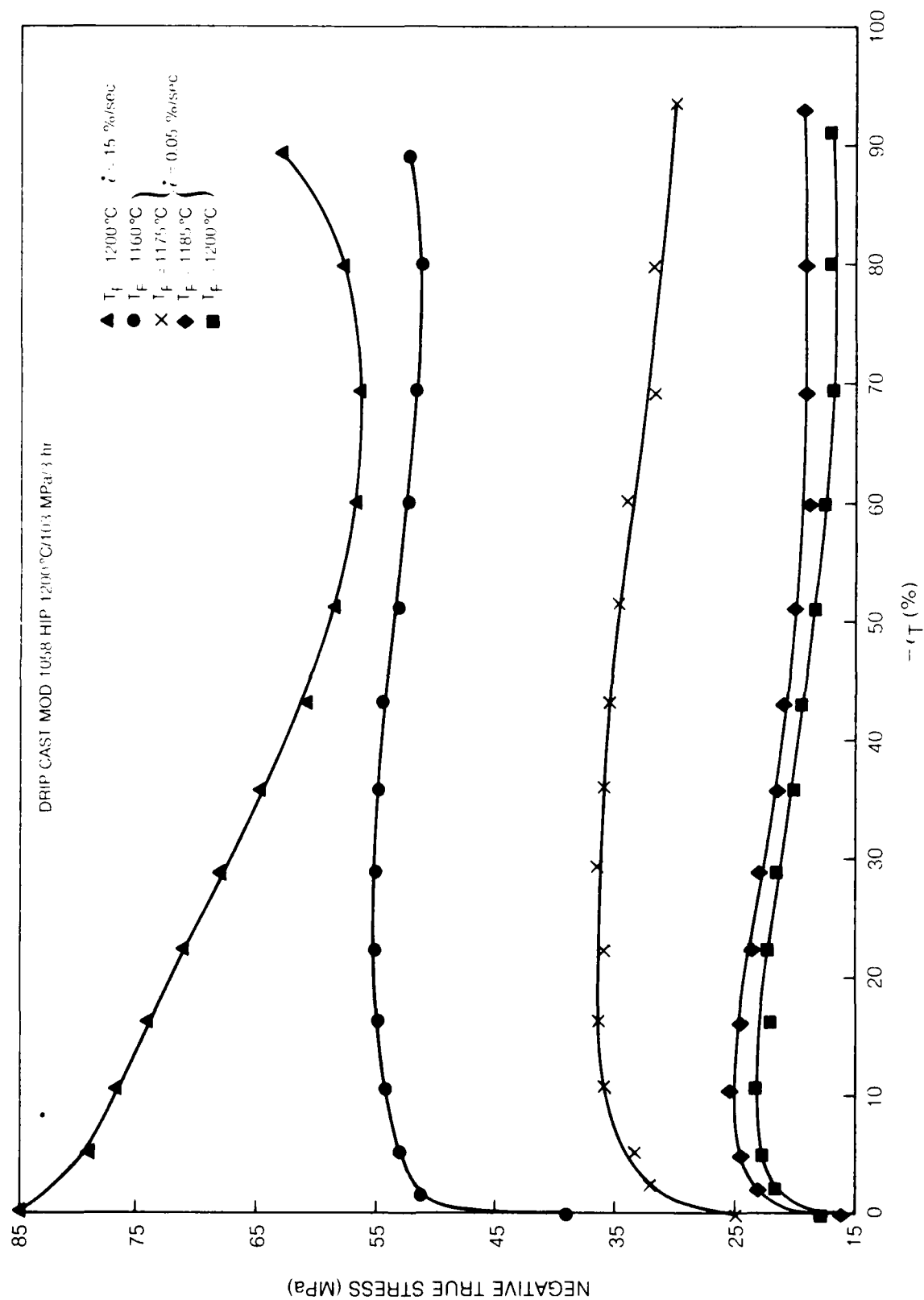
DRIP + HIP MODIFIED IN-100 BEFORE AND AFTER FORMING AT 1175°C AT 0.05% s⁻¹

(b) AFTER

(a) BEFORE

81 12 8 18

FORMING/STRAIN RATE SENSITIVITY TEST OF DRIP + HIP IN-100

MOD 1058 DRIP CAST + HIP, T_F 1200°C

$-\epsilon_T$ (%)

$-\sigma_T$ (MPa)

81-12-8-9
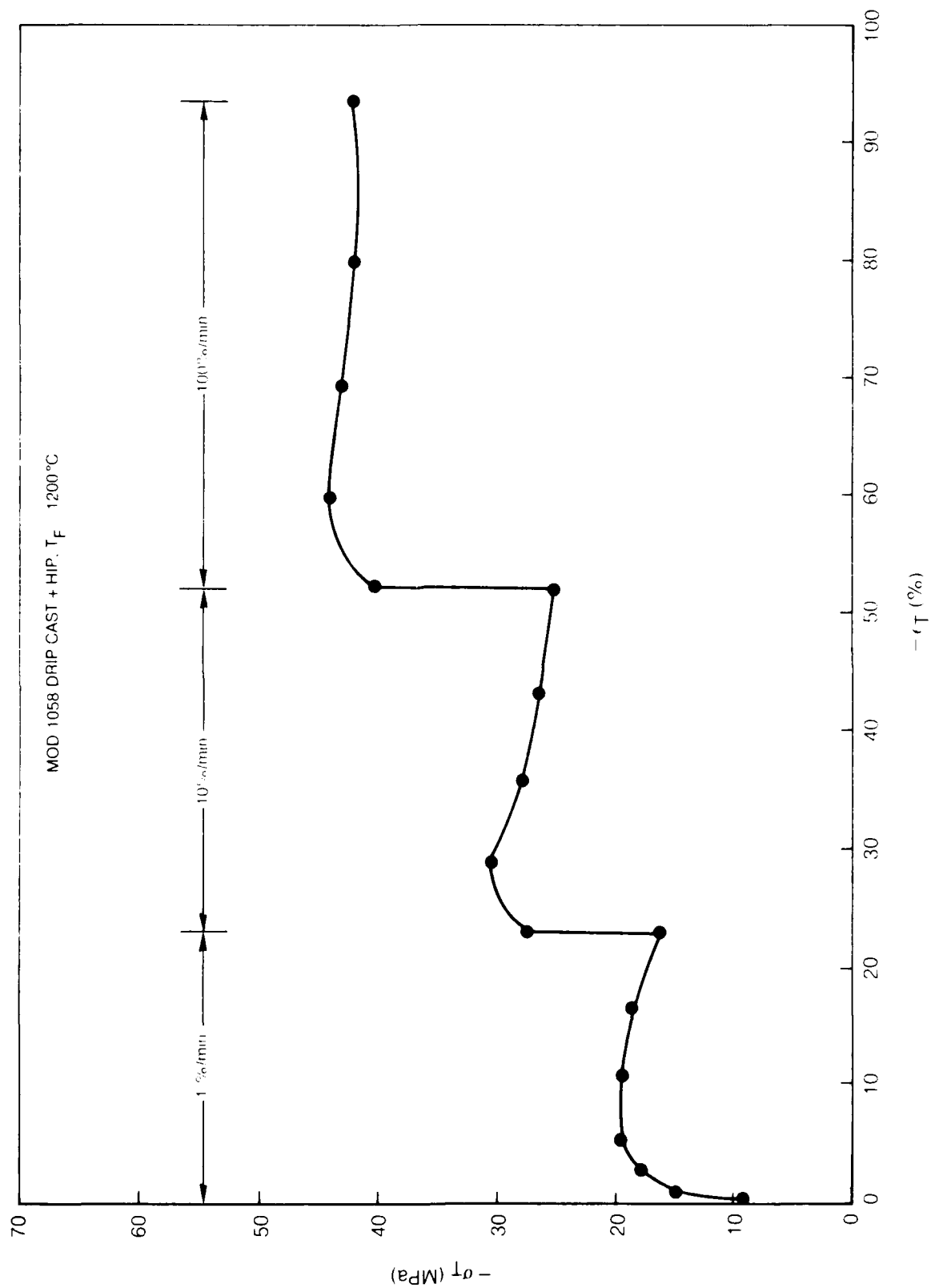
LONGITUDINAL SECTION (i.e. COMPRESSIVE STRESS AXIS IS VERTICAL) FOR DRIP + HIP
MODIFIED IN-100 FORMED AT 1200°C INITIALLY AT 1% min^{-1} WITH TWO 10X JUMPS
ENDING AT 100% min^{-1} STRAIN RATE
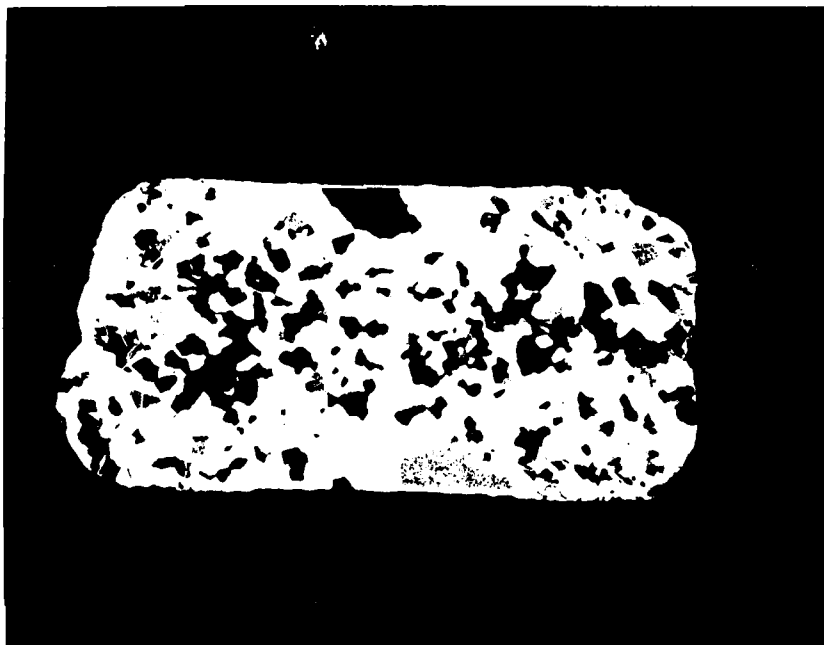
1000μm

CROSS-SECTION OF DISC RING OF MOD 1058 AFTER HIP
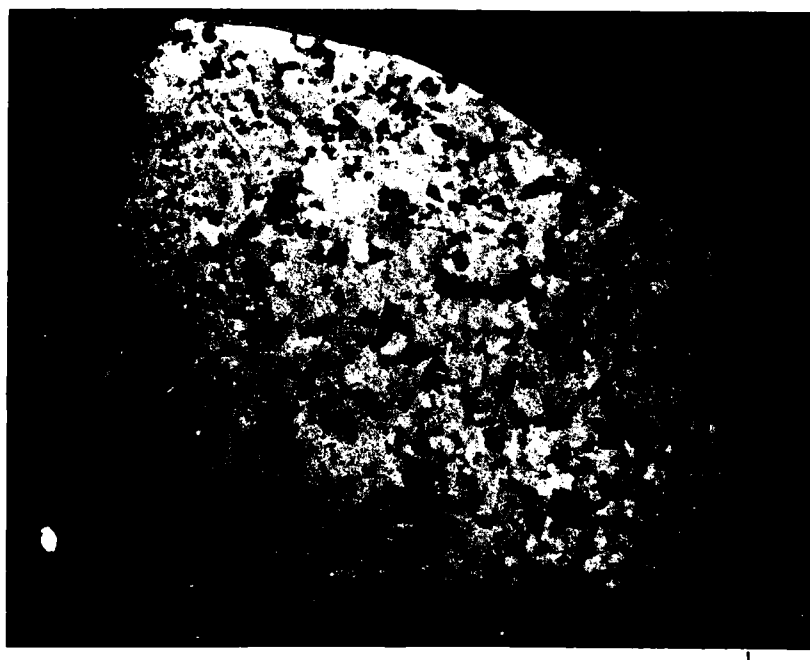
CROSS-SECTION OF DISC SPECIMEN AFTER COMPRESSIVE DEFORMATION TO DETERMINE STRAIN RATE SENSITIVITY

T = 1082 °C

RECRYSTALLIZATION OF MOD PWA 1058 AS A FUNCTION OF TRUE STRAIN

a) $\epsilon = 2\%$

b) $\epsilon = 5\%$

83 5 102 36

END
FILMED
I11

MICROCOPY RESOLUTION TEST CHART

NATIONAL BUREAU OF STANDARDS 1963 A
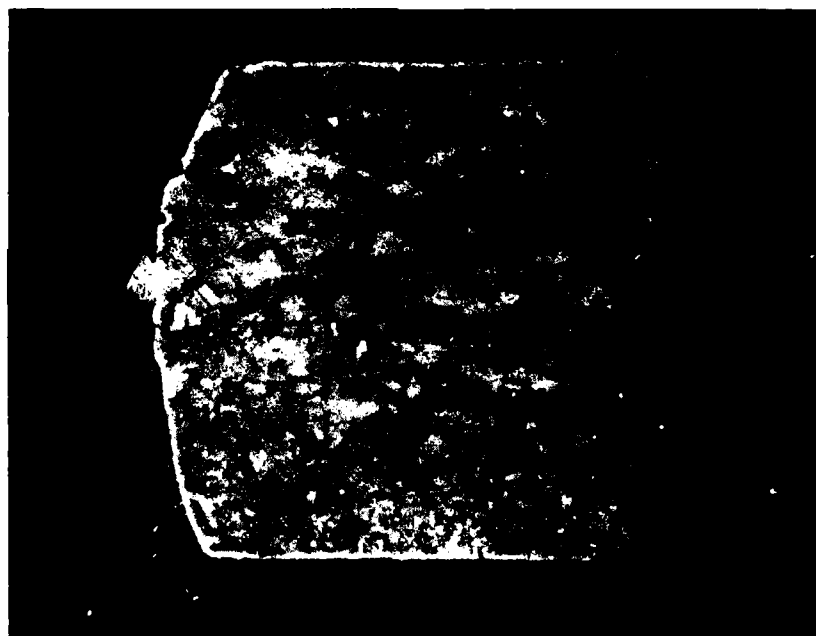
RECRYSTALLIZATION OF MOD PWA 1058 AS A FUNCTION OF TRUE STRAIN

$$\dot{\epsilon} = 0.005\% \ sec^{-1}$$
$$T = 1204\,°C$$

c) $\epsilon = 10\%$

1 mm

d) $\epsilon = 15\%$
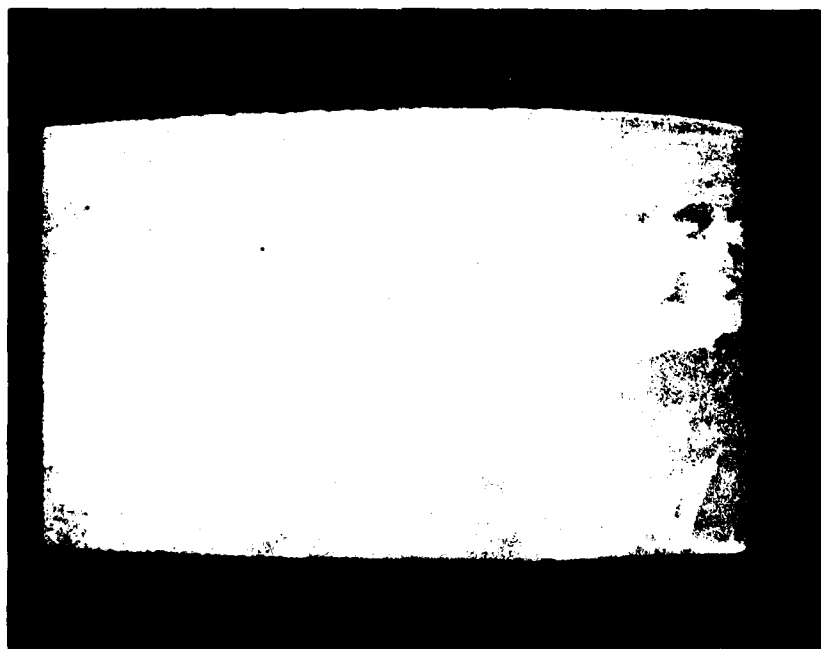
RECRYSTALLIZATION OF MOD PWA 1058 AS A FUNCTION OF TRUE STRAIN RATE

$\epsilon = 5\%$

$T = 1204\ ^{\circ}C$

a) $\dot{\epsilon} = 0.005\ \%\ \text{sec}^{-1}$

1.0 mm

b) $\dot{\epsilon} = 0.035\ \%\ \text{sec}^{-1}$

FIG. 3-53 (CONT.)
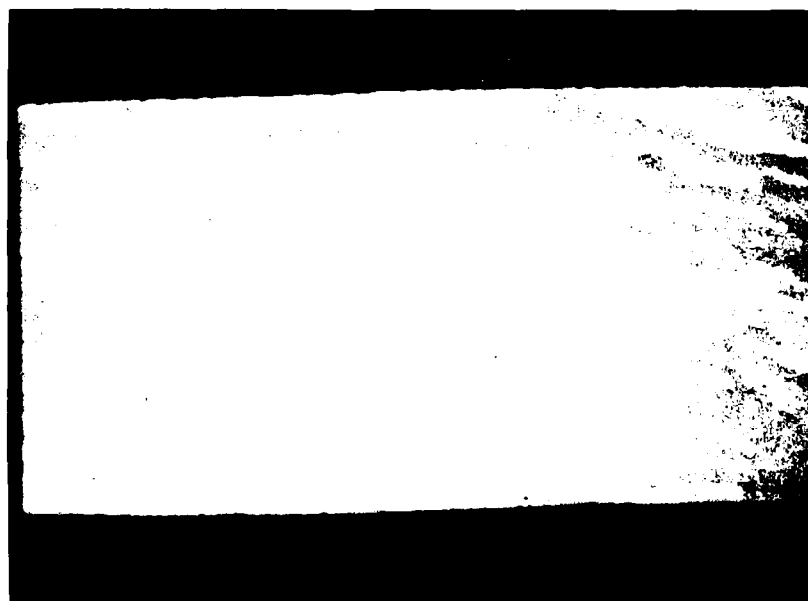
RECRYSTALLIZATION OF MOD PWA 1058 AS A FUNCTION OF TRUE STRAIN RATE

$\epsilon = 5\%$

$T = 1204\,^{\circ}C$

c) $\dot{\epsilon} = 0.250\%\ \text{sec}^{-1}$

1 0 mm

d) $\dot{\epsilon} = 12.500\%\ \text{sec}^{-1}$

83-5-102-35

FIG. 3-54
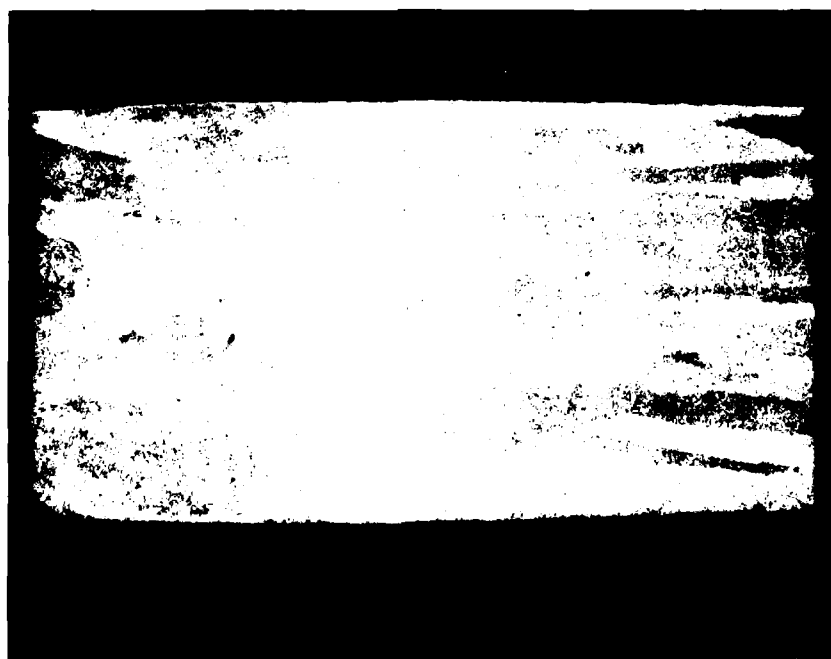
GRAIN BOUNDARY IRREGULARITIES IN DEFORMED MOD 1058 WITH DIFFERENT STRAIN RATES

a) $\dot{\epsilon} = 0.005\%\ sec^{-1}$
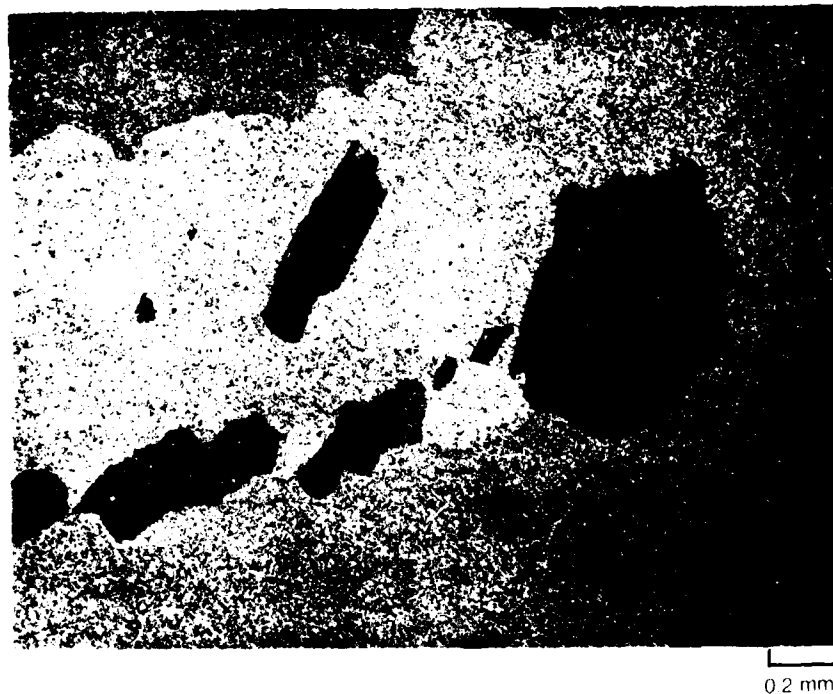
0 2 mm

b) $\dot{\epsilon} = 12.5\%\ sec^{-1}$

83-5-102-20

FIG. 3-55

GRAIN SUBSTRUCTURE OF PWA 1056 AFTER DEFORMATION
AT VARIOUS STRAIN RATES

T = 1080 °C

$\epsilon \sim 60\%$

a) $\dot{\epsilon} = 0.06\%$ sec^{-1}
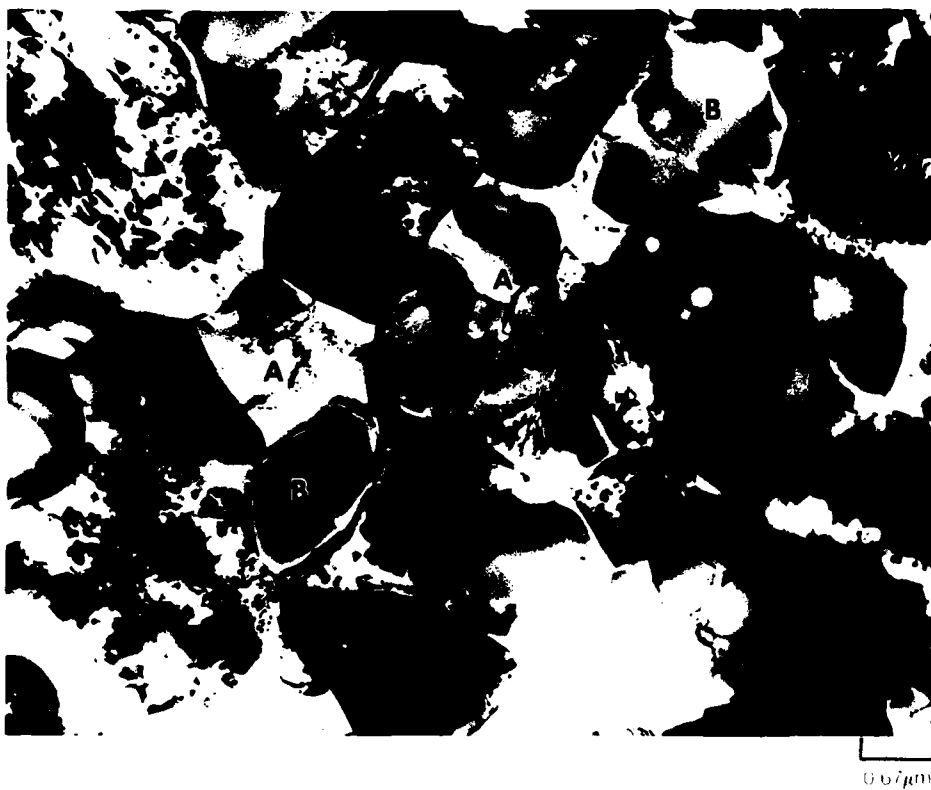
0.67μm

83-5-102-24

FIG. 3-55(CONT.)

GRAIN SUBSTRUCTURE OF PWA 1056 AFTER DEFORMATION
AT VARIOUS STRAIN RATES

T = 1080 °C
ε = 60%

b) $\epsilon = 0.60\%\text{SEC}^{-1}$

0.67μm

**GRAIN SUBSTRUCTURE OF PWA 1056 AFTER DEFORMATION
AT VARIOUS STRAIN RATES**

T = 1080°C
ε = 60%

c) $\dot{\epsilon} = 6.00\%\ \text{sec}^{-1}$

0.67μm

FIG. 3-56

CELL WALL DEVELOPMENT IN A LARGE γ' GRAIN

0 18μm

LARGE γ' GRAINS IN DEFORMED PWA 1056

a) BRIGHT FIELD

0.3 μm
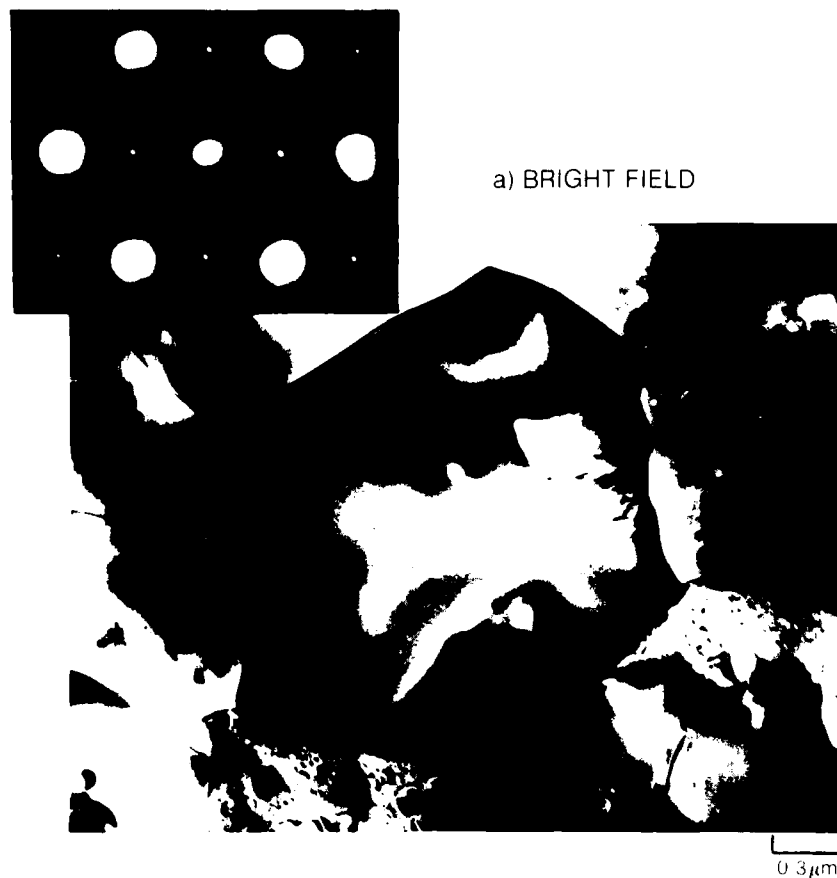
b) DARK FIELD USING <100> SUPERLATTICE SPOT

(A) LARGE γ' IN $\gamma+\gamma'$ GRAINS WITH (B) $\gamma'/\gamma+\gamma'$ SUB-BOUNDARY

a) BRIGHT FIELD

0 3μm

b) DARK FIELD

83-5-102-27

MICROSTRUCTURE OF CHILL CAST MOD 1058 AFTER DEFORMATION ABOVE THE γ' SOLVUS TEMPERATURE

a) $\dot{\epsilon} = 0.06\%\ sec^{-1}$

b) $\dot{\epsilon} = 6.00\%\ sec^{-1}$

83-5-102-28

FIG. 3-60
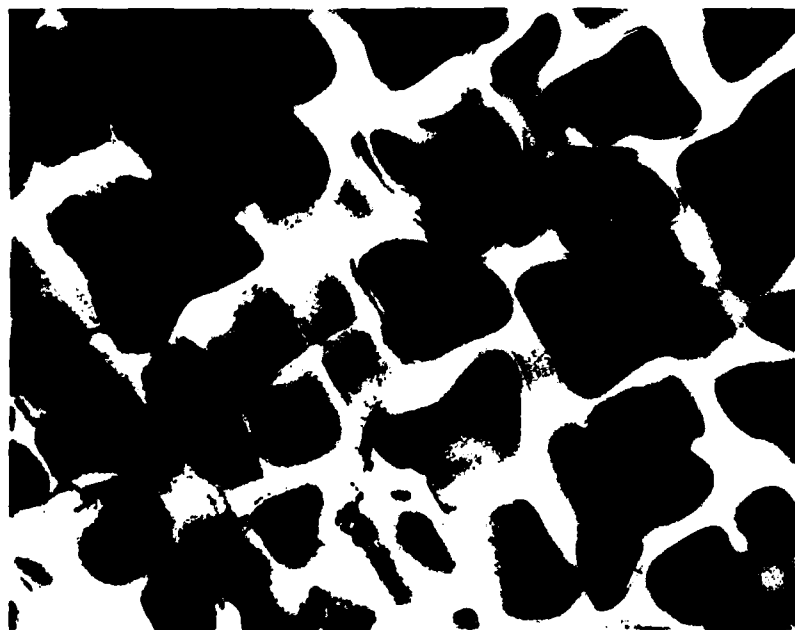
**YIELD STRESSES AND INITIAL DEFORMATION BEHAVIOR OF PWA 1444
SINGLE CRYSTALS (COMPRESSION)**
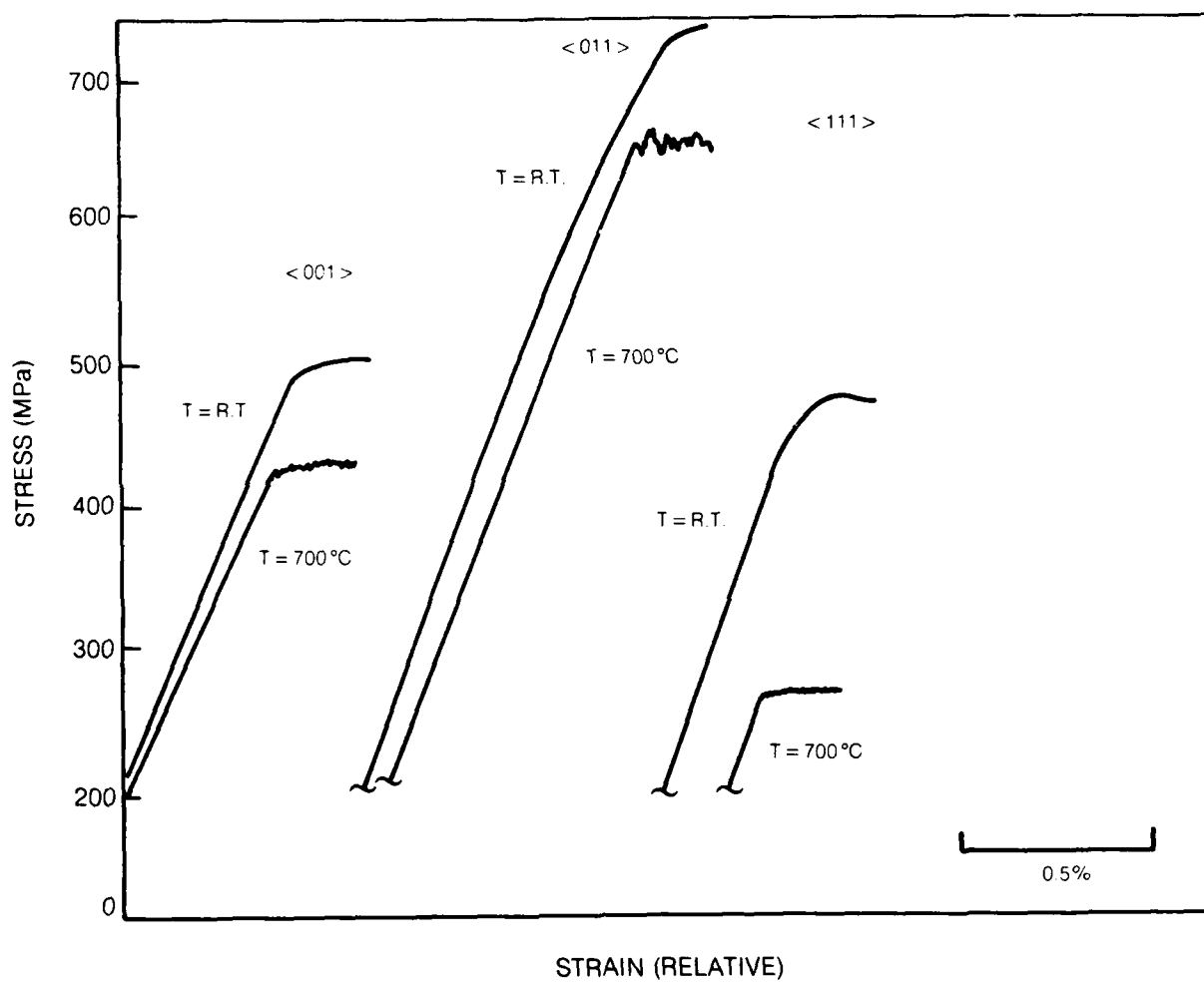
COMPRESSIVE FORMING CURVE FOR [001] PWA 1444 AT 1190°C AND 0.5% SEC⁻¹

FIG. 3-62
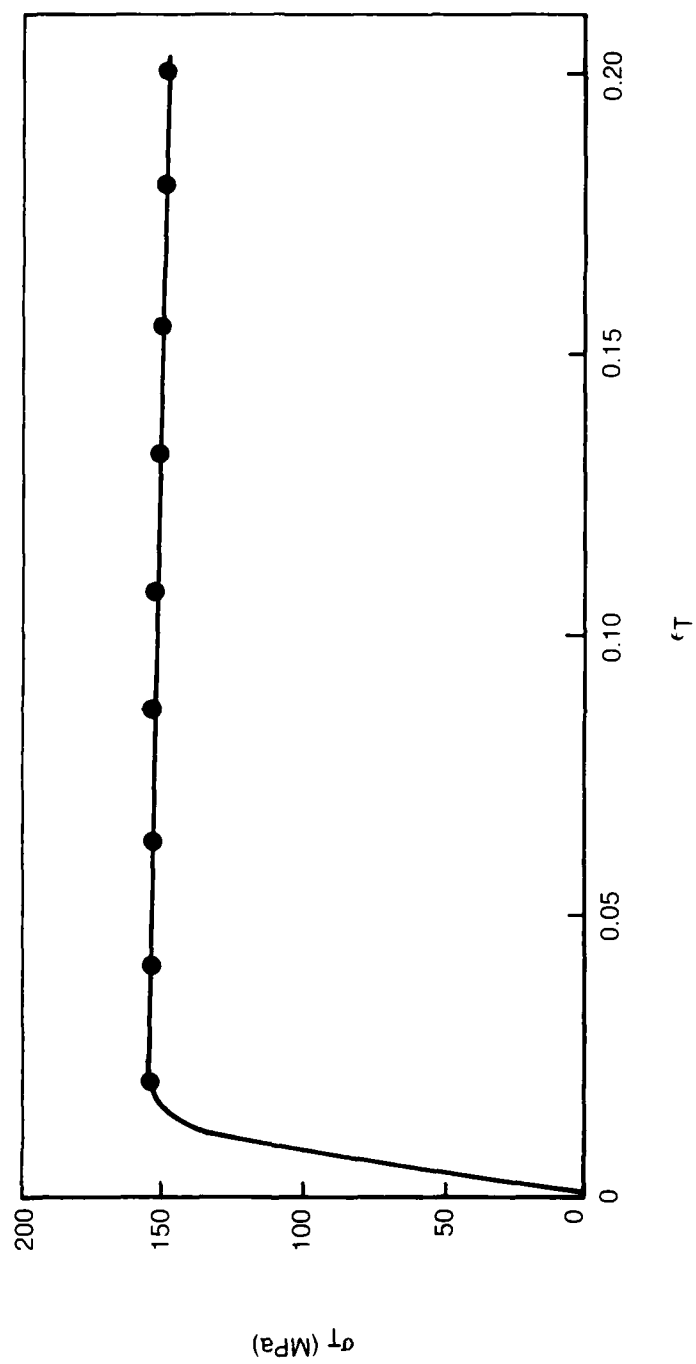
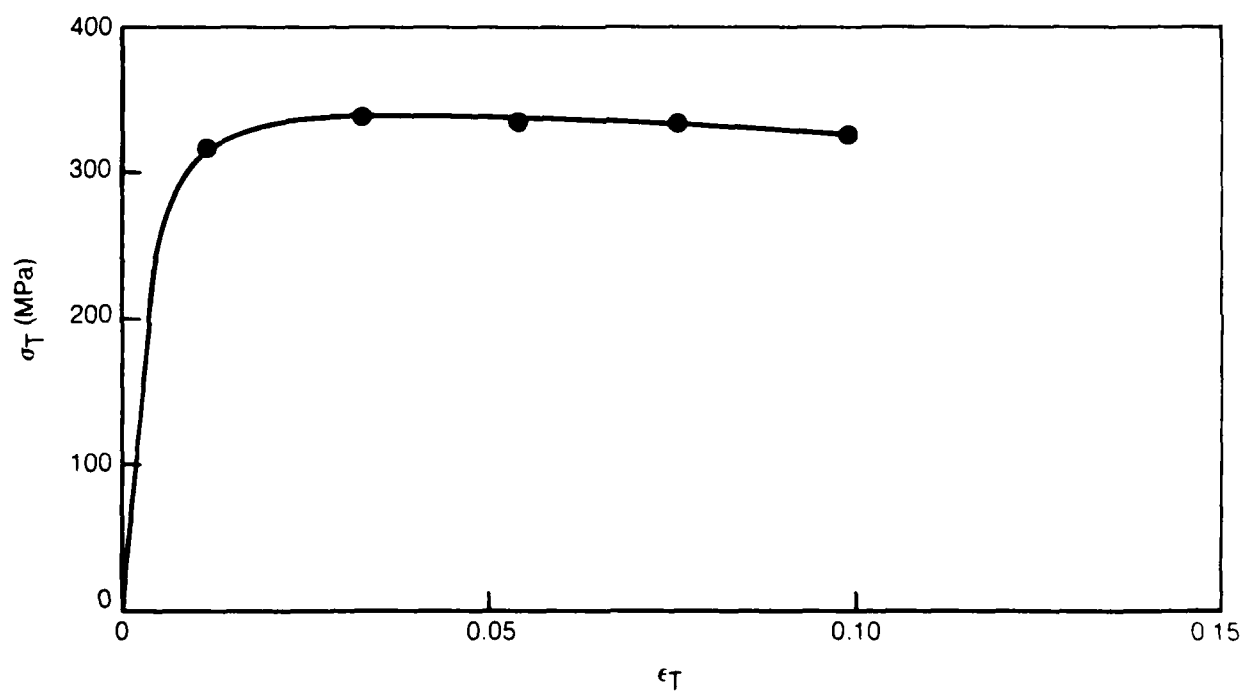**COMPRESSIVE FORMING CURVE FOR [001] PWA 1444 AT 1090°C AND 0.5% SEC^{-1}**
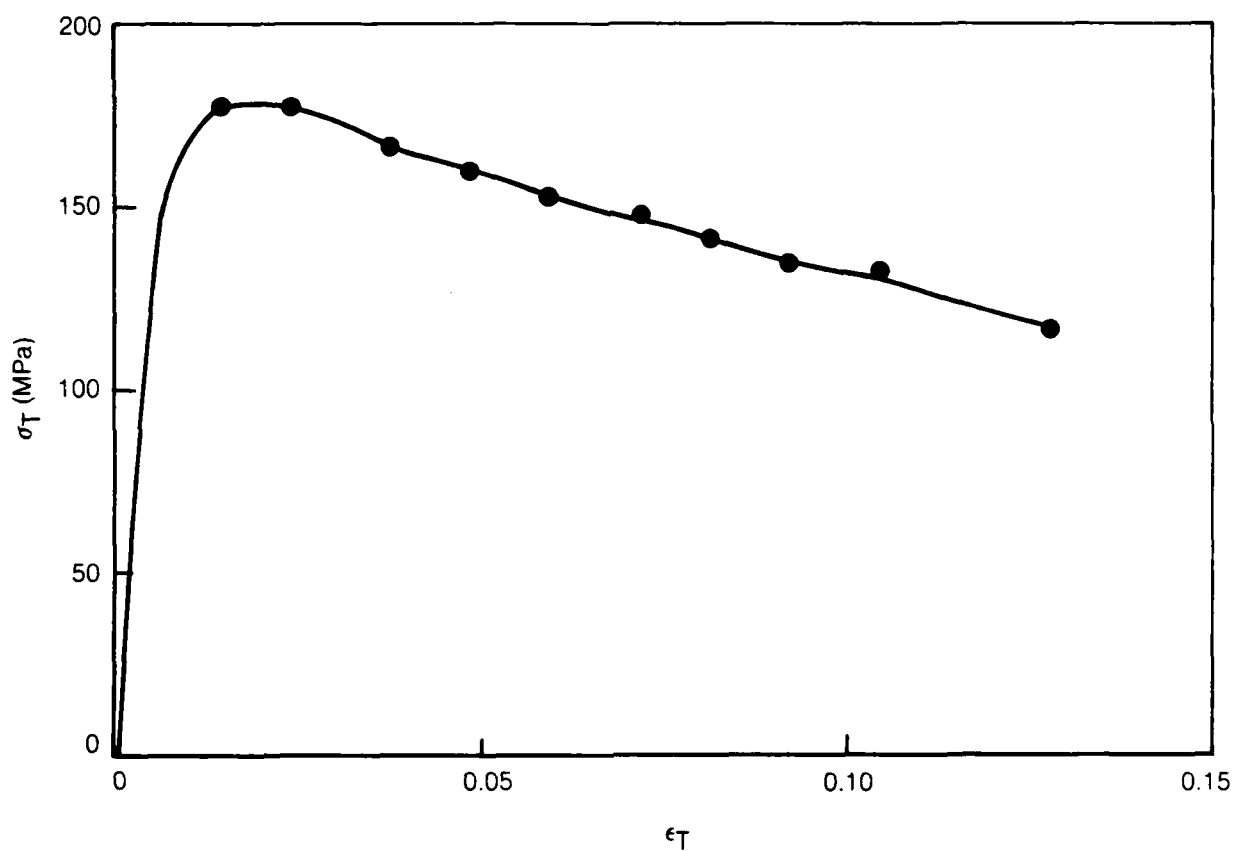
COMPRESSIVE FORMING CURVE FOR [100] PWA 1444 AT 990°C AND 0.5% SEC^{-1}

FIG. 3-64
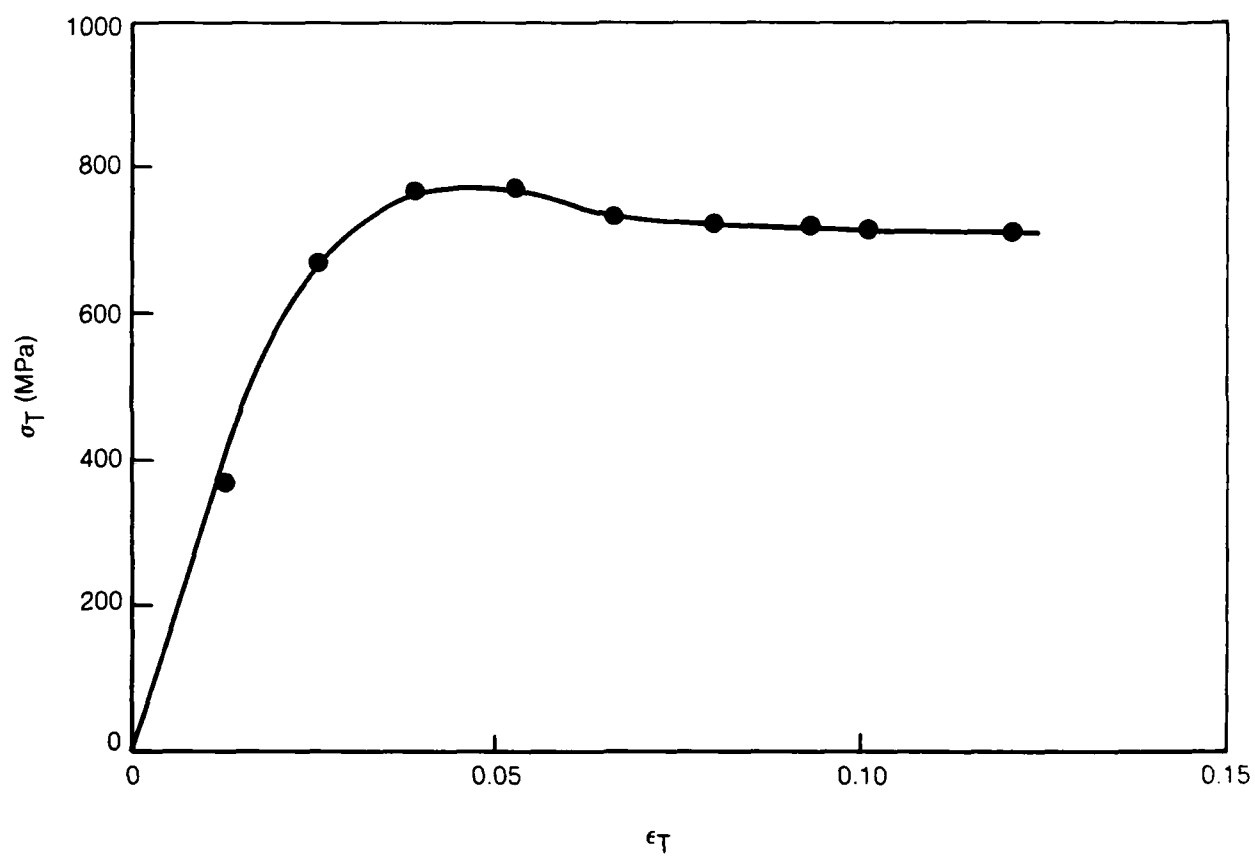
COMPRESSIVE FORMING CURVE FOR [001] PWA 1444 AT 890°C AND 0.5% SEC^{-1}

83—5—102—41

FIG. 3-65
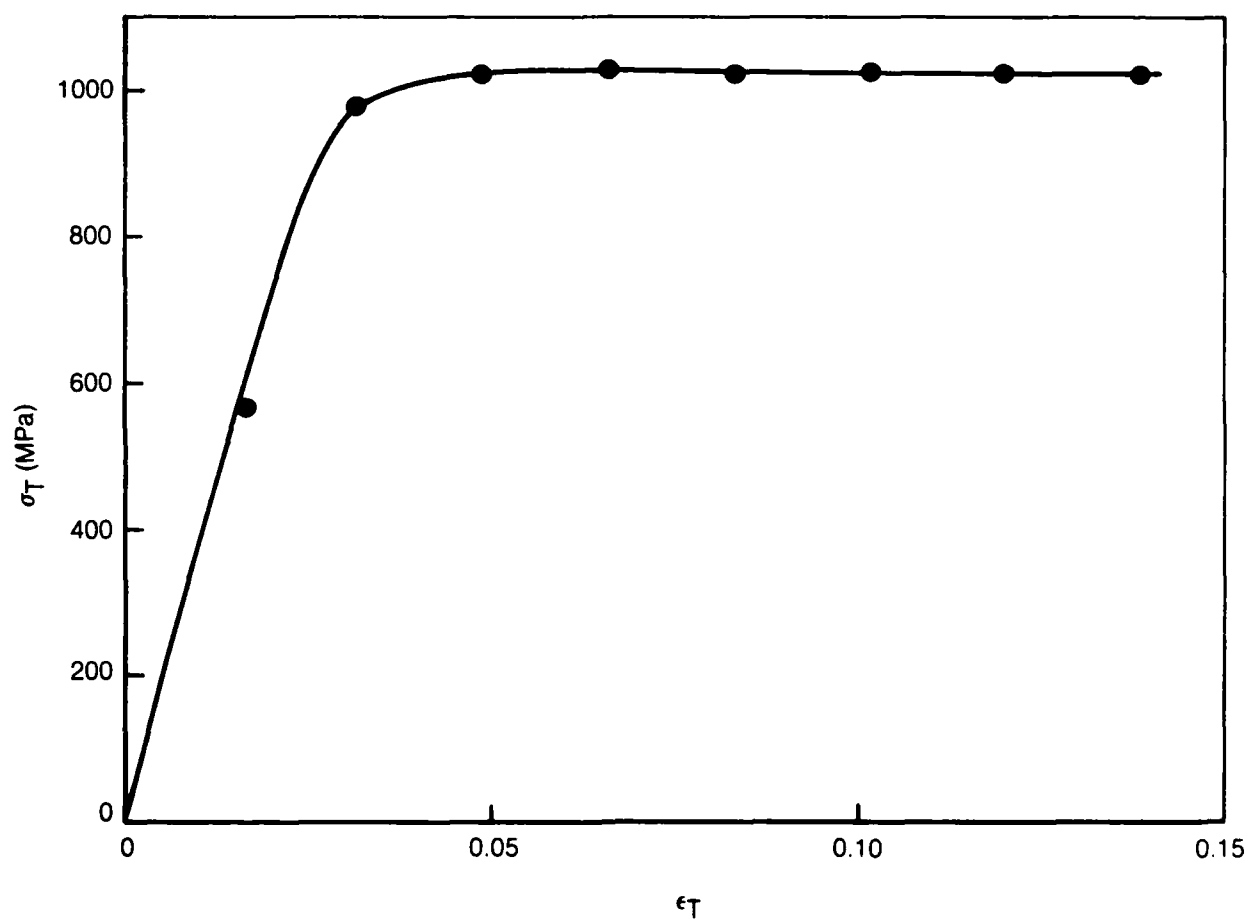
COMPRESSIVE FORMING CURVE FOR [011] PWA 1444 AT 1190°C AND 0.5% SEC⁻¹

FIG. 3-66
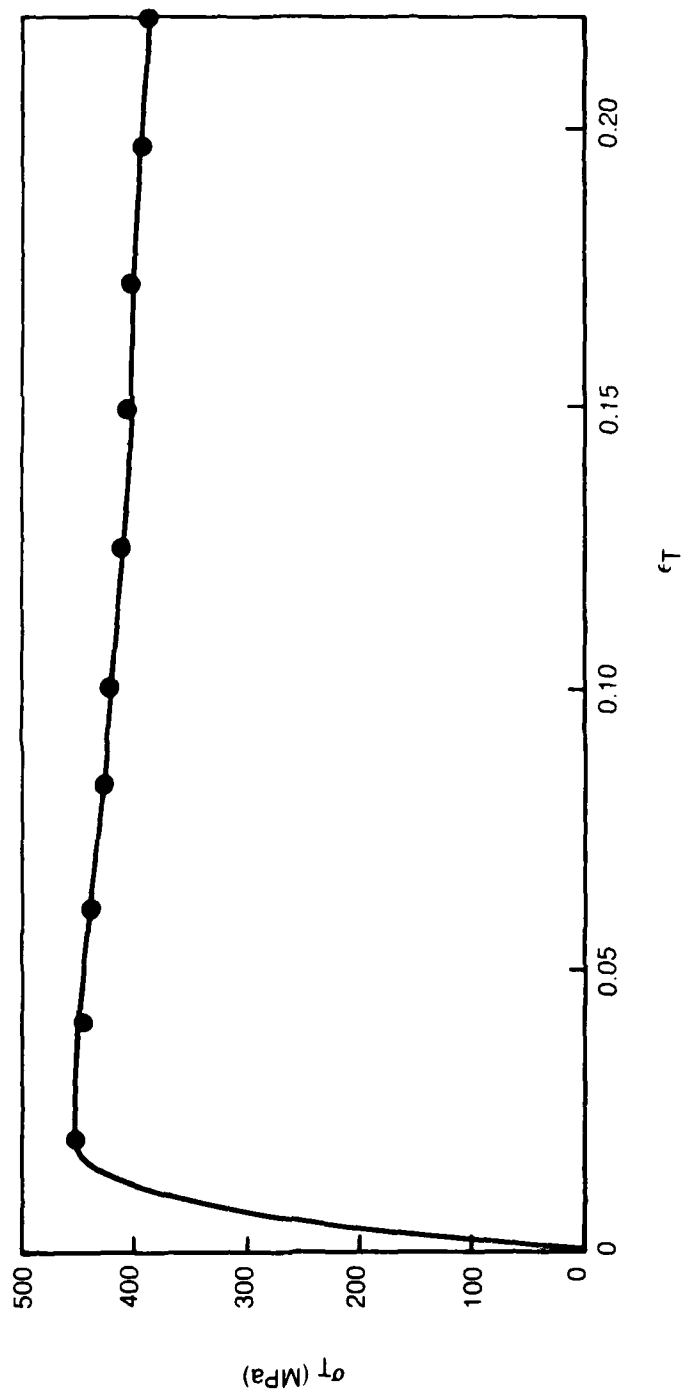
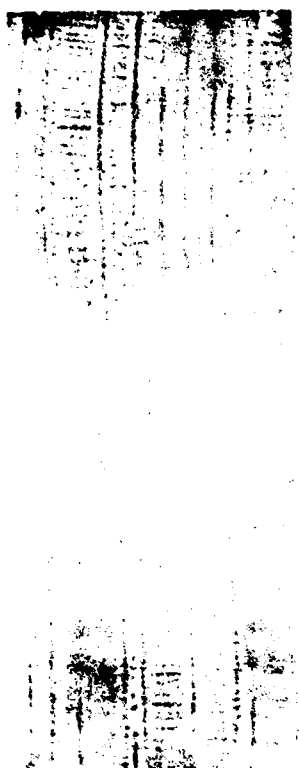COMPRESSIVE FORMING CURVE FOR [011] PWA 1444 AT 1090°C AND 0.5% SEC^{-1}

FIG. 3-67
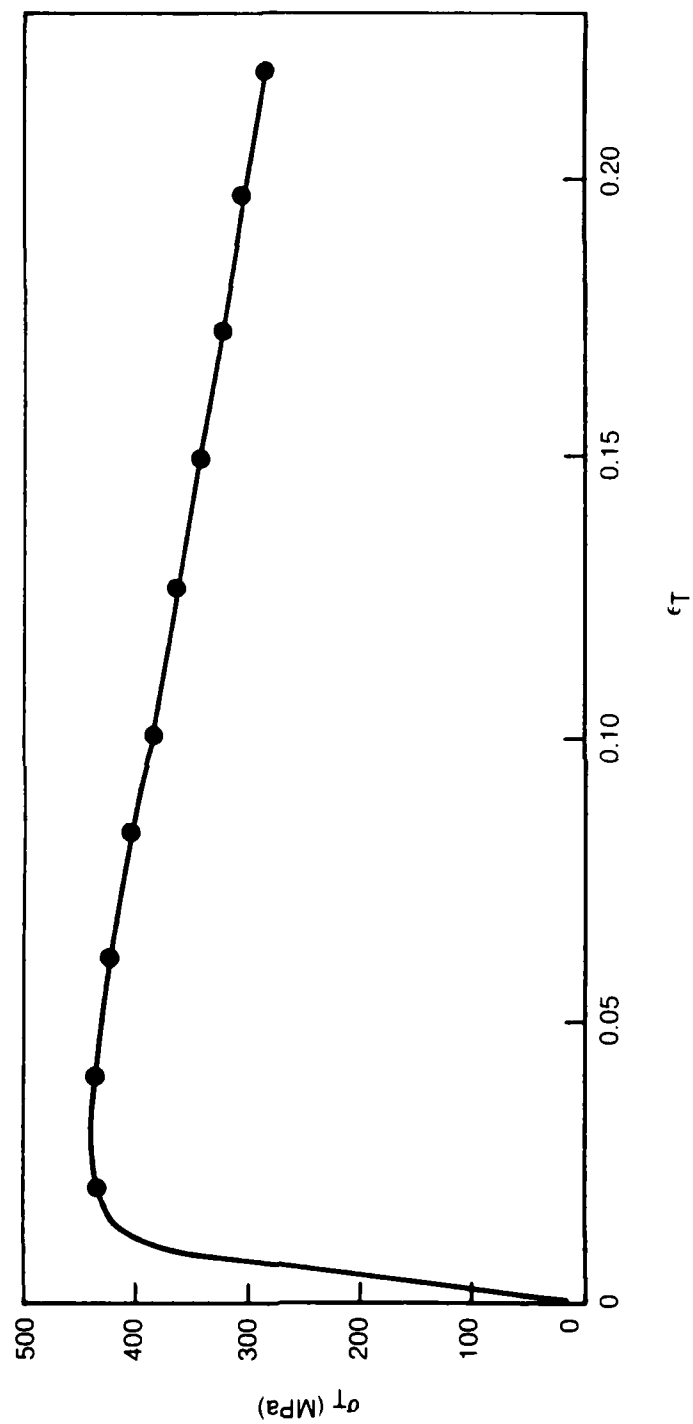
COMPRESSIVE FORMING CURVE FOR [111] PWA 1444 AT 1190°C AND 0.5% SEC^{-1}

83-5-102-44
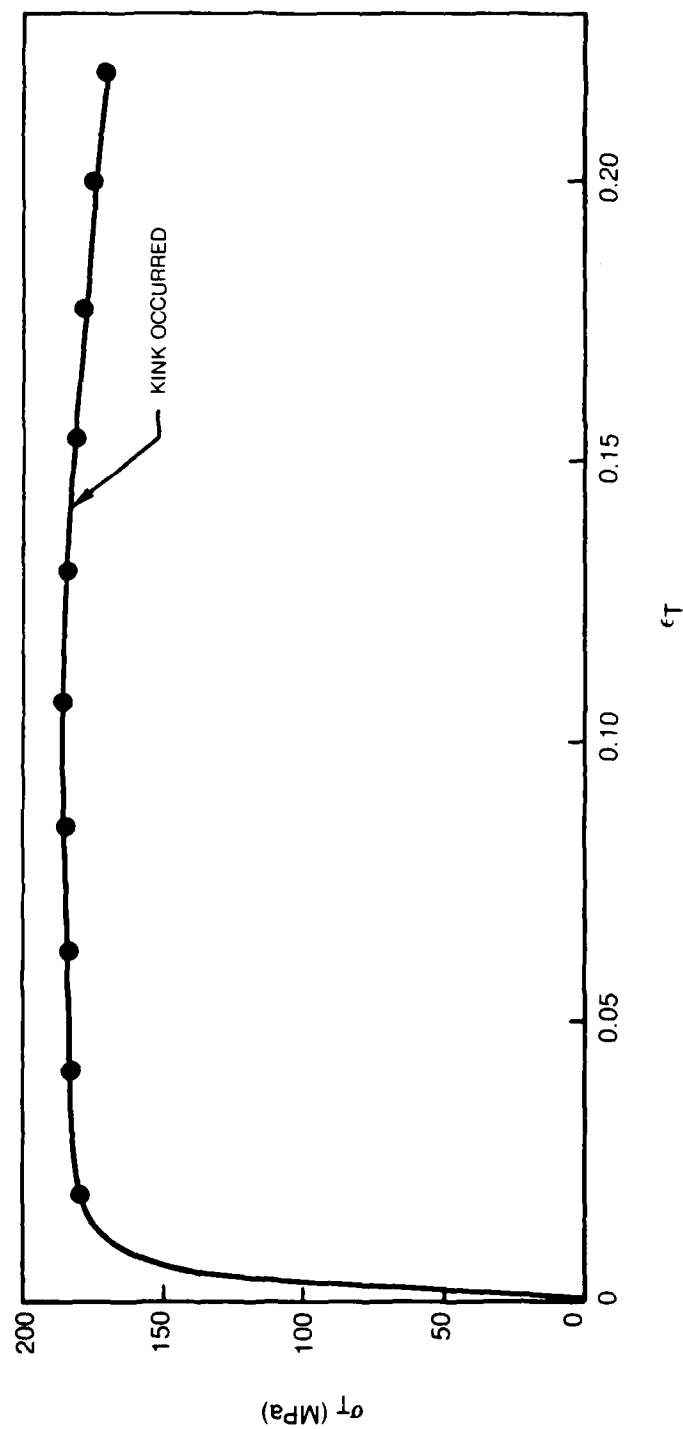
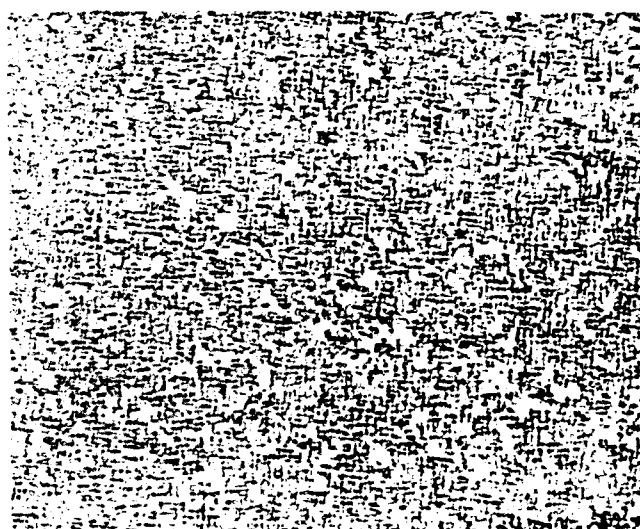**COMPRESSIVE FORMING CURVE FOR [111] PWA 1444 AT 1090°C AND 0.5% SEC^{-1}**

FIG. 3-69

COMPRESSIVE FORMING CURVE FOR [111] PWA 1444 AT 890°C AND 0.5% SEC^{-1}
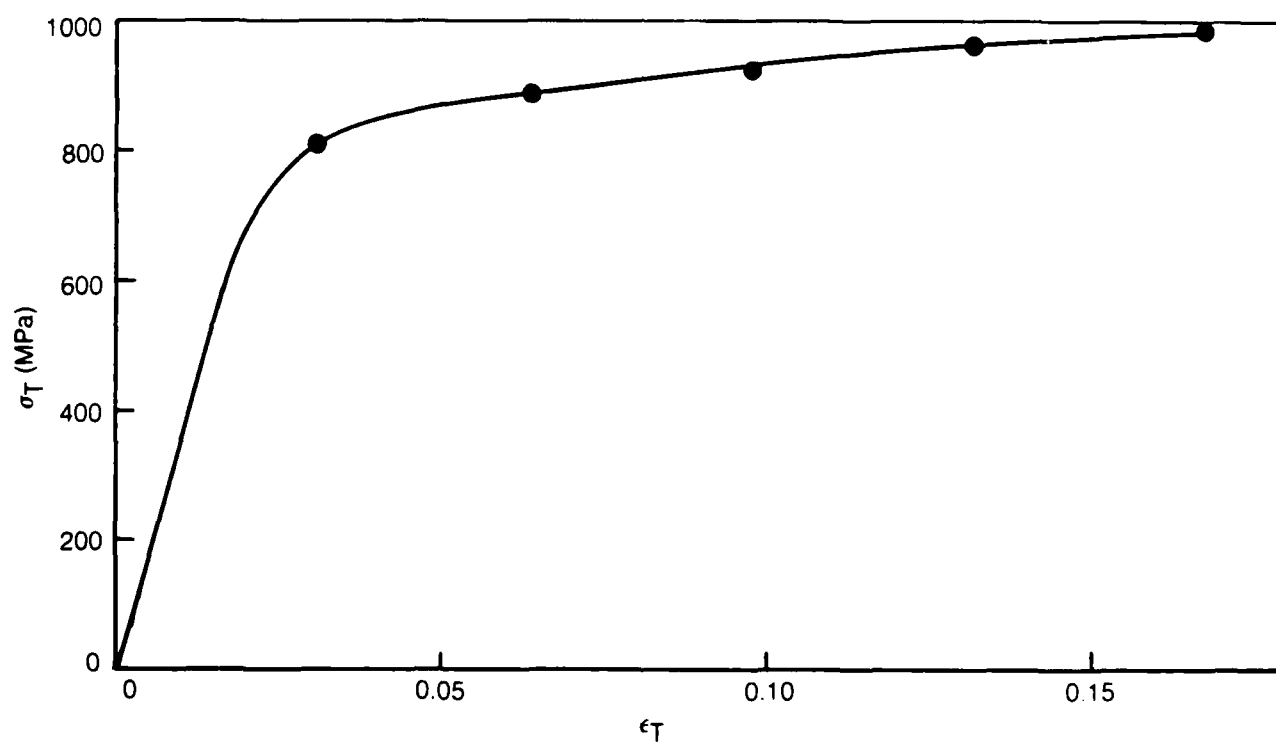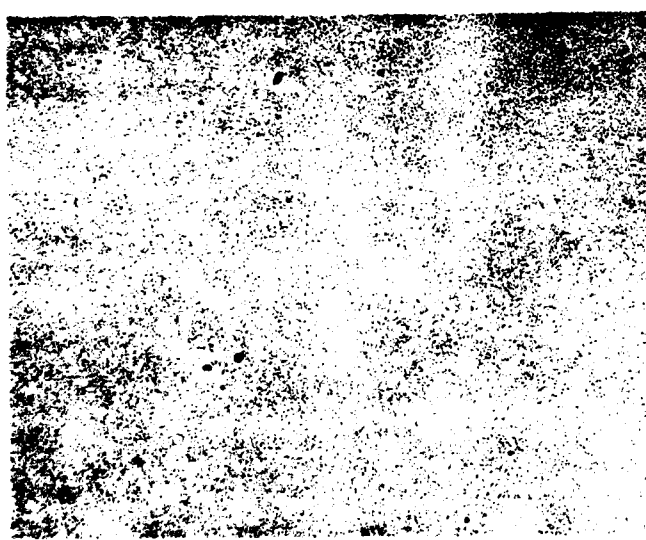
FULLY HEAT TREATED <100> PWA 1444

a) LONGITUDINAL COMPRESSION
AFTER 10% STRAIN.

b) MICROSTRUCTURE AFTER 1 hr
AT 1190°C.

c) TRANSVERSE VIEW AFTER 1190°C
FORMING + 15 min AT 1245°C
+ AIR COOL TO RE-SOLUTION A
LARGE PERCENTAGE OF THE
COARSENED γ'.

d) SAME AS (c) SHOWING SMALL
VOLUME FRACTION COARSE γ' TO
PREVENT RECRYSTALLIZATION.

83 5- 102 17

DISTRIBUTION LIST

No. of Copies	To
12	Dr. Alan Rosenstein, Bldg. 410, Air Force Office of Scientific Research, Bolling Air Force Base, Washington, DC 20332
1	Dr. G. R. Leverant, Dept. of Materials Sciences, Southwest Research Institute, 6220 Culebra Road, San Antonio, TX 78284
1	Prof. Julia Weertman, Dept. of Materials Science, Northwestern Univ., Evanston, IL 60201
1	Prof. N. Stoloff, Mat. Engrg. Dept., Rensselaer Polytechnic Institute, Troy, NY 12181
1	Prof. J. K. Tien, Columbia Univ., 1137 S. W. Mudd, New York, NY 10027
1	Prof. H. D. Brody, School of Engrg., Univ. of Pittsburgh, Pittsburgh, PA 15621
1	Mr. Bhatka B. Rath, Physical Metallurgy Branch, Naval Research Laboratory, Washington, DC 98314
1	Prof. A. J. McEvily, Jr., Metallurgy Dept., Univ. of Connecticut, Storrs, CT 06268
1	Prof. S. M. Copley, Dept. of Materials Science, Univ. of Southern California, Los Angeles, CA 90007
	Air Force Wright Aeronautical Labs, Metals Processing, Wright-Patterson Air Force Base, OH 45433
1	Attn: Mr. A. M. Adair
1	Dr. H. Lipsitt
	Air Force Materials Laboratory, Wright-Patterson Air Force Base, OH 45433
	Attn: Branch Chief
1	AFWAL/MLLS
1	AFWAL/MLLM
1	AFWAL/MLLN
1	Dr. N. E. Paton, Rockwell International Science Center, 1049 Camino dos Rios, Thousand Oaks, CA 91360
1	Dr. B. A. MacDonald, Code 471, Dept. of the Navy, Office of Naval Research, Arlington, VA 22217

END

FILMED

9-83

DTIC